

Nonisolated High Step-Up DC–DC Converters: Comparative Review and Metrics Applicability

Hadi Tarzamni ¹, Student Member, IEEE, Homayon Soltani Gohari ², Mehran Sabahi ³,
and Jorma Kyyrä ⁴, Member, IEEE

Abstract—Due to the extensive role of nonisolated high step-up dc–dc converters (NHSDC)s in industrial applications and academic research works, many of these pulswidth modulation converters have been presented in recent years. For each of these NHSDCs, some claims are introduced to verify its capabilities and features, which have been investigated in some review papers with different frameworks. Dissimilar to previous review papers, which have focused on the classification and derivation of voltage boosting techniques, this article aims to evaluate the converters from various topological and operational points of view and determine the superiority of each technique and converter according to applications. Some of these metrics are voltage gain, stresses, ripple, cost, power density, weight, size, control complexity, and components count, which lead to a comprehensive comparative study. Then, as the main purpose of this article, the effectiveness of these metrics is assessed to show how well they can lead us to fair comparison results. Moreover, some new figures of merit are proposed in this article to provide a helpful guideline in power electronic converters comparison studies. Finally, the feasibility discussion of single- and multiobjective figures of merit is followed by a general practical conclusion and outlook about the NHSDC structures.

Index Terms—DC–DC converters, high step-up power conversion, metrics applicability, pulswidth modulation (PWM), single- and multiobjective figures of merit, topological and operational features, voltage boosting techniques.

I. INTRODUCTION

BASED on the drawbacks and shortcomings of the conventional pulswidth modulation (PWM) boost converters, many research and industrial projects have attempted to alleviate or eliminate the drawbacks along with improving topological and operational features under the title of nonisolated high step-up dc–dc converters (NHSDC)s [1], [2], [3], [4], [5], [6], [7], [8], [9], [10], [11], [12], [13], [14], [15], [16], [17], [18],

Manuscript received 28 December 2022; revised 5 March 2023; accepted 21 March 2023. Date of publication 3 April 2023; date of current version 6 December 2023. This work was supported by the Finnish Electronic Library, Finland, under the FinELib Consortium’s agreement with IEEE. Recommended for publication by Associate Editor F. Azcondo. (Corresponding author: Hadi Tarzamni.)

Hadi Tarzamni and Jorma Kyyrä are with the Department of Electrical Engineering and Automation, Aalto University, 02150 Espoo, Finland (e-mail: hadi.tarzamni@aalto.fi; jorma.kyyra@aalto.fi).

Homayon Soltani Gohari is with the Department of Electrical Engineering, K. N. Toosi University of Technology, Tehran 1969764498, Iran (e-mail: hsoltani@email.kntu.ac.ir).

Mehran Sabahi is with the Faculty of Electrical and Computer Engineering, University of Tabriz, Tabriz 51666-15813, Iran (e-mail: sabahi@tabrizu.ac.ir).

Color versions of one or more figures in this article are available at <https://doi.org/10.1109/TPEL.2023.3264172>.

Digital Object Identifier 10.1109/TPEL.2023.3264172

[19], [20], [21], [22], [23], [24], [25], [26], [27], [28], [29], [30], [31], [32], [33], [34], [35], [36], [37], [38], [39], [40], [41], [42], [43], [44], [45], [46], [47], [48], [49], [50], [51], [52], [53], [54], [55], [56], [57], [58], [59], [60], [61], [62], [63], [64], [65], [66], [67], [68], [69], [70], [71], [72], [73], [74], [75], [76], [77], [78], [79], [80], [81], [82], [83], [84], [85], [86], [87], [88], [89], [90], [91], [92], [93], [94], [95], [96], [97], [98], [99], [100], [101], [102], [103], [104], [105], [106], [107], [108], [109], [110], [111], [112], [113], [114], [115], [116], [117], [118], [119], [120], [121], [122], [123], [124], [125], [126], [127], [128], [129], [130], [131], [132], [133], [134], [135], [136], [137], [138], [139], [140], [141], [142], [143], [144], [145], [146], [147], [148], [149], [150], [151], [152], [153], [154], [155], [156], [157], [158], [159], [160], [161], [162], [163], [164], [165], [166], [167], [168], [169], [170], [171], [172], [173], [174], [175], [176], [177], [178], [179], [180], [181], [182], [183], [184], [185], [186], [187], [188], [189], [190], [191], [192], [193], [194], [195], [196], [197], [198], [199], [200], [201], [202], [203], [204], [205], [206], [207], [208], [209], [210], [211], [212], [213], [214], [215], [216], [217], [218], [219], [220], [221], [222], [223], [224], [225], [226], [227], [228], [229], [230], [231], [232], [233], [234], [235], [236], [237], [238], [239], [240], [241]. These research projects have led to numerous converters in publications, some of which have close similarities to the extent that the novelty and contribution are the challenging issues among the recently published and peer-reviewed articles. To clarify their functionalities and solve the confusion among the researchers and readers, some literature works aimed to review, classify, and generalize the synthesis methodologies of the NHSDCs [1], [2], [3], [4], [5], [6], [7], [8], [9], [10].

Because of the critical role of the NHSDCs in the photovoltaic (PV) systems, authors have established a PV application-oriented review on these converters in [1]. Focusing on the grid-connected operation, some common voltage lifting methods have been analyzed and classified. Moreover, some helpful arguments have been provided about the superiority of the NHSDCs over isolated structures along with the shortcomings of the conventional PWM boost converter. The authors have tried to provide a conceptual solution to achieve a high step-up converter featuring low cost and high efficiency. Although they have considered the challenges of each type of the reviewed converters, the topological and operational characteristics of the structures have not been compared. The main aim of Li and He [1] is to study the configuration process of some specific

converters in PV applications. Another comparative study of the NHSDCs, originating from the conventional PWM boost topology, has been presented in [2], where the converters have been classified according to their conversion ratio width. The derivation process of the topologies has been explained, and some common operational and topological features, such as voltage gain, switches voltage stress, components count, modularity, and duty cycle range, have been considered as the comparison metrics. However, other crucial figures of merit, such as current stress, voltage and current ripples, soft switching performance, control complexity, cost, size, weight, efficiency, power density, sensitivity, and applicability, are not evaluated. In addition, although a larger variety of converters have been analyzed in comparison to [1], the impedance source and extendable and bidirectional converters are not taken into account in [2]. A similar framework has been followed in [3] with focusing on the high-frequency topologies, which are classified into coupled inductor-, switched cell-, and transformer-based structures. In other words, some high step-up and step-down dc–dc configurations with soft switching capability have been considered in [3].

The NHSDCs have been investigated in some literature works relying on the coupled inductors and voltage multiplier cells (VMC)s configurations. In [4], the coupled inductor-based NHSDCs, derived from the conventional PWM boost and fly-back (FL) structures, have been reviewed. The studied converters have been classified into five categories according to the utilized voltage boosting approaches that are followed by their derivation process. These categories are cascaded, stacked, multiwinding, integrated, and interleaved structures. The topological characteristics have been evaluated briefly, and the operational comparison has been established under some limited design conditions for only five topologies. Although the article has summarized the advantages and disadvantages of the reviewed topologies, its study is restricted to the coupled inductor-based converters. In [5], a synthesis methodology, using coupled inductors and VMCs, has been introduced to accomplish ultrahigh voltage gain converters. The authors have reviewed different combinations of structures and their resultant converters and have categorized them based on the number of utilized voltage boosting approaches as the single-, double-, and triple techniques. Then, five selected converters have been compared from different points of view and the experimental results have been provided. Although the comparison study of Andrade et al. [5] is limited, it has verified that many NHSDCs can be suggested by different permutations of voltage boosting techniques. As a similar effort in [6], a generalized methodology to derive a family of NHSDCs has been suggested by employing coupled inductors and VMCs where its boost-, buck-, and buck–boost-oriented topologies have been compared in terms of some basic figures of merit. As two applicable criteria, the converters output power regulation and the effect of switching frequency on the power losses have been assessed in these three topologies. The main purpose of Schmitz et al. [6] is to compare the capabilities of the boost, buck, and buck–boost converters rather than the voltage boosting techniques. In two other similar works [7], [8], the

authors have introduced an efficient and practical methodology to synthesize the NHSDCs from basic structures by focusing on the differential connection style. In these papers, various types of derived converters have been assessed with regard to the utilized voltage lift methods, operation limitations, design considerations, modulation types, and components count reduction. In general, the authors of [7] and [8] aim to verify the differential connection capabilities rather than analyzing the voltage boosting approaches.

One of the well-organized reviews about the NHSDCs has been provided in [9], in which the converters are categorized into five major categories based on isolation, power flow direction, input port feeding type, soft switching capability, and the presence of right-half-plane zero. Moreover, the voltage boosting techniques have been investigated in five classifications of switched capacitor (SC), switched inductor (SI), magnetically coupled, VMC, and multistage configurations. As an interesting part of this article, the applications and power range of each class have been widely studied. Although the converters are comprehensively classified with various examples and their pros and cons are discussed, most of the comparisons are general and qualitative giving no precise evaluation. A similar procedure has been followed in [10] while concentrating on the unidirectional NHSDCs applicable in the fuel cell (FC) vehicles.

As studied in the proceeding paragraphs, the main aims of the previously published review papers are to generalize synthesis methodologies, classify voltage boosting techniques, analyze the NHSDCs characteristics, and present some discussions about their merits and demerits. Although they provide some helpful sets of guidelines for the NHSDCs configurations, none of them provides an applicable, clear, and comprehensive evaluation for this growingly dominant category of power electronic converters. In addition, the evaluation metrics, which are considered in the comparison studies, are sometimes employed:

- 1) without considering their required condition;
- 2) without a comprehensive point of view;
- 3) without common assumptions;
- 4) with biased conclusions.

Moreover, some of these figures of merit are not practically decisive and reliable. These issues result in some unfair, vague, incomplete, and sometimes invalid comparison outcomes. This article aims to fill these gaps between the NHSDCs and evaluation metrics by presenting a comprehensive comparative review of the NHSDCs as well as an extensive comparison guideline. During the effectiveness analysis of the evaluation metrics, some improved figures of merit are proposed. It is noteworthy that, most of the assessments about the metrics applicability can be generalized to the other categories of power electronic converters. The framework and assumptions of this article are listed as follows.

- 1) Since most of the high step-up dc–dc converters can be reconfigured as multiport converters, the single-input single-output topologies are evaluated in this study.

- 2) Because most of the conference papers are published as journal articles in their improved version, the high-impact factor journals are taken into account.
- 3) In order to assess the latest publications and ignore the repetition of reviewed ones in the previous review papers, this article concentrates on the publications of the recent decade (2010–2023). It tries to cover the completely distinct converters introduced in this period.
- 4) In some literature works, a family of converters is introduced, where these converters are separately evaluated in this study only if they present significantly different features. Converters of these papers are specified in the Appendix (see Appendix A).
- 5) In order to prepare a fair comparison, the whole converters are redesigned under the same operation conditions.

The rest of this article is organized as follows. In Section II, a brief review of the NHSDCs is provided along with concise and comprehensive illustrations. Section III is the main part of the article that presents an extensive evaluation of the NHSDCs and their associated voltage boosting techniques, applicability assessment of the topological and operational figures of merit, improved comparison metrics, discussions about the NHSDCs applications, and acceptable comparison conditions. Section IV is devoted to the impedance source and extendable topologies. Eventually, Section V concludes the article with some practical discussions, comparison guidelines, and outlook.

II. VOLTAGE BOOSTING TECHNIQUES: A BRIEF REVIEW

The high step-up dc–dc converters are basically responsible to transfer the low input voltage level to the higher values in the output port by periodic charging and discharging of passive components through an appropriate control scheme of semiconductors. The main aim of this process is to provide the desired regulated high voltage to the load, and to satisfy some topological and operational requirements according to the applications as well. In the previously published literature, different voltage boosting techniques are classified, synthesized, and explained in various frameworks [1], [2], [3], [4], [5], [6], [7], [8], [9], [10]. Employing charge pump, magnetic coupling, SC, SI, combined switched capacitor and inductor (SCI), VMC, voltage lift, multistage and multilevel structures, and interleaving techniques are some of the common methodologies with some probable overlaps in nomination. These methodologies can be implemented in any step-up dc–dc converter, such as conventional PWM boost, buck–boost, Cuk, Sepic, Zeta, and FL converters. Since the purpose of this article is not categorizing or obtaining the techniques, the fundamental discussions are not included. Nevertheless, a concise demonstration of the NHSDCs voltage boosting methodologies as well as other features is provided in Fig. 1. In this figure, the basic topology is the conventional PWM boost converter (drawn in black bold lines) and other required parts for high step-up conversion are added as some auxiliary modules or units. The placement and connection of these units match their real configurations that are employed

either for voltage gain increment or operation improvement, such as voltage clamping and soft switching.

III. EVALUATION OF THE NHSDCs, BASED ON THE CURRENT AND NEWLY PROPOSED FIGURES OF MERIT

As the main part of this article, the NHSDCs are studied, evaluated, and compared from different topological and operational points of view. Along with these assessments, the effectiveness of comparison metrics is also discussed, and some improved metrics are proposed to lead to a fair judgment between the NHSDCs as well as their associated voltage boosting techniques. The most common comparative figures of merit in the NHSDCs are categorized in Fig. 2, where the topological features refer to the power electronic components and the layout of the converters regardless of their operation and control drive. Meanwhile, the operational features are the whole characteristics of the converters after they are driven by a control unit. The single-objective features are listed in Fig. 2 and the multiobjective features related to each category are introduced in the following sections. In order to compare fairly, the following assumptions are considered in this article.

- 1) Evaluations are carried out for the continuous conduction mode (CCM) of all converters because it is more common in a high step-up operation. Moreover, the ideal CCM voltage gain of the PWM NHSDCs is independent of load, switching frequency, and passive components values' that make the evaluation easier.
- 2) In analyzing the effect of duty cycle (D), it varies in the whole applicable range of $0.1 \leq D \leq 0.9$ except in the interleaved and impedance source converters. The parameter D is usually more (or less) and less than 0.5 in the interleaved and impedance source NHSDCs, respectively.
- 3) In analyzing the effect of magnetically coupled components turns ratio (N), it varies in the range of $1 \leq N \leq 10$. The parameter N is defined as the secondary to the primary winding turns ratio, where it is also considered for the tertiary to the primary winding turns ratio in the triple-winding cores.
- 4) In these cases, one operation point is required and one parameter should be considered as a constant, $D = 0.7$ and $N = 3$ are assumed. Moreover, the redesigning of the converters for the comparison study is performed with the switching frequency of $f_S = 50$ kHz (except for some resonant structures) as the most popular in the NHSDCs. Note that the design and comparison of the converters can be repeated for any desired operation point.
- 5) Extended structures are investigated separately, and for a fair comparison among them, the number of extended cells is $K = 3$.

A. Topological Features

1) *Numerical Characteristics*: Comparing the components count of converters is the most primitive and simple approach to evaluate the superiority of a converter, which is carried out in almost all of the NHSDC-related papers. Table I presents some numerical characteristics of the NHSDCs, where the first

TABLE I
(CONTINUED.)

[161]	5	0	3	0	3	4	12	9	78.32	917.1	467891.4	0.1149	-0.7084	-0.6127	-0.6150	-0.6382	✓		
[163]	3	6	3	0	3	6	18		80.96	941.1	468579								
[164]	2	3	2	0	2	3	10	10	53.49	644.8	327363.2	0.1869	-0.4596	-0.2443	-0.2815	-0.2907			
[165]	2	3	2	0	2	3	10	12.33	53.49	644.8	327363.2	0.2305	-0.4449	-0.2294	-0.2666	-0.2757			
[168]	2	4	1	0	1	4	11		34.13	193	71396.2								
[171]	2	4	3	0	3	3	12		68.68	905.6	460438.6								
[174]	2	8	2	0	2	8	20		68.24	697.3	336852.2								
[175]	4	0	1	0	1	3	8	6.66	45.16	392	199181.8	0.1474	-0.3992	-0.1443	0.0006	-0.0010	✓		
[176]	3	4	2	0	2	3	12		60.52	659.8	331596.2								
[178]	2	1	2	0	2	1	6	5.66	47.59	623.8	323567.6	0.1189	-0.4292	-0.1862	-0.2841	-0.3093			
[178]	2	2	2	0	2	2	8	6.66	50.54	634.3	325465.4	0.1317	-0.4517	-0.2228	-0.2903	-0.3075			
[178]	2	3	2	0	2	3	10	7.66	53.49	644.8	327363.2	0.1432	-0.4743	-0.2594	-0.2965	-0.3057			
[179]	3	3	3	0	3	3	12	27.88	72.11	909.6	462885.6	0.3866	-0.5292	-0.4011	-0.4849	-0.5049			
[180]	2	4	3	0	3	1	10	8	66.38	895.6	458429	0.1205	-0.5980	-0.4451	-0.5956	-0.6216			
[180]	2	7	4	0	4	1	14	10.33	85.17	1167.4	593290.4	0.1212	-0.7669	-0.7040	-0.9071	-0.9340			
[181]	3	4	3	0	3	2	12		63.84	703.1	337091.4								✓
[182]	4	0	2	0	2	2	8	13.33	57.4	642.3	330359.4	0.2322	-0.4769	-0.2800	-0.2571	-0.2766			
[184]	4	4	4	0	4	5	17	10	94.83	1189.9	601310.6	0.1054	-0.8633	-0.8470	-0.9363	-0.9556			
[184]	4	4	4	0	4	4	16	6.66	93.68	1184.9	600305.8	0.0710	-0.8731	-0.8516	-0.9517	-0.9745			
[185]	2	4	2	0	2	4	12	13.33	56.44	655.3	329261	0.2361	-0.4675	-0.2660	-0.2728	-0.2739			
[186]	1	4	3	0	3	4	12	18.89	64.6	901.1	458103.4	0.2924	-0.5123	-0.3493	-0.5324	-0.5510			
[187]	2	2	2	0	2	2	8	13.44	50.54	634.3	325465.4	0.2659	-0.4092	-0.1793	-0.2468	-0.2640			
[188]	2	4	3	0	3	5	14	14.33	70.98	915.6	462448.2	0.2018	-0.6032	-0.4715	-0.5790	-0.5908			
[189]	2	2	3	0	3	3	10	10.33	65.08	894.6	458652.6	0.1587	-0.5707	-0.4112	-0.5794	-0.6072			
[190]	1	3	3	0	3	5	12	8	63.95	900.6	458215.2	0.1250	-0.5743	-0.4097	-0.6016	-0.6211			
[191]	2	2	2	0	2	2	8	6.66	50.54	634.3	325465.4	0.1317	-0.4517	-0.2228	-0.2903	-0.3075			
[192]	2	3	2	0	2	3	10	14.44	53.49	644.8	327363.2	0.2699	-0.4317	-0.2159	-0.2530	-0.2622			
[193]	1	4	3	0	3	4	12	13.44	64.6	901.1	458103.4	0.2080	-0.5465	-0.3842	-0.5673	-0.5859			
[193]	1	4	3	0	3	4	12	18.89	64.6	901.1	458103.4	0.2924	-0.5123	-0.3493	-0.5324	-0.5510			
[194]	4	7	6	0	6	9	26		95.93	909	369644								✓
[197]	1	5	3	0	3	3	12	22.22	65.25	901.6	457991.6	0.3405	-0.4977	-0.3374	-0.5116	-0.5293			
[198]	4	7	4	0	4	3	18	21.66	97.93	1196.4	601980	0.2211	-0.8204	-0.8174	-0.8693	-0.8824			
[200]	1	3	2	0	2	2	8	10.11	47.11	630.3	323018.4	0.2146	-0.3966	-0.1506	-0.2634	-0.2794			
[201]	2	5	3	0	3	4	14	7.66	62.71	709.1	336654	0.1221	-0.5643	-0.3938	-0.3737	-0.3282			✓
[203]	2	2	2	0	2	3	9	6.66	42.77	432.3	200787.8	0.1557	-0.3759	-0.1095	-0.0477	-0.0049			✓
[204]	6	0	5	0	5	5	16	8.51	93.64	1028.2	485236.2	0.0908	-0.8611	-0.8392	-0.7516	-0.6834	✓		✓
[205]	6	0	3	0	3	3	12		82.4	921.6	470226.6						✓		
[207]	2	3	2	0	2	3	10	15.55	53.49	644.8	327363.2	0.2907	-0.4247	-0.2088	-0.2459	-0.2551			
[208]	2	4	4	0	4	2	12		72	948.9	465933.8								✓
[209]	4	0	2	0	2	3	9	6.66	58.55	647.3	331364.2	0.1137	-0.5300	-0.3395	-0.3059	-0.3218	✓		
[210]	4	0	2	0	2	2	8	11.11	57.4	642.3	330359.4	0.1935	-0.4908	-0.2942	-0.2714	-0.2908	✓		
[211]	5	0	2	0	2	3	10	6.66	63.78	656.8	334704.2	0.1044	-0.5810	-0.4158	-0.3173	-0.3299	✓		
[212]	3	3	1	0	1	3	10		45.33	399	198520.8								
[213]	3	2	3	0	3	4	12	5.66	71.46	909.1	462997.4	0.0792	-0.6623	-0.5341	-0.6268	-0.6477	✓		
[214]	4	8	8	0	8	9	29		124.51	1425.1	634901.8								✓
[215]	3	0	2	0	2	3	8	3.33	53.32	637.8	328024.2	0.0624	-0.4998	-0.2846	-0.3159	-0.3351			
[216]	2	3	2	0	2	3	10	15.44	53.49	644.8	327363.2	0.2886	-0.4254	-0.2095	-0.2466	-0.2558			
[217]	2	4	2	0	2	4	12		56.44	655.3	329261								✓
[218]	2	5	0	1	5	5	13	23.33	53.48	431.7	198976.4	0.4362	-0.3758	-0.1587	0.0599	0.1063	✓		✓
[219]	1	3	1	1	3	2	8		48.98	635.6	323018.4								✓
[220]	1	4	1	1	3	5	12	16.66	54.23	656.1	326925.8	0.3072	-0.4250	-0.2124	-0.2524	-0.2469	✓		
[221]	2	2	1	1	3	4	10	9.83	54.71	649.6	327475	0.1796	-0.4726	-0.2632	-0.2884	-0.2921	✓		✓
[222]	1	4	1	1	3	5	12		54.23	656.1	326925.8								✓
[223]	1	4	0	2	4	5	12	23.33	56.1	661.4	326925.8	0.4158	-0.4014	-0.1969	-0.2159	-0.2041	✓		
[224]	1	5	0	1	3	6	13	23.16	45.66	416.6	196641.2	0.5072	-0.3005	-0.0458	0.0769	0.1109	✓		
[225]	1	5	2	0	2	7	15	7.83	56.46	666.3	329828.4	0.1386	-0.5022	-0.3016	-0.3212	-0.3106	✓		
[226]	2	4	2	0	2	4	12	17.93	56.44	655.3	329261	0.3176	-0.4386	-0.2365	-0.2433	-0.2444	✓		
[227]	1	4	4	0	4	7	16	5.66	81.44	1171.4	593300.2	0.0694	-0.7598	-0.6796	-0.9419	-0.9639	✓		
[228]	2	5	1	0	1	4	12	10	44.85	405.5	197971.6	0.2229	-0.3752	-0.1184	0.0059	0.0232			
[229]	3	2	4	0	4	3	12		83.7	1159.4	594175								✓
[230]	1	2	2	0	2	3	8	4.33	46.46	629.8	323130.2	0.0931	-0.4265	-0.1782	-0.2998	-0.3168	✓		
[231]	1	5	3	0	3	7	16	4.15	69.85	921.6	462010.8	0.0594	-0.6561	-0.5204	-0.6515	-0.6550	✓		
[232]	1	4	2	0	2	5	12	7.66	52.36	650.8	326925.8	0.1462	-0.4632	-0.2429	-0.3037	-0.3046	✓		
[233]	1	4	2	1	4	4	12		66.47	906.4	458103.4								✓
[234]	1	3	2	0	2	4	10	5.5	49.41	640.3	325028	0.1113	-0.4480	-0.2137	-0.3050	-0.3139	✓		
[235]	1	5	1	2	5	7	16	22.16	73.59	932.2	462010.8	0.3011	-0.5795	-0.4594	-0.5487	-0.5395	✓		
[236]	1	2	0	1	3	2	6		35.66	380.1	189943								✓
[237]	6	1	2	0	2	5	14	6.66	73.11	681.8	340946.8	0.0910	-0.6722	-0.5518	-0.3474	-0.3451	✓		✓
[238]	1	2	2	0	2	3	8	4.33	46.46	629.8	323130.2	0.0931	-0.4265	-0.1782	-0.2998	-0.3168	✓		
[238]	1	4	2	0	2	5	12	7.66	52.36	650.8	326925.8	0.1462	-0.4632	-0.2429	-0.3037	-0.3046	✓		
[238]	1	4	1	1	3	5	12	17.66	54.23	656.1	326925.8	0.3256	-0.4187	-0.2060	-0.2459	-0.2405	✓		
[239]	1	2	1	1	3	3	8		48.33	635.1	323130.2								✓
[240]	2	3	2	0	2	3	10		53.49	644.8	327363.2								✓
[240]	2	6	3	0	3	3	14		72.28	916.6	462224.6								✓
[241]	1	3	3	0	3	3	10	3.33	61.65	890.6	456205.6	0.0540	-0.5812	-0.4061	-0.6195	-0.6462	✓		

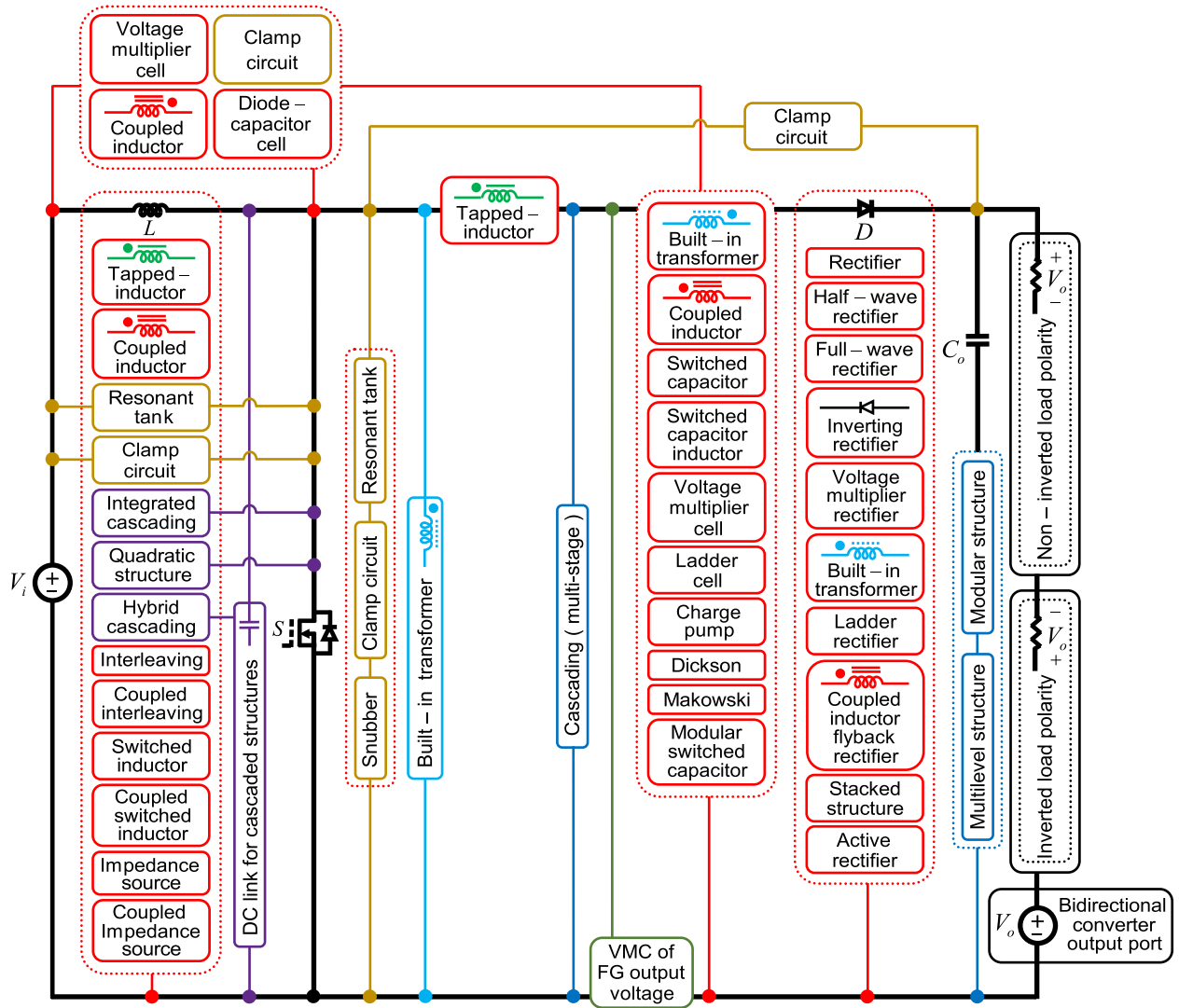


Fig. 1. Summarization of voltage boosting techniques and power conditioning units of NHSDCs applied to the conventional PWM boost converter.

seven columns are dedicated to the components count, and the best and the worst candidates are highlighted in green and red in each column, respectively. According to these numbers, the following points are concluded.

- 1) The minimum number of power switches (which will be named switches in the rest of the article) is one, which reflects the principle of power electronic converters for the existence of at least one controlled semiconductor in an independent converter. As it is clear, 79 converters ($\approx 35\%$) of this list have one switch, which enables them with straightforward switching algorithms, and wide duty cycle ranges. This capability helps the single-switch structures to be suitably simple candidates for applications with high variation of operation points, such as renewable energy systems. From the structural point of view, all types of capacitive and inductive voltage boosting techniques, except interleaving and using active configurations of clamps, snubbers, switched cells, and resonant tanks, can be implemented with a single switch.

On the other hand, to accomplish high voltage gain (G), it is inevitable to use a higher number of diodes in the VMC, SC, and SI units, output rectifier, stacked structure, integrated cell, soft switching tank, passive clamp, and snubber circuit. According to Table I, most of the NHSDCs with one switch have four or more diodes. Therefore, the number of switches cannot reflect a useful and practical insight from a converter superiority, and the summation of switches and diodes is replaced in some literature works, where [36], [46], [63], [69], [85], [96], [105], [145], [163], [174], [180], [194], [198], and [214] consist of the highest semiconductors count. With a close look at these converters, it is recognized that using a three-phase interleaved topology with a common active clamp [36], a two-phase topology with two active resonant tanks and an SCI unit [46], high-order SC cells [63], [96], [163], [174], a two-phase interleaved topology with three SC and SCI units [69], a two-phase interleaved topology with two SC units and two output rectifier circuits [85], a two-phase interleaved topology with integrated cascading and two output rectifier circuits [105], an interleaved topology with four passive

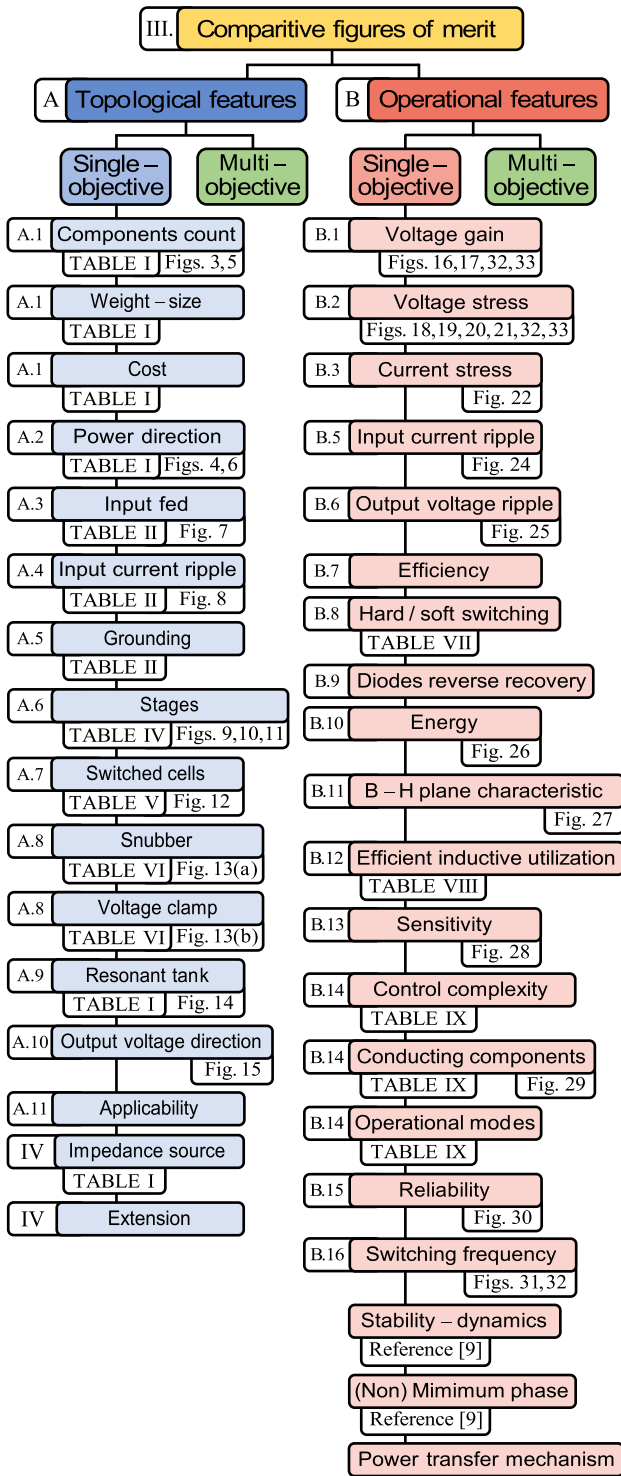


Fig. 2. Categorization of the most important characteristics in NHSDCs while addressing the number of associated sections, tables, and figures.

clamp circuits [145], a combination of passive and active SI units [180], a two-phase interleaved topology with complicated SC units and soft switching auxiliary circuits [194], two SI and one SC units [198], and a multiphase interleaved topology with a soft switching mechanism [214] increase the semiconductors count. All the aforementioned approaches, which lead to high

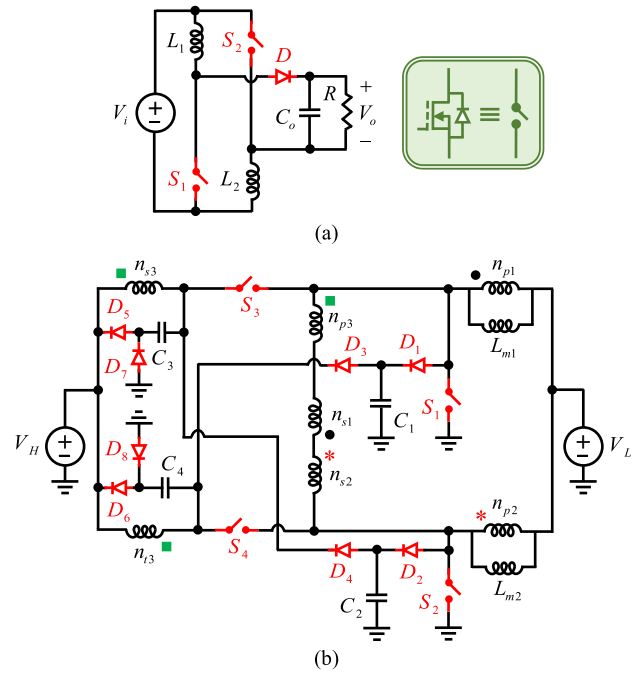


Fig. 3. Comparison of two NHSDCs semiconductors count. (a) Low [178] and (b) high [145] number of semiconductors.

counts of semiconductors, are employed to increase the voltage gain and power of the converters, and their high semiconductors count should not be considered as a drawback separate from other operational features. As another evidence, although low semiconductors count in [178], [215], [230], and [238] may lead to more simple configurations, their output voltage gain and power are low, which restrict their applicability. To compare the wide variety of semiconductors count, Fig. 3 shows two NHSDCs with low (3) and high (12) counts.

Accordingly, the total semiconductors count presents an incomplete vision of the gate drives of switches and the reverse recovery condition of diodes. Furthermore, since the specifications of semiconductors are not considered, this number does not lead to a useful practical point of view even when comparing the converters of the same family.

- About 40% of the converters operate with two switches where the second switch is employed in the interleaved branch [16], [39], [100], [151], cascaded (multistage) unit [124], soft switching auxiliary circuit [27], [53], [218], active clamp circuit [36], [38], [57], active SI unit [165], [178], [180], [187], combined SCI unit [91], [94], [191], impedance source network [221], [240], or complementary with the first switch [12], [189], [203]. Note that except for the synchronous PWM boost converter, which is realized with the replacement of the rectifying diode by a switch in the conventional PWM boost converter (see Fig. 4), the bidirectional NHSDCs employ more than two switches. The synchronous PWM boost converter is not usually categorized as a high step-up topology; however, it is the basic structure in most of the bidirectional NHSDCs.

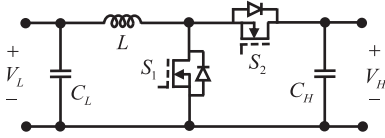


Fig. 4. Synchronous PWM boost converter.

- 3) In the previously published literature, it has been usually considered that semiconductors have the highest impact on the total cost of a converter, and the low number of semiconductors results in a cheap converter. According to the results in Table I, the converters in [30], [66], [122], [125], [126], [168], [212], and the converters in [28], [35], [109], [228] with six and seven semiconductors, respectively, are cheaper than [178], [215], and [239] with three in the same operation point and design specifications. Thus, the number of semiconductors is not a precise, comprehensive, and reliable criterion to evaluate the cost metric.
- 4) A combined SI and high-order SC structure in [63], two-phase interleaved topologies with separated SC cells in each phase in [69] and [174], a two-phase interleaved topology with two combined SI and SC cells and two output rectifier circuits in [85], a topology with multiphase rectifier in [214], and a two-phase interleaved topology with passive clamp circuits in [145] are the converters with the highest diode count.
- 5) Passive components, specifically the magnetic cores, count has been considered as the most effective metric on a converter's volume and weight. This number can be used as a criterion of superiority for a converter in comparison studies if the following points are taken into account.
 - a) The switching frequency should be the same.
 - b) The compared converters are assessed in the same operation point and power, or if they are not in the same operation point, the effect of power and voltage gain should also be considered.
 - c) If the converter is evaluated individually, the volume and weight of the heatsink(s) should also be calculated as a decisive factor; otherwise, if the converter is compared with others in the same power, the heatsink size and volume can be ignored. This is due to the approximately same characteristic of the utilized heatsinks in the NHSDCs if they are implemented in the same operation points and power. Note that ignoring the volume and size of the heatsink(s) does not lead to any physical meaning and it is only used as a comparison assumption to eliminate the thermal considerations and simplify the evaluation.
 - d) It is suggested to investigate the number of windings along with the number of magnetic cores.
- 6) Using multiwinding magnetics (coupled inductors, conventional transformers, and built-in transformers) increases the voltage gain of the NHSDCs. They add more degrees of freedom to the converter and result in high efficiency if the parasitic inductances energy is recycled.

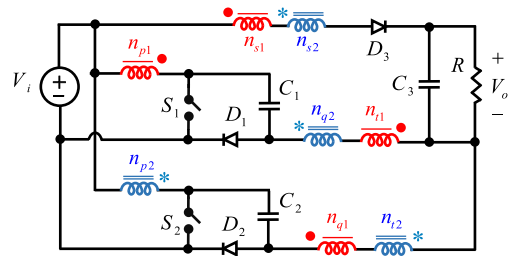


Fig. 5. Example of an NHSDC with a high number of windings [100].

However, the number of windings directly affects the magnetic cores' window size and, consequently, the converters' size and weight. According to Table I, the least number of windings is one, which is dedicated to the single-winding single-inductor converters [152], [168], [175], [212], [228]. Among these converters, [152], [168], and [175] are listed as the low-weight topologies in Table I. On the other hand, a two-phase topology with two active resonant tanks [46], a two-phase interleaved structure with two four-winding coupled inductors [100], and a multiphase resonant structure [214] have the most windings. As an example, Fig. 5 illustrates the employment of eight windings in an NHSDC to reach high output voltage gain [100]. From the application point of view, magnetic coupling has wide applications in renewable energies, microgrids, data centers, telecommunication, physics, high-power power supplies, and bidirectional topologies.

- 7) The converters in [178] and [180], and the converters in [46], [63], [174], [194], [214] have the least and the most capacitors, respectively. The least number of capacitors in [178] and [180] is due to relying on the active SI units to increase the output voltage level. On the other hand, the high number of capacitors is caused by a two-phase topology with two active resonant tanks [46], a high-order SC structure [63], a two-phase interleaved topology with separated SC cells [174], a two-phase interleaved topology with complicated SC units and a soft switching auxiliary circuit [194], and a multiphase resonant structure [214]. It should be noted that the input filter capacitor is not included in this count.
- 8) In some literature, total components count has been considered as a figure of merit to evaluate converters [11], [80], [84], [121], [143], [146], [177], [179], [237]. Nevertheless, it seems meaningless to add the counts of switches, diodes, magnetic cores, and capacitors since it is an unweighted components count (UCC) metric bearing no practical and physical concept.

Then, the critical question is: "Can components counts' reflect a meaningful and practical vision from a converter to be considered as reliable comparison metrics?" Based on the discussion, the answer is probably "No." The best promising solution to cope with this issue is to transform these components counts into some physical concepts. The most common physical metrics related to the components are cost [11], [80], [137], size [137], and weight, all of which are dependent on the frequency, power, operation

point, design safety margins, and printed circuit board (PCB) arrangement. With a closer look at the cost criterion, for a fair cost comparison of converters, the following conditions should be met.

- 1) The converters should be designed with the same power and switching frequency.
- 2) Since the quality of utilized components affects the final price, the converters should be designed with the same components and material types.
- 3) The voltage and current safety margins and thermal considerations of the components should be the same.
- 4) All converters have to be cooled with the same approach.
- 5) The price is dependent on the market and manufacturer; for instance, magnetic components are cheaper in some countries.
- 6) The operation region of the converters should be considered the same to reach similar operational features as input current and output voltage ripples (OVRs). From a logical point of view, it is clearly hard to satisfy the whole conditions simultaneously. The problem becomes even more challenging when you notice that each unique converter can be designed with various combinations of input voltage level, magnetic components turns ratio, duty cycle, switching frequency, and load to reach a certain power value, and these combinations result in different design, cost, volume, and weigh. Therefore, it looks like the conventional price comparison as a single-objective metric in the previous articles is not effective enough.

To solve this issue, the NHSDCs are redesigned under the same $D = 0.7$, $N = 3$, $f_S = 50$ kHz and components type (family) with dimensioning of the heatsink for the ambient temperature of 35°C . In addition, unique input current and OVRs are considered, where the results of cost, weight, volume, and voltage gain are tabulated in Table I. Note that the duty cycle is assumed as $D = 0.35$ for the impedance source converters. The parameter N is considered as the primary to the secondary winding turns ratio for [59], [72], [86], [98], [220], which is followed only in Table I of this article to have equal design and comparison assumptions. It is evident that this design condition leads to different power levels for the converters due to their distinct voltage gain. To compensate for this difference and eliminate the load value effect, two multiobjective metrics are suggested for the cost evaluation; the fractional gain-cost (FGC) function defined as “gain/cost,” and the subtractive gain-cost (SGC) function equal to “normalized gain-normalized cost.” However, normalization is not required for FGC. The metrics can be generalized by adding some coefficients (α_G and α_C) to strengthen the importance of each factor based on the application and other preferences as follows:

$$\text{FGC} = \frac{\alpha_G \hat{G}}{\alpha_C \text{Cost}}, \quad \text{SGC} = \alpha_G \hat{G} - \alpha_C \hat{\text{Cost}}. \quad (1)$$

The factors \hat{G} and $\hat{\text{Cost}}$ are the normalized forms of voltage gain and cost, respectively, which can be defined as the division of each converter voltage gain and cost by 1) the highest voltage gain and cost of the compared converters branch ($\hat{G} = G/G_{\max}$ and $\hat{\text{Cost}} = \text{Cost}/\text{Cost}_{\max}$) to make all of them ≤ 1 ; or 2) the corresponding voltage gain and cost of an individual converter

in the branch that the converter with G_{\max} or Cost_{\max} is the suitable candidate. Since two definitions of SGC lead to different ratings of the converters, an improved SGC (ISGC) is introduced with some modification in normalization as

$$\hat{G} = \frac{G - G_{\min}}{G_{\max} - G_{\min}}, \quad \hat{\text{Cost}} = \frac{\text{Cost} - \text{Cost}_{\min}}{\text{Cost}_{\max} - \text{Cost}_{\min}}. \quad (2)$$

The numerical results of FGC, SGC with $\hat{G} = G/G_{\max}$, and $\hat{\text{Cost}} = \text{Cost}/\text{Cost}_{\max}$, and ISGC are assessed in Table I with $\alpha_G = \alpha_C = 1$, where the ratings of the converters have some similarities in general. For instance, [36], [161], [184], [204], [213] and [50], [65], [86], [87], [109], [110], [112], [139], [148] are listed among the least and the most desired converters in three metrics, respectively. However, in a pair comparison of the converters with close operation characteristics, the results are different. As an example among many, [69] is more, more, and less cost-effective than [86] in FGC, SGC, and ISGC, respectively. The difference between these metrics is common and comes from the mathematical nature of the problem, in which fractional and subtractive functions with different normalization base values behave the voltage gain and cost metrics of FGC, SGC, and ISGC with different weights. In other words, all these three metrics are practically and mathematically correct, and the usage of each depends on the application and design interests. FGC is the simplest metric, which is known as cost-to-worth function, with no need for normalization. However, if FGC is considered as a criterion to select the optimized operation area of a converter, the solver might encounter difficulties in computing the first and the second derivatives. Moreover, the variation range of FGC is larger. On the other hand, SGC and ISGC lead to a well-defined optimization problem and the derivatives are calculated with less error. The base values for normalization and weight coefficients dramatically affect the final decision; therefore, their appropriate selection is a bit tricky.

With this definition, the same procedure can be followed for the weight and size metrics, where only the improved subtractive gain-weight (ISGW) and gain-size (ISGS) functions with coefficients of $\alpha_G = \alpha_W = \alpha_S = 1$ are presented in Table I. According to ISGW, the suggested converters in [36], [184], [227], [180], [39], [198], [149], [204], [231] and in [110], [112], [50], [109], [87], [66], [65], [109], [86], [78] are the least and the most preferred, respectively. In addition, the converters with the worst and the best ISGS are [184], [227], [184], [36], [180], [39], [198], [149], [204], [231] and [110], [112], [50], [109], [87], [66], [109], [65], [78], [146], respectively.

In order to evaluate more comprehensively, the multiobjective metrics of ISGC, ISGW, and ISGS can be combined in one metric, where the most practical suggestion is $\alpha_G \hat{G} - \alpha_C \hat{\text{Cost}} - \alpha_S \hat{\text{Size}}$. Since size and weight are not completely independent of each other, they are not used simultaneously in this function. Considering the aforementioned metric, the introduced converters in [110], [66], [37], [87], [76], [109], [95], [71] present the best performance, respectively.

2) *Unidirectional–Bidirectional Power Flow*: Generally, unidirectional or bidirectional power flow is not considered as a superiority for NHSDCs, and it is mainly selected based on the application. In industrial applications and academic research, most of the NHSDCs have been unidirectional topologies due

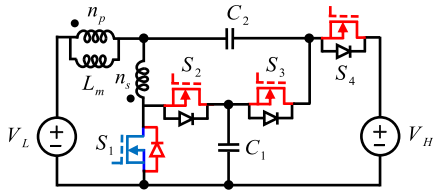


Fig. 6. Example of a bidirectional NHSDC [59]. (The components in blue, red, and black operate in step-up, step-down, and both directions, respectively).

to their high applications. These topologies consist of some switches and diodes, where the diodes are employed in a single-direction power flow mechanism. There is one exception in unidirectional topologies in which diodes are replaced by switches to reduce conduction loss. On the other hand, bidirectional NHSDCs, which are popular in storage systems, renewable energy-based systems, uninterruptable power supplies, transportation electrification, elevators, battery chargers, and smart grids, are implemented with switches (current-bidirectional semiconductors) instead of diodes. These growingly dominant topologies are identified in Table I (the column named BI), and Fig. 6 represents an example. They operate as the boost and buck converters in the forward (FW) and reverse power flow, respectively. There are two exceptions in which diodes are also used in the bidirectional NHSDCs: 1) as snubber or clamp circuit components [133], [136], [137], [213], and 2) as components operate only in one power transfer direction [145], [229]. Based on Table I, the highest number of switches belongs to the bidirectional converters: a bidirectional converter with an active resonant network in [204], a three-phase interleaved bidirectional converter in [205], and a bidirectional converter with an SC cell and a quasi-Z-source (ZS) network in [237]. Moreover, [110] and [204] are the most and the least preferred bidirectional topologies, respectively, from the ISGC, ISGW, and ISGS points of view. The bidirectional converters are more popular in multiport converters with various types of sources, loads, and energy storage links. Meanwhile, they encounter the following challenges or drawbacks in design and operation.

- 1) The high number of active switches increases their cost and control complexity.
 - 2) Their power flow control in multiport structures needs more sensors and more complicated algorithms.
 - 3) Since the time period of reverse regenerative power transfer is usually short and uncontrolled in the applications, such as battery chargers and electric vehicles (EV)s, the converter components should be designed for higher voltage and current ratings than the ratings required for the FW power direction.
 - 4) The dynamic of shifting between operation scenarios, such as charging, load power consumption, and regeneration, is challenging.
- 3) *Current Fed (CF)–Voltage Fed (VF)*: Based on the inductive or capacitive input filter of a dc–dc converter, it is defined as a CF or a VF topology, respectively, which specifies the applications of each. Note that by ignoring some special and

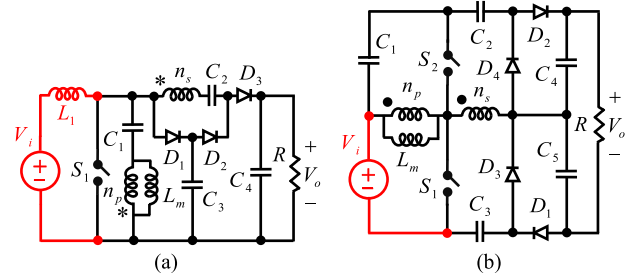


Fig. 7. Examples of NHSDCs, based on the input port feeding type. (a) CF [33]. (b) VF [22].

limited types of converters, the reciprocity theorem in electrical circuitry necessitates the input CF and VF converters to contain a capacitive and an inductive output filter, respectively. Fig. 7 illustrates two examples of CF and VF topologies. Since the current source is not built in the real world, it is modeled through the series connection of a voltage source and an inductor, where the inductor should be designed meticulously enough. The CF topologies are intrinsically boost converters, ignoring the effect of VMCs and magnetic components turns ratio, that makes them suitable for high-voltage direct current (HVdc), X-ray devices, radar, dc microgrids, electric transportation, and low-voltage renewable energy applications such as FC and PV. Nevertheless, their dynamic response is slow due to right-half-plane zero.

On the other hand, the VF topologies are intrinsically buck converters, have fast dynamic response, operate without any right-half-plane zero, do not tolerate shoot-through conditions, and are appropriate for low-power applications. It should be noticed that there are some NHSDCs with the basic structure of a boost converter and an input CF configuration; however, by adding some switching VMCs [14], [22], [24], [29], [35], [37], [40], [63], [66], [95], [113], [116], [135], [158], clamp circuits [107], [125], [130], soft switching cells [169], and impedance networks [225] to the input port, the converter is reformed to a VF topology. This type of VF converters (see Fig. 7(b) as an example) still keeps the voltage boost characteristic of the basic CF topology, which is reflected in their voltage gain equations.

Continuous input current helps the CF converters to extract the input source power uninterruptedly and operate with a large range of soft switching, wide input voltage variation, and high efficiency. However, the input capacitive filter should be designed very properly to save the input energy in discontinuous input current intervals of the VF converters. Table II categorizes the NHSDCs due to their input filter in the input fed (IF) column. According to Tables I and II, the suggested CF converters in [110] and [36] present the best and the worst results, respectively, with regard to ISGC. The corresponding ratings are assigned to [66] and [198] in the VF topologies, respectively. The additional results for ISGW and ISGS are tabulated in Table III.

- 4) *Input Current Ripple (ICR)*: Low ICR is required for some types of power sources, such as renewable energies. In order to evaluate the ICR characteristic of NHSDCs, the converters are categorized into seven groups with the ratings of “A” (very

TABLE II
CLASSIFICATION OF NHSDCS ACCORDING TO ICR, INPUT PORT FEEDING TYPE (IF), AND GND

Ref	ICR	IF	GND	Ref	ICR	IF	GND	Ref	ICR	IF	GND	Ref	ICR	IF	GND
[11]	D	CF	CG	[71]	F	CF	CG	[130]	G	VF	FG	[184]	B	CF	CG
[12]	D	CF	CG	[72]	F	VF	CG	[131]	B	CF	FG	[185]	B	CF	FG
[12]	F	CF	CG	[73]	C	CF	CG	[132]	C	CF	CG	[186]	D	CF	FG
[13]	B	CF	CG	[74]	F	VF	CG	[132]	C	CF	CG	[187]	G	VF	FG
[14]	G	VF	CG	[74]	F	VF	CG	[133]	F	CF	CG	[188]	E	VF	FG
[15]	F	VF	CG	[74]	F	VF	CG	[134]	D	CF	CG	[189]	E	VF	FG
[16]	C	CF	CG	[75]	F	CF	CG	[135]	G	VF	CG	[190]	D	CF	CG
[17]	D	CF	CG	[76]	F	CF	CG	[136]	F	CF	CG	[191]	E	VF	CG
[18]	A	CF	CG	[77]	C	CF	FG	[137]	F	CF	CG	[192]	D	CF	CG
[18]	A	CF	CG	[78]	F	VF	CG	[138]	F	CF	CG	[193]	D	CF	FG
[19]	C	CF	CG	[78]	F	VF	CG	[139]	D	CF	CG	[193]	D	CF	FG
[20]	C	CF	CG	[79]	F	VF	CG	[140]	G	VF	CG	[194]	D	CF	FG
[21]	F	CF	CG	[80]	F	VF	FG	[141]	G	VF	FG	[195]	D	CF	CG
[22]	G	VF	FG	[81]	C	CF	FG	[142]	F	CF	CG	[196]	G	VF	CG
[23]	D	CF	CG	[82]	C	CF	CG	[143]	D	CF	CG	[197]	D	CF	CG
[24]	G	VF	CG	[83]	F	CF	CG	[144]	D	CF	CG	[198]	E	VF	FG
[25]	B	CF	CG	[84]	F	VF	CG	[145]	C	CF	CG	[199]	D	CF	CG
[26]	G	VF	FG	[85]	C	CF	CG	[146]	F	CF	CG	[200]	G	VF	CG
[27]	G	VF	CG	[86]	D	CF	CG	[147]	F	CF	CG	[201]	E	VF	CG
[28]	F	CF	CG	[87]	F	CF	CG	[148]	F	CF	CG	[202]	D	CF	CG
[29]	G	VF	CG	[88]	F	CF	CG	[149]	E	CF	FG	[203]	D	CF	CG
[30]	F	CF	FG	[88]	F	CF	CG	[150]	B	CF	FG	[204]	D	CF	CG
[31]	F	CF	CG	[89]	D	CF	CG	[150]	B	CF	FG	[205]	A	CF	FG
[32]	C	CF	CG	[90]	D	CF	CG	[151]	B	CF	CG	[206]	A	CF	CG
[33]	D	CF	CG	[91]	D	CF	CG	[151]	B	CF	CG	[207]	D	CF	CG
[34]	C	CF	CG	[92]	F	VF	FG	[152]	D	CF	FG	[208]	B	CF	CG
[35]	G	VF	CG	[93]	G	VF	FG	[153]	D	CF	FG	[209]	D	CF	CG
[36]	C	CF	CG	[94]	F	VF	FG	[154]	D	CF	CG	[210]	B	CF	CG
[37]	F	VF	CG	[95]	G	VF	FG	[155]	G	VF	FG	[211]	B	CF	CG
[38]	G	VF	CG	[96]	E	VF	FG	[156]	B	CF	FG	[212]	D	CF	CG
[39]	B	CF	CG	[97]	D	CF	CG	[157]	B	CF	FG	[213]	D	CF	CG
[40]	G	VF	CG	[98]	B	CF	CG	[158]	E	VF	FG	[214]	A	CF	FG
[41]	G	VF	CG	[99]	C	CF	CG	[159]	D	CF	CG	[215]	G	VF	CG
[42]	C	CF	CG	[100]	E	VF	FG	[159]	D	VF	CG	[216]	E	VF	CG
[43]	C	CF	FG	[101]	E	VF	FG	[159]	G	VF	CG	[217]	G	VF	CG
[44]	C	CF	FG	[102]	C	CF	CG	[160]	D	CF	CG	[218]	G	VF	FG
[45]	F	VF	CG	[103]	F	VF	FG	[161]	A	CF	FG	[219]	E	VF	CG
[46]	C	CF	CG	[104]	D	CF	CG	[162]	B	CF	FG	[220]	D	CF	CG
[47]	C	CF	CG	[105]	D	CF	CG	[163]	F	CF	CG	[221]	D	CF	CG
[47]	C	CF	CG	[106]	G	VF	CG	[164]	B	CF	FG	[222]	D	CF	CG
[48]	G	VF	CG	[107]	F	VF	CG	[164]	B	CF	FG	[223]	G	VF	CG
[49]	D	CF	CG	[108]	F	CF	CG	[164]	A	CF	FG	[224]	F	CF	CG
[50]	F	CF	CG	[109]	F	CF	CG	[165]	E	VF	FG	[225]	E	VF	FG
[51]	G	VF	FG	[109]	F	CF	CG	[166]	B	CF	FG	[226]	D	CF	FG
[52]	F	CF	FG	[110]	C	CF	CG	[167]	B	CF	CG	[227]	G	VF	FG
[53]	G	VF	CG	[111]	F	CF	FG	[168]	G	VF	CG	[228]	D	CF	CG
[54]	C	CF	CG	[112]	D	CF	CG	[169]	E	VF	CG	[229]	G	VF	FG
[55]	D	CF	CG	[113]	F	VF	CG	[170]	E	CF	FG	[230]	G	VF	CG
[56]	G	VF	FG	[114]	E	VF	CG	[171]	B	CF	CG	[231]	D	CF	FG
[57]	D	CF	CG	[114]	E	VF	CG	[172]	A	CF	CG	[232]	G	VF	CG
[57]	D	CF	CG	[115]	D	CF	CG	[173]	B	CF	CG	[233]	D	CF	CG
[57]	D	CF	CG	[116]	E	VF	CG	[174]	B	CF	FG	[234]	D	CF	CG
[58]	C	CF	CG	[117]	D	CF	CG	[175]	D	CF	CG	[235]	G	VF	FG
[59]	F	CF	CG	[118]	C	CF	CG	[176]	E	VF	FG	[236]	G	VF	CG
[60]	F	VF	CG	[119]	C	CF	FG	[177]	G	VF	CG	[237]	D	CF	CG
[61]	F	CF	CG	[120]	F	CF	FG	[178]	E	VF	FG	[238]	E	VF	CG
[62]	F	VF	CG	[121]	D	CF	CG	[178]	E	VF	FG	[238]	E	VF	CG
[63]	F	VF	CG	[122]	F	CF	CG	[178]	E	VF	FG	[238]	E	VF	CG
[64]	C	CF	FG	[123]	F	VF	CG	[179]	E	VF	FG	[239]	D	CF	CG
[65]	C	CF	CG	[124]	F	CF	CG	[180]	E	VF	FG	[240]	D	CF	FG
[66]	F	VF	CG	[125]	F	VF	CG	[180]	E	VF	FG	[240]	D	VF	FG
[67]	F	CF	CG	[126]	F	VF	CG	[181]	B	CF	FG	[241]	D	CF	CG
[68]	D	CF	CG	[127]	G	VF	FG	[182]	D	CF	FG				
[69]	C	CF	CG	[128]	D	CF	CG	[183]	G	VF	FG				
[70]	C	CF	FG	[129]	F	VF	FG	[184]	B	CF	CG				

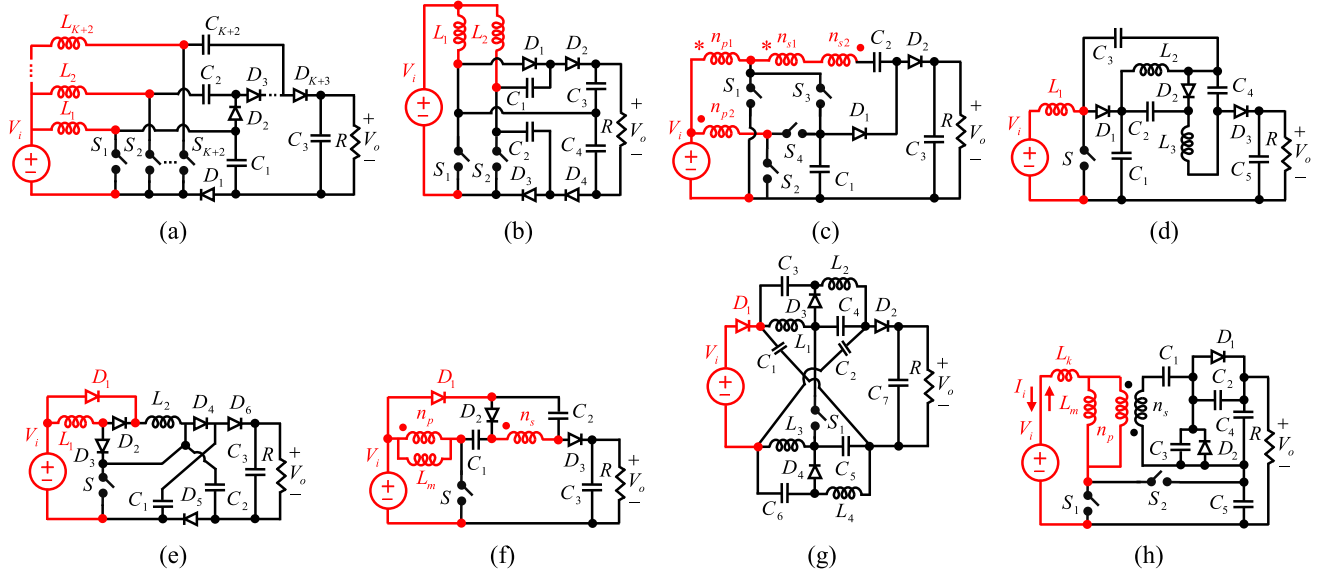


Fig. 8. Examples of NHSDCs according to the ICR groups. (a) A [164]. (b) B [185]. (c) C [42]. (d) D [190]. (e) E [158]. (f) F [37]. (g) G [227]. (h) G [27].

TABLE III
EVALUATION OF NHSDCs IN EACH CATEGORY ACCORDING TO THE ISGC, ISGW, AND ISGS RESULTS

Categories		ISGC	ISGW	ISGS
Current fed	Highest	[110]	[110]	[110]
	Lowest	[36]	[36]	[184]
Voltage fed	Highest	[66]	[66]	[66]
	Lowest	[198]	[227]	[227]
Common ground	Highest	[110]	[110]	[110]
	Lowest	[36]	[36]	[184]
Floating ground	Highest	[95]	[52]	[52]
	Lowest	[198]	[227]	[227]
Single-stage	Highest	[66]	[109]	[109]
	Lowest	[180]	[227]	[227]
Multistage	Highest	[112]	[112]	[112]
	Lowest	[213]	[213]	[213]
Interleaved	Highest	[110]	[110]	[110]
	Lowest	[36]	[36]	[184]
Multilevel	Highest	[86]	[86]	[28]
	Lowest	[184]	[184]	[184]
Switched capacitor	Highest	[65]	[66]	[66]
	Lowest	[184]	[184]	[184]
Switched inductor	Highest	[187]	[101]	[101]
	Lowest	[198]	[180]	[180]
SCI	Highest	[112]	[112]	[112]
	Lowest	[46]	[149]	[149]
With snubber or clamp	Highest	[65]	[109]	[109]
	Lowest	[36]	[36]	[36]
Unidirectional	Highest	[112]	[112]	[112]
	Lowest	[36]	[36]	[184]
Bidirectional	Highest	[110]	[110]	[110]
	Lowest	[204]	[204]	[204]

low) to “G” (very high), which are expressed in Table II. These groups are dedicated to: extended interleaved CF topologies (A), interleaved CF topologies (B), interleaved structures with an input coupled inductor or an FL operation (C), single-phase topologies with a single input inductor (D), VF converters with a parallel input inductive power path (E), single-phase structures

with an input coupled inductor or an FL operation (F), and VF topologies with discontinuous or partially negative input current (G). To clarify this classification, some examples are shown in Fig. 8. Regarding the categorization, interleaving is the most desired and applicable methodology to reduce ICR which features n times switching frequency in the input current for n phases [105], phase shift between the corresponding waveforms of phases, lower components current stress, easier demagnetization of the coupled inductors between phases [13], improved magnetic performance [16], [20], [32], [46], and usually lower OVR. Note that if the input inductors of two interleaved stages are coupled with each other, the ICR of the windings in-phase voltages configuration (dotted points on the same side) is less than the out-of-phase condition.

5) *Grounding (GND)*: Common ground (CG) between input and output ports is usually preferred in NHSDCs due to easier switch gate driving, output voltage measurement, and feedback system implementation, especially in motor drives, PVs, and EVs. In addition, parasitic components and electromagnetic interference (EMI) are coped better in CG topologies. However, there are still industrial applications, such as power supplies with floating ground (FG) structures, which are usually resulted from the presence of a voltage quadrupler [22], [43], a VMC [26], [52], [70], [77], [157], a voltage doubler [30], [81], [96], [120], [130], [141], a soft switching cell [44], [92], an SC [150], [152], [153], [155], [156], [158], [161], an SI [51], [93], [101], an SCI [56], [64], [94], [95], [111], [119], [127], [131], [149], an SC and an SI [80], [165], [176], [187], [188], [198], and a coupled inductor [100], [103], [129]. In this article, the NHSDCs are investigated, and they are categorized according to their common or FG structure in Table II. Furthermore, the results of ISGC, ISGW, and ISGS are presented in Table III.

6) *Stages*: Besides single-stage (SS) configurations with various types of VMCs or (and) magnetic coupling, the combination

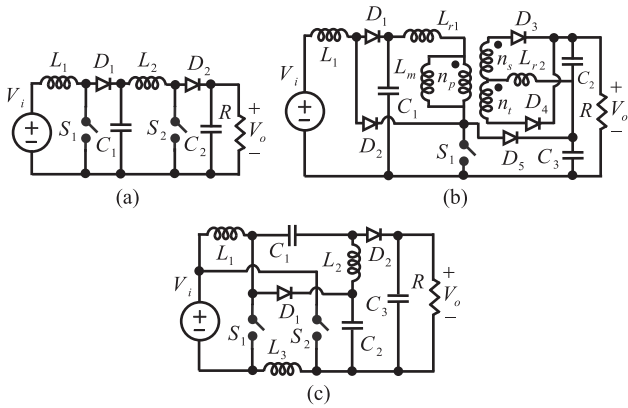


Fig. 9. Examples of multistage (cascaded) NHSDCs. (a) Two-stage cascaded boost converter. (b) Integrated structure [68]. (c) Integrated structure with more than one switch [189].

of two or more voltage boosting modules/converters in different connection styles has been an attractive approach to achieve high voltage gain and power values in NHSDCs. The most common connection styles are multistage, interleaving, and multilevel methods, where even more than one method can be employed simultaneously. Although the components count, cost, weight, and size are increased in these configurations, they provide some helpful capabilities. HVDC, renewable energies, high-power microgrids, high-power power supplies, X-ray devices, and electrified transportation are some of their applications. In the following, some features of the aforementioned connection styles are elaborated.

- 1) **Multistage:** This type of voltage boosting technique, usually called cascading, is employed by the series connection of identical or different step-up converters. The simplest topology for this category is realized by the combination of two conventional PWM boost converters, where the output port of the first is connected to the input port of the second converter [see Fig. 9(a)]. This converter, called a two-stage cascaded boost converter, can be extended to more cascaded stages; however, the total efficiency of the converter decreases due to the multiplication of the converters' efficiency by each other. One straightforward approach to suppress low-efficiency drawback is to drive the first low-voltage stage with high frequency and the second high-voltage stage with low frequency, where solving an optimization problem leads to the best results for switching frequency values with optimized efficiency, size, weight, cost, ripples, dynamics, and reliability. The serious obstacle with this solution relates to its more complicated control unit. Moreover, the problems with system stability and high output rectifier diode's reverse recovery loss remain [1].

The other solution is to integrate the cascaded converters, which decreases the number of switches [see Fig. 9(b)]. These high-voltage low-power integrated converters, which are divided into some groups such as hybrid cascaded [17], [193], quadratic [55], [68], etc., provide wider output voltage range,

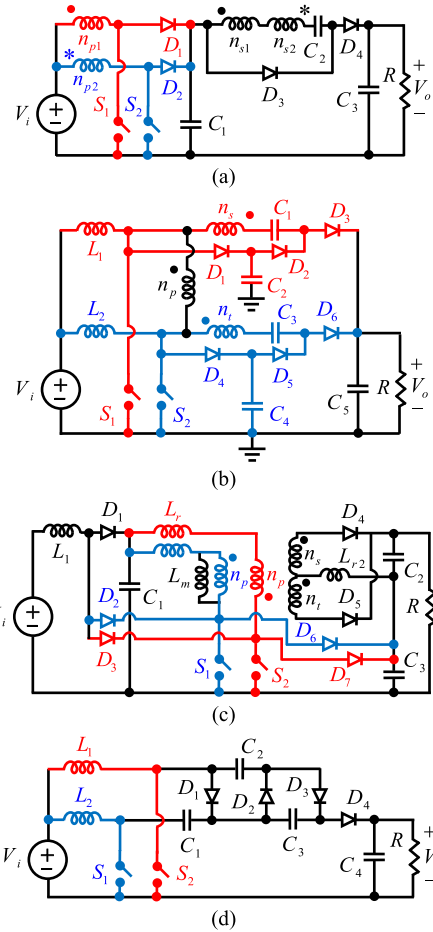


Fig. 10. Examples of interleaved NHSDCs with (a) common VMC [20], (b) separated VMCs [25], (c) interleaving in the input port of the second stage in a two-stage cascaded converter [105], and (d) integrated VMC [151].

higher output voltage sensitivity with respect to the duty cycle, easier passive components design procedure, less EMI, less passive components count, less instability, and smaller size. Nevertheless, they suffer from high current and voltage stress on the main switch and output rectifier diode(s), respectively. Moreover, the switches in the integrated converters with more than one switch cannot be driven independently [see Fig. 9(c)] [189]. Note that the connected converters in the NHSDC multistage configuration can also be a step-up inverter and a voltage multiplier rectifier in the first and second stages, respectively [154].

- 2) **Interleaving:** High input current and its high ripple are the main challenges in high-voltage high-power NHSDCs, which make the input port components' design harder and size larger. To overcome these issues, interleaving has been being suggested with a parallel connection of two or more identical converters in the input port, which can be extended to the output port. Fig. 10 demonstrates some examples of interleaved converters, where Fig. 10(a)–(d) shows interleaved topologies: in the input port with a common VMC [20], in the input and output ports with separated VMCs [25], in the input port of the second stage in a

two-stage cascaded converter [105], and with an integrated VMC [151], respectively. Interleaving: helps to satisfy low reverse recovery loss of converter diodes and low dc flux in the magnetic cores if the input inductors are coupled [1], [18], [20], [25], [32], [39], [42], [46], [54]; increases power density [42], [58]; increases the input current frequency with multiplying each branch frequency by the number of interleaved branches [105]; usually enhances converter reliability [242]; usually helps to recycle the magnetics' leakage energy; provides modularity capability of increasing converter power with acceptable efficiency values [18], [19]; realizes wide operation range; decreases the passive components size; enhances transient response; and decentralizes the power loss heat [1]. On the other hand, identical implementation of the corresponding components, input current sharing, more limited duty cycle range, control difficulties, symmetrical operation of branches, utilization of more components, high cost, and usually high output voltage sensitivity are the main challenges.

3) *Multilevel*: As a common and practical solution for high voltage stress on the output port components while satisfying high voltage gain, multilevel structures have been suggested. These high-voltage high-power topologies are realized by the series connection of modules' output ports to achieve low proportional voltage stress of output port components (especially rectifier diodes and capacitors) according to the high total output voltage. Multilevel structures decrease the converters dependence on the magnetic components, which leads to lower weight and EMI. Their variation is from two- or three-level stacked configurations [12], [68], [147] to extendable modular converters [18], [19], [150], [153], [166], [202], where modular structures present high fault tolerance (reliability) behavior. On the other hand, their output voltage regulation is hard since the ground node is not accessible to all output ports. Unlike SS converters with a lower number of high-voltage output port components, the modular multilevel topologies have more low-voltage and cheap components, for which a multiobjective optimization problem should be defined and solved based on the application requirements to achieve an optimized number of levels. One very popular configuration of the multilevel structures is the conventional three-level boost converter that has been developed with regard to the voltage spikes, efficiency, and voltage gain [127]. Fig. 11 expresses two examples of multilevel converters.

According to the discussion, the NHSDCs are classified into four groups in Table IV with regard to their stages. It is worth mentioning that, in some literature, multistage and interleaving [206], multistage and multilevel [17], [57], [68], [84], [88], [92], [94], [97], [120], [128], [139], [147], interleaving and multilevel [16], [18], [19], [44], [64], [70], [73], [77], [81], [85], [96], [107], [132], [149], [150], [157], [162], [166], [167], [174], [184], [185], [194], [205], and all of the three styles [105], [211] are utilized simultaneously. In addition, the best and the worst performances of these connection

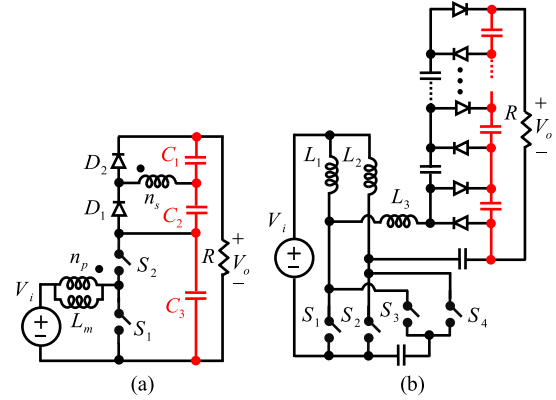


Fig. 11. Examples of multilevel NHSDCs. (a) Stacked structure [12]. (b) Extendable structure [150].

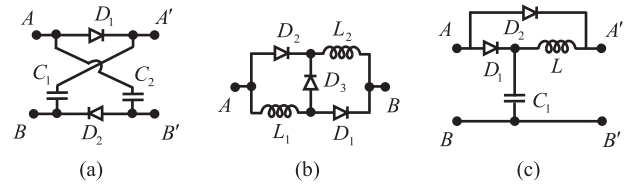


Fig. 12. Basic switched networks. (a) SC. (b) SI. (c) SCI.

styles are presented with respect to ISGC, ISGW, and ISGS in Table III.

7) *Switched Capacitor and Switched Inductor Cells: Features and Drawbacks*: One theoretically simple but harder-to-implement technique for voltage boosting is replacing the inductor and the capacitor of conventional boost converters with various types and levels of SIs and SCs, respectively. The reason for this nomination, SI and SC, is their operation principle with charging and discharging of only inductors and only capacitors by changing the configuration of these networks through some switching semiconductors, respectively. A well-known technique for this purpose is to charge and discharge the inductors or capacitors in parallel and in series, respectively, to enhance the input voltage to higher levels [80], [93], [101], [165], [187], [198]. Fig. 12(a) and (b) illustrates the basic SI and SC networks, respectively. The most significant points about SI and SC structures are summarized as follows.

- 1) Regardless of different nominations such as charge pump [143], [156], voltage lift [99], self-lift, VMC [20], [21], [25], [32], [33], [58], [75], [82], [94], [97], voltage multiplier rectifier [22], ladder cell [168], voltage doubler [30], [81], [96], [120], [130], [141], and voltage quadrupler [22], [43] in previous literature, any network with capacitors and semiconductors to increase the voltage level is uniformly named SC in this article. The same rule is also followed for the SIs, the networks with inductors, and semiconductors.
- 2) Due to the capacitive power transfer in the SC circuits and no need for magnetic cores, their weight and cost

TABLE IV
NHSDCs ACCORDING TO THEIR STAGES (SS: SINGLE STAGE; MS: MULTISTAGE; INT: INTERLEAVED; ML: MULTILEVEL)

Ref	SS	MS	INT	ML	Ref	SS	MS	INT	ML	Ref	SS	MS	INT	ML	Ref	SS	MS	INT	ML
[11]	✓				[71]	✓				[130]	✓				[184]				✓
[12]				✓	[72]				✓	[131]			✓		[185]			✓	✓
[12]				✓	[73]			✓	✓	[132]			✓	✓	[186]		✓		
[13]			✓		[74]	✓				[132]			✓	✓	[187]	✓			
[14]	✓				[74]	✓				[133]		✓			[188]		✓		
[15]				✓	[74]	✓				[134]	✓				[189]		✓		
[16]			✓	✓	[75]		✓			[135]	✓				[190]	✓			
[17]		✓		✓	[76]	✓				[136]		✓			[191]	✓			
[18]			✓	✓	[77]			✓	✓	[137]	✓				[192]				✓
[18]			✓	✓	[78]	✓				[138]	✓				[193]		✓		
[19]			✓	✓	[78]	✓				[139]		✓		✓	[193]		✓		✓
[20]			✓		[79]		✓			[140]	✓				[194]			✓	✓
[21]				✓	[80]	✓				[141]	✓				[195]				✓
[22]				✓	[81]			✓	✓	[142]	✓				[196]	✓			
[23]				✓	[82]			✓		[143]	✓				[197]		✓		
[24]	✓				[83]	✓				[144]		✓			[198]				✓
[25]			✓		[84]		✓		✓	[145]			✓		[199]	✓			
[26]	✓				[85]			✓	✓	[146]	✓				[200]		✓		
[27]				✓	[86]				✓	[147]		✓		✓	[201]	✓			
[28]				✓	[87]	✓				[148]	✓				[202]				✓
[29]	✓				[88]		✓		✓	[149]			✓	✓	[203]				✓
[30]				✓	[88]		✓		✓	[150]			✓	✓	[204]				✓
[31]				✓	[89]	✓				[150]			✓	✓	[205]			✓	✓
[32]			✓		[90]	✓				[151]			✓		[206]		✓	✓	
[33]	✓				[91]		✓			[151]			✓		[207]		✓		
[34]			✓		[92]		✓		✓	[152]	✓				[208]			✓	
[35]	✓				[93]		✓			[153]				✓	[209]				✓
[36]			✓		[94]		✓		✓	[154]		✓			[210]			✓	
[37]	✓				[95]			✓	✓	[155]	✓				[211]		✓	✓	✓
[38]				✓	[96]			✓	✓	[156]			✓		[212]	✓			
[39]			✓		[97]		✓		✓	[157]			✓	✓	[213]		✓		
[40]				✓	[98]			✓		[158]	✓				[214]			✓	
[41]				✓	[99]			✓		[159]		✓			[215]		✓		
[42]			✓		[100]			✓		[159]		✓			[216]	✓			
[43]			✓		[101]	✓				[159]		✓			[217]	✓			
[44]			✓	✓	[102]			✓		[160]		✓			[218]	✓			
[45]	✓				[103]		✓			[161]	✓				[219]	✓			
[46]			✓		[104]			✓		[162]			✓	✓	[220]		✓		✓
[47]			✓		[105]		✓	✓	✓	[163]			✓		[221]		✓		✓
[47]			✓		[106]	✓				[164]			✓		[222]		✓		
[48]	✓				[107]			✓	✓	[164]			✓		[223]	✓			
[49]	✓				[108]	✓				[164]			✓		[224]				✓
[50]		✓			[109]	✓				[165]	✓				[225]		✓		
[51]	✓				[109]	✓				[166]			✓	✓	[226]		✓		
[52]	✓				[110]			✓		[167]			✓	✓	[227]	✓			
[53]				✓	[111]				✓	[168]	✓				[228]	✓			
[54]			✓		[112]		✓			[169]	✓				[229]		✓		
[55]		✓			[113]	✓				[170]			✓		[230]	✓			
[56]	✓				[114]		✓			[171]			✓		[231]				✓
[57]		✓			[114]		✓			[172]			✓		[232]				✓
[57]		✓			[115]	✓				[173]			✓		[233]	✓			
[57]		✓		✓	[116]	✓				[174]			✓	✓	[234]				✓
[58]			✓		[117]			✓	✓	[175]	✓				[235]				✓
[59]	✓				[118]			✓		[176]		✓			[236]	✓			
[60]		✓			[119]			✓	✓	[177]	✓				[237]	✓			
[61]				✓	[120]		✓		✓	[178]	✓				[238]	✓			
[62]		✓			[121]	✓				[178]	✓				[238]	✓			
[63]	✓				[122]	✓				[178]	✓				[238]	✓			
[64]			✓	✓	[123]		✓		✓	[179]				✓	[239]	✓			
[65]			✓		[124]		✓			[180]	✓				[240]	✓			
[66]	✓				[125]	✓				[180]	✓				[240]	✓			
[67]	✓				[126]	✓				[181]			✓		[241]		✓		
[68]		✓		✓	[127]			✓	✓	[182]									
[69]			✓		[128]		✓		✓	[183]		✓		✓					
[70]			✓	✓	[129]		✓			[184]			✓	✓					

are relatively lower, and they encounter less EMI issues [154], [159], [162]. However, since the power density in an electric field is less than a magnetic field, SCs present less power density. To overcome this obstacle, higher switching frequency is suggested provided that the switching losses and spikes are suppressed.

3) The SC and SI circuits have the capability of cascading, integration, and modularity, all of which help to increase their voltage gain to very high values in much higher orders of stages and levels theoretically. However, these values are unachievable in practice due to higher power loss, especially in the components with higher voltage

stress. Thus, efficiency restricts increasing the number of modules, and a cooptimization is required to find the best order with regard to efficiency and voltage gain.

- 4) Since the inductors of an SI network are in series at least in one switching mode, they should be implemented similarly to prevent any freewheeling current and power loss. This makes the prototyping of the network more difficult and sensitive to the components values, which happens in the parallel connection of capacitors too.
- 5) In all types of SCs, such as voltage doubler and quadrupler, Dickson, Makowski, Greinacher, and Cockcroft–Walton circuits, the more the network stages order, the higher the voltage gain. However, the voltage increment profile can be linear, exponential, or in a Fibonacci series sequence.
- 6) By using coupled inductors in SI networks, the voltage gain is improved, the number of magnetic cores and weight are decreased, the design is more flexible with the tunable coupled inductor turns ratio, the diodes reverse recovery issue may be mitigated, and usually the core leakage energy is recycled. However, it makes the EMI, switching voltage spikes, and thermal design more challenging.
- 7) A high current spike in switching transitions or inrush current is another challenge in SCs, which reduces the efficiency and power density dramatically, and prevents the network extension to higher orders. This obstacle is worsened in high nominal current values; hence, SCs are desired for high-voltage low-power applications, and the placement is close to the output low-current port. One common solution is to add one or more power or resonant inductors to the SCs to decrease switching power loss while increasing voltage gain [23], [78]. The same procedure can be repeated for the SI networks by adding one or more capacitors, which leads to more power transfer rate, voltage gain, and efficiency simultaneously. In this article, the switching networks consisting of capacitors, inductors, and semiconductors are named SCI, where an example is expressed in Fig. 12(c).
- 8) Clamp [36], [38], [86], [127], soft switching [11], [18], [22], [46], [48], [128], [130], soft charging, and snubber [55], [143], [173], [212], [213], [222] circuits are usually used to suppress high voltage stress, current spikes, and power loss on converter semiconductors.
- 9) Adding a small resonant inductor to some SC cells results in zero current switching (ZCS) condition for the switching devices [20], [25], [31], [32], which enables them to operate with higher switching frequency and power density [3].
- 10) It is suggested to locate the VMCs after the main switch (between the switch and high-voltage output port) to decrease the voltage stress across it; meanwhile, it results in higher current stress through the same switch paper [16] [21], [24], [33], [34], [39], [40], [41], [42], [43], [54], [65], [66], [77], [151], [158]. Note that lower voltage and higher current stresses lead

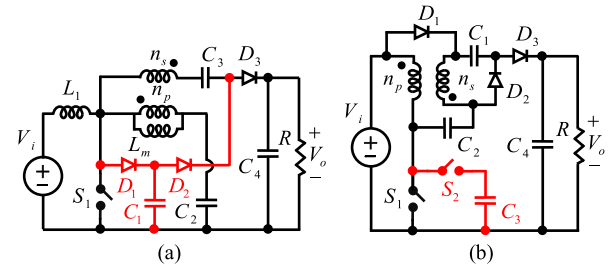


Fig. 13. Examples of auxiliary circuits. (a) Snubber [143]. (b) Active clamp [38].

to more variety of switches choice with less drain-source resistance, which may reduce the switch power loss and the stored energy in the internal parallel capacitor.

- 11) Although using high-order SC, SI, and SCI cells enhances the converter voltage gain, it increases the number of passive and active components. Based on Table I, the highest counts of switches, diodes, inductors, and capacitors are allocated, respectively, to a bidirectional SC-based topology [237], two-phase interleaved topologies with two or three SC and SCI units [69], [85], [174], a two-phase interleaved topology with Dickson SC cells and soft switching auxiliary circuits [194], and a two-phase topology with two active resonant tanks and an SCI unit [46].

In this article, the NHSDCs are checked and the usage of SC, SI, and SCI cells is identified in Table V, where the SC-, SI-, and SCI-based converters with the highest and the lowest ISGC, ISGW, and ISGS are also presented in Table III. According to Table V, most of the converters use these switching techniques where some topologies such as [51], [77], [78], [80], [101], [115], [160] employ two techniques simultaneously. The results of Tables I and V express that there is not a meaningful correlation between using two techniques and ISGC, ISGW, and ISGS metrics. In other words, these converters spread from high to low ISGC, ISGW, and ISGS values.

8) *Snubber and Clamp Circuits*: Using snubber and clamp circuits is a well-known approach to suppress voltage stress [11], [12], [14], [15], alleviate current spikes [25], recycle leakage energy [20], [22], [42], decrease switching loss [13], [16], [22], and improve efficiency and power density [24]. These circuits are divided into active (with switch) and passive (without switch) topologies. Since the aim of this article is not focusing on the types and operation principles of these circuits, they are not studied in detail. Meanwhile, as an important point among many, their regenerative operation increases the total efficiency by transferring the stored energy of their passive components, the clamp capacitor as an example, to the output port efficiently [11]. This type of circuit is sometimes named a lossless clamp or snubber. Fig. 13(a) and (b) demonstrates two examples of snubber and clamp circuits, respectively. In addition, the converters with these auxiliary circuits are listed in Table VI in which the letters “P” and “A” represent passive and active types,

TABLE V
NHSDCs ACCORDING TO THE USAGE OF SWITCHED NETWORKS (SC: SWITCHED CAPACITOR; SI: SWITCHED INDUCTOR, SCI: COMBINED SWITCHED CAPACITOR AND INDUCTOR)

Ref	SC	SI	SCI	Ref	SC	SI	SCI	Ref	SC	SI	SCI	Ref	SC	SI	SCI	Ref	SC	SI	SCI
[11]			✓	[58]			✓	[106]	✓			[153]	✓			[195]			✓
[12]	✓			[59]			✓	[107]	✓			[154]	✓			[196]			✓
[12]	✓			[60]			✓	[108]				[155]	✓		✓	[197]			✓
[13]		✓		[61]			✓	[109]	✓			[156]	✓			[198]	✓	✓	
[14]			✓	[62]				[109]				[157]	✓			[199]			✓
[15]				[63]			✓	[110]				[158]	✓		✓	[200]			
[16]	✓			[64]			✓	[111]				[159]	✓			[201]			✓
[17]				[65]	✓		✓	[112]				[159]	✓	✓		[202]			
[18]				[66]	✓			[113]	✓			[159]	✓			[203]			
[18]				[67]			✓	[114]				[160]	✓		✓	[204]			
[19]	✓			[68]				[114]				[161]	✓			[205]			
[20]			✓	[69]	✓		✓	[115]	✓			[162]	✓			[206]	✓		
[21]	✓			[70]	✓			[116]				[163]	✓			[207]			
[22]	✓			[71]			✓	[117]	✓			[164]	✓			[208]			
[23]			✓	[72]			✓	[118]				[164]	✓			[209]			
[24]	✓			[73]			✓	[119]				[164]	✓			[210]			
[25]			✓	[74]			✓	[120]	✓			[165]	✓	✓		[211]			
[26]	✓			[74]			✓	[121]	✓			[166]	✓			[212]			
[27]	✓			[74]			✓	[122]				[167]	✓			[213]			
[28]			✓	[75]	✓			[123]				[168]	✓			[214]			
[29]			✓	[76]			✓	[124]				[169]	✓			[215]			
[30]	✓			[77]	✓		✓	[125]	✓			[170]	✓			[216]			
[31]			✓	[78]	✓		✓	[126]	✓			[170]	✓			[217]			
[32]			✓	[78]	✓		✓	[127]				[171]	✓			[218]			✓
[33]			✓	[79]			✓	[128]	✓			[172]	✓			[219]			
[34]	✓			[80]	✓	✓		[129]				[173]	✓			[220]			
[35]			✓	[81]			✓	[130]				[174]	✓			[221]			✓
[36]			✓	[82]			✓	[131]				[175]	✓			[222]	✓		✓
[37]			✓	[83]			✓	[132]	✓			[176]	✓	✓		[223]			✓
[38]			✓	[84]	✓			[132]	✓			[177]	✓			[224]			✓
[39]	✓			[85]			✓	[133]				[178]		✓		[225]			
[40]	✓			[86]			✓	[134]				[178]		✓		[226]			✓
[41]	✓			[87]			✓	[135]				[178]		✓		[227]			
[42]	✓			[88]	✓			[136]				[179]	✓	✓		[228]	✓		
[43]	✓			[88]	✓		✓	[137]	✓			[180]	✓	✓		[229]			
[44]				[89]			✓	[138]				[180]		✓		[230]			
[45]			✓	[90]	✓			[139]	✓			[181]	✓			[231]	✓		
[46]			✓	[91]			✓	[140]				[182]	✓			[232]	✓		
[47]			✓	[92]				[141]				[183]	✓			[233]			
[47]			✓	[93]		✓		[142]				[184]	✓			[234]	✓		
[48]			✓	[94]			✓	[143]				[184]	✓			[235]	✓		
[49]			✓	[95]			✓	[144]				[185]	✓			[236]			
[50]				[96]	✓		✓	[145]				[186]	✓			[237]	✓		
[51]		✓	✓	[97]				[146]	✓			[187]	✓	✓		[238]			
[52]			✓	[98]	✓		✓	[147]				[188]	✓	✓		[238]			
[53]	✓			[99]			✓	[148]				[189]			✓	[238]			
[54]	✓		✓	[100]				[149]				[190]			✓	[239]			
[55]				[101]		✓	✓	[150]	✓			[191]			✓	[240]			
[56]		✓		[102]	✓		✓	[150]	✓			[192]			✓	[240]		✓	
[57]	✓			[103]	✓		✓	[151]	✓			[193]			✓	[241]			
[57]	✓			[104]	✓			[151]	✓			[193]			✓				
[57]	✓			[105]				[152]	✓			[194]	✓		✓				

respectively. Since snubber and clamp circuits can be added to any converter, it is not much fair to compare them with the rest of the NHSDCs. Accordingly, the best and the worst topologies of Table VI with respect to ISGC, ISGW, and ISGS are tabulated in Table III.

9) *Resonant Tank*: Soft switching is an interesting subject in power electronics; therefore, various types of resonant tanks with different connections and configurations have been presented as one of the popular soft switching methodologies. According to the literature review, the soft switching techniques based on resonance operation are not usually introduced by implementing on a high step-up converter due to their sinusoidal voltage or (and) current stress, which is much higher in high step-up topologies. However, some NHSDCs with resonant operation

in some switching time intervals have been presented, which are listed in the last column (Res.) of Table I. According to control modulation, these resonant topologies are generally divided into variable [27], [100], [181], [183], [194], [203], [208], [214] and fixed [11], [23], [53], [55], [67], [72], [73], [88] frequency converters, which are sometimes nominated as frequency and PWM, respectively. In some detailed categorization, resonant [33], [183], [203], [208], [214], quasi-resonant [11], [23], [117], multiresonant [48], [74], [169], [194], switched-resonant [46], [57], [67], and zero voltage transition (ZVT) [90], [101], [173], [181], [218] topologies are the most common with resonant operation. Nevertheless, some important points should be considered about these converters: 1) Resonant inductor is the leakage inductance or a small, usually air-core, inductor to profit the

TABLE VI
NHSDCs ACCORDING TO THE USAGE OF SNUBBER (SN) AND CLAMP (CLP) CIRCUITS (P: PASSIVE, A: ACTIVE)

Ref	Sn	Clp	Ref	Sn	Clp	Ref	Sn	Clp	Ref	Sn	Clp	Ref	Sn	Clp	Ref	Sn	Clp	Ref	Sn	Clp
[11]		P	[36]		A	[58]		P	[82]		P	[106]	P	P	[128]		A	[150]		A
[12]	P	P	[38]		A	[59]		A	[83]		P	[107]		P	[130]		A	[162]	P	
[12]	P	P	[40]		P	[60]		P	[84]		P	[109]		P	[131]		A	[171]		A
[13]		A	[41]		P	[63]		P	[85]		P	[109]		P	[132]		A	[173]	P	
[14]		P	[42]	A	A	[64]		A	[86]		P	[111]		P	[132]		A	[194]		A
[15]		P	[44]	P	P	[65]		P	[87]		P	[113]		P	[133]	P		[201]		P
[16]		A	[45]		P	[66]		P	[88]		P	[115]		P	[134]		P	[202]		A
[20]		P	[46]		P	[69]		P	[88]		P	[116]		A	[134]		P	[204]		P
[21]		A	[48]		A	[70]		P	[89]		A	[117]	P		[135]		A	[206]		P
[22]		A	[49]		P	[71]		P	[90]	P	P	[118]		P	[136]		A	[212]	A	
[23]	P	P	[52]		P	[72]		P	[92]		P	[119]		P	[137]		P	[213]	P	
[24]		P	[53]		A	[73]		A	[94]		A	[120]		A	[140]		P	[218]	P	A
[25]		P	[54]		P	[75]	P	P	[97]		P	[121]		P	[141]		A	[222]	P	
[26]		P	[55]	P		[76]		P	[98]		A	[122]		P	[142]		A	[223]		P
[27]		P	[56]		P	[78]		P	[99]		P	[123]		P	[143]	P				
[29]		P	[57]		A	[78]		P	[100]	A		[125]		P	[145]		P			
[32]		P	[57]		A	[79]		A	[101]		A	[126]		P	[146]		P			
[33]		A	[57]		A	[81]		P	[102]		P	[127]	P	A	[148]		A			

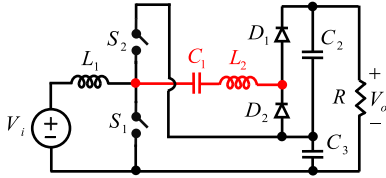


Fig. 14. Example of utilizing a series resonant tank [203].

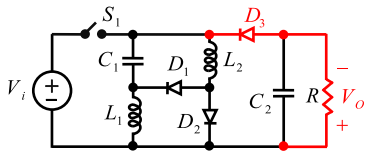


Fig. 15. Example of the inverted output voltage [200].

linear magnetic characteristic of air. Therefore, the resonant inductors should not be treated similar to the power inductors in comparison studies with respect to size, weight, and cost, which is followed in Table I. 2) Variable frequency operation is a big challenge for the components design, which is highlighted in the EMI filters. 3) In some literature, it is observed that the resonant converters with soft switching capability are compared with hard switching topologies, and their higher components count is considered as a demerit. This type of evaluation is unfair unless the effect of the resonant tank is considered on efficiency, size, weight, cost, voltage and current stress, switching frequency, and voltage gain simultaneously. Fig. 14 shows an example of utilizing a series resonant tank in an NHSDC.

10) *Output Voltage Direction*: As depicted in Fig. 1, the NHSDCs usually have the same input–output voltage direction, which mostly originated from the conventional PWM boost converter. This makes the output voltage regulation easier. Meanwhile, a limited number of topologies based on the conventional PWM buck–boost [155], [200], [207] or negative VMC [166], [186] structures present inverted output voltage. An example of these converters is illustrated in Fig. 15.

11) *Applicability in Renewable Energy Systems*: Although lack of galvanic isolation, lower safety, leakage current due to parasitic capacitances in PV application, and challenging harmonic issues when connecting to an inverter are the drawbacks or deficiencies of NHSDCs, they have wide industrial applications as an independent stage or a preconditioning stage connected to other topologies. From a general prospect, the NHSDCs are employed in PV, EV, and FC systems, power supplies, medical devices, data centers, aircraft, electrical machinery, home appliances, chargers, electroplating and welding machines, electrolyzers, thermoelectric generators, electrostatic filters, microgrids, X-ray, and high-voltage vacuum tube drivers.

As one of the leading applications for the NHSDCs, renewable energy power conditioning systems owe a large share in research, industry, and investment. Accordingly, they are mostly claimed in the literature, which should be evaluated more meticulously. To be more clear, the applications such as PVs, FCs, and EVs often require CG, CF, and low-input-current-ripple structures to improve the converter functionality with regard to EMI, parasitic elements, leakage currents, gate driving, and output voltage regulation. For instance, although claimed, [14], [21], [24], [26], [40], [41], [51], [53], [72], [78], [79], [83], [87], [155], [187], [227], [230], [235] and [24], [26], [51], [64], [96], [131], [152], [155], [158], [162], [187], [189], [193], [225], [227], [231], [235] have restricted applicability in renewable energy systems due to input current (discontinuous current or high ripples) and GND issues, respectively.

B. Operational Features

1) *Steady-State Voltage Gain*: As the main task of an NHSDC, achieving high voltage gain, along with retaining other topological and operational metrics, is of high importance, which helps to improve its industrial applicability. Although the fundamental of all NHSDCs is transferring the input low-voltage port energy to the output high-voltage load by charging and discharging passive components in some time intervals through switching the semiconductors, employment or combination of different approaches, such as enhancing components count, converters configuration, switching pattern, and switch(es) ON state,

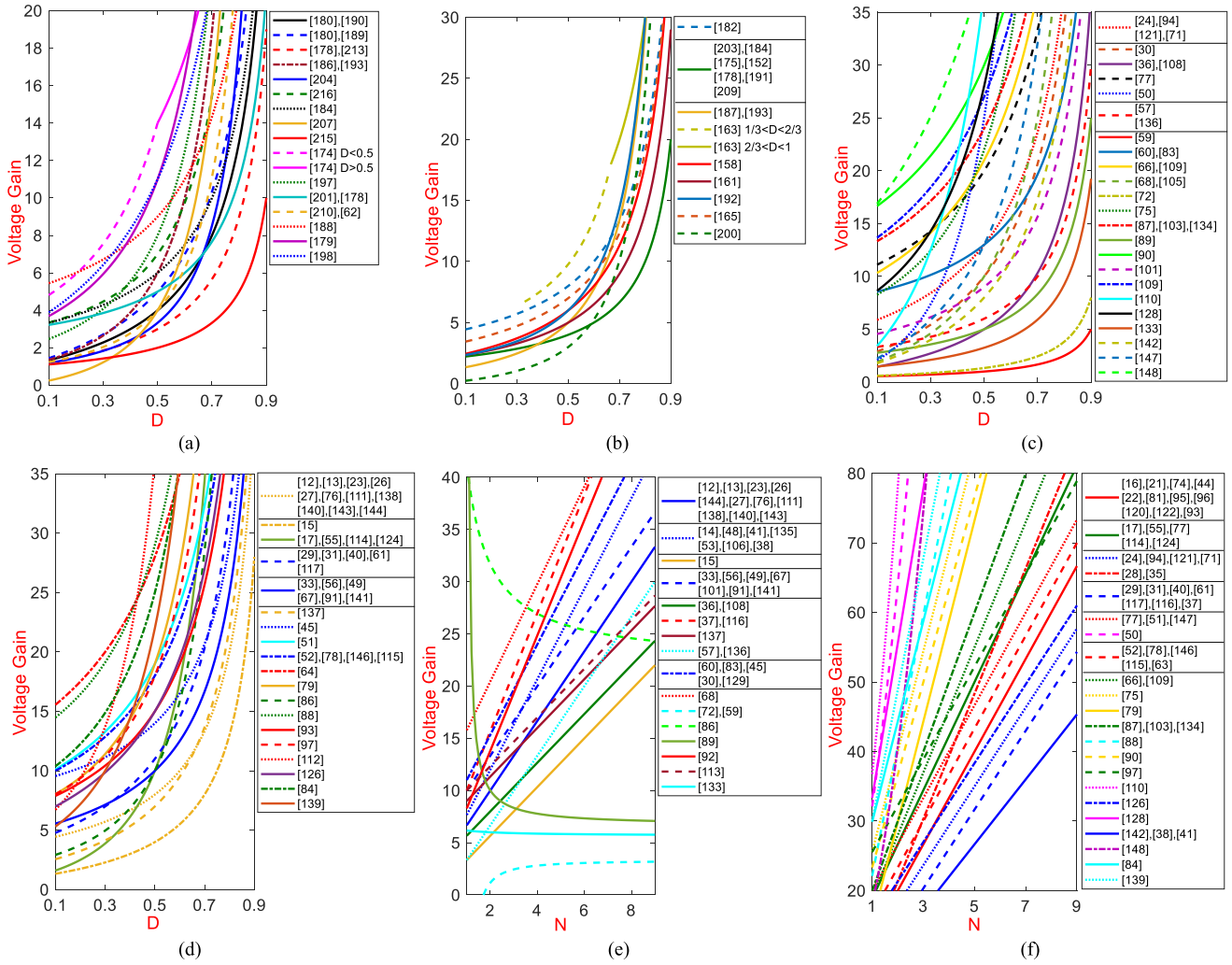


Fig. 16. Voltage gain comparison of NHSDCs with regard to (a), (b) duty cycle for the converters with only D -dependent voltage gain, (c), (d) duty cycle, and (e), (f) coupled magnetic components turns ratio.

lead to higher voltage gain. Note that similar to any engineering system, improving one feature, such as voltage gain, realized by losing one or more other merits. In Fig. 16, the ideal CCM voltage gain of the converters is assessed elaborately with regard to D and N , for which the following points are concluded. It is worth mentioning that Fig. 16(a) and (b) is allocated to the converters with only D -dependent voltage gain, whereas Fig. 16(c)–(f) presents the voltage gain of the converters with both D and N in their equations. Dividing the converters into two groups in Fig. 16(c) and (d) is only done for better visibility, which is also followed in Fig. 16(e) and (f). In addition, since the acceptable duty cycle range of some interleaved topologies is limited to $0.5 \leq D$, their voltage gain diagrams are drawn separately in Fig. 17.

- 1) The highest voltage gain values in the whole range of D variation are allocated to: [64] with an interleaved multilevel topology employing an SCI; [87], [109], and [134] with SS configurations employing two SCI units, three-winding coupled inductors, and only one switch; [88] with a multistage multilevel configuration employing

an SC and a three-winding coupled inductor; [90] with an SS configuration employing a three-winding coupled inductor and a high-order SC; [103] with a multistage configuration employing two coupled inductors, and two SC and SCI units; and [148] with a SS configuration employing an SCI unit and a three-winding coupled inductor. Furthermore, in the interleaved converters with $0.5 \leq D$, the topologies with three coupled inductors and three SC and SCI units [65], [69] and two coupled inductors, one SC unit as a voltage multiplier rectifier, and a multilevel configuration [132] owe the highest voltage gain (see Fig. 17). According to these topologies, ultrahigh voltage gain is accomplished through the simultaneous usage of capacitive and inductive approaches, where the role of multiwinding coupled inductors is more decisive.

- 2) Using Table I, none of the aforementioned high voltage gain converters, except [65] and [69] with limited D and more than 16 components, are among the topologies with the highest components count. Thus, the configuration of

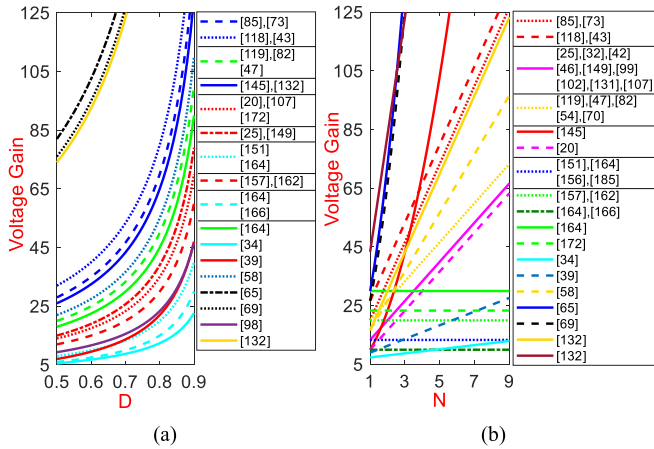


Fig. 17. Voltage gain comparison of the interleaved NHSDCs with regard to (a) duty cycle and (b) coupled magnetic components turns ratio.

the components takes a more influential role than their count. Moreover, the authors of [87] and [109] present high ISGC, ISGW, and ISGS too.

- 3) Comparing Fig. 16(a), (b) with Fig. 16(c), (d) concludes that using coupled inductors leads to higher voltage gain than inductors due to their more efficient inductive utilization, which is highlighted in higher N values.
- 4) For any operation in lower duty cycle values, [64], [90], and [148] have the highest voltage gain.
- 5) Voltage gain equations of the interleaved topologies in [163] and [174] differ when the conduction periods of interleaved phases have or do not have overlap [see Fig. 16(a) and (b)].
- 6) The suggested converters in [133], [152], [175], [178], [184], [191], [203], [209], and [215] are selected as the topologies with the lowest voltage gain values with regard to D ; meanwhile, [152] and [175] have low weight. In addition, [184] is on the list of undesired topologies with respect to ISGC, ISGW, and ISGS metrics. Note that the low voltage gain of [59] and [72] in Fig. 16(c) is because of their reciprocal turns ratio definition.
- 7) The ascending ramp of the voltage gain diagrams is high in [50], [110], and [112], which leads to high voltage gain but hard output voltage regulation. In some literature works, a high voltage gain value in low D is considered an achievement, which should be analyzed more carefully. In fact, for the same load, power, and voltage gain, the converter driven under lower D has higher switch current stress to satisfy the required average current in shorter time durations, which leads to higher switch RMS current and conduction power loss. Consequently, decreasing the efficiency restricts the output power and desired voltage gain.
- 8) Since N usually appears as a linear combination in the numerator of the voltage gain equations, most of the profiles in Fig. 16(e) and (f) are linear, except [59], [72], [86], [89], and [133]. As mentioned earlier, in order to keep the uniformity of figures, N is defined as the secondary to

the primary winding turns ratio of the coupled inductors or built-in transformers, which is reciprocal in [59], [72], [86], [98], and [220]. This is the reason for the nonlinear behavior of [86]. However, N originally appears in the voltage gain equation denominator of [59], [72], [89], and [133].

- 9) With regard to N variation, [50], [65], [69], [75], [79], [84], [88], [90], [110], [128], [132], and [139] provide the highest voltage gain values, which are due to the usage of two (or more) coupled inductors [50], [65], [69], [75], [79], [88], [110], [132], employment of switched cells [65], [69], [75], [79], [84], [88], [90], [128], [132], [139], and coimplementation of multistage and multi-level structures [84], [88], [128], [139]. Consider that only [50], [65], [110], and [139] have high ISGC, ISGW, and ISGS in this list. On the other hand, [15], [34], [36], [57], [108], [113], [133], [136], [137], [164], and [166] have the least values. The SS configuration usage [36], [108], [113], [137] and lack of switched cells [15], [36], [133], [136] are the main reasons for their low voltage gain.
- 10) Even with utilizing a three-winding coupled inductor, the suggested converter in [133] provides the least sensitivity with respect to N . Therefore, changing N is not a solution for voltage gain increment in this converter.
- 11) Among the converters with a low number of semiconductors and passive components, respectively, [50], [110], [129] and [50], [110], [124] have high voltage gain.
- 12) Among bidirectional structures, [133], [175], [209], [211], [213], [237] and [50], [110], [145] owe the lowest and highest voltage gains, respectively. The introduced topologies in [43], [65], [69], [73], [85], [110], [118], and [132] feature low ICR and high voltage gain simultaneously. In addition, the converters in [90], [109], [148], in [43], [65], [69], [85], [110], [118], [132], in [50], [75], [84], [88], [112], [123], [128], [139] and in [86], [84], [85], [88], [123], [128], [132], [139] provide the highest voltage gain values among SS, interleaved, multistage, and multilevel topologies, respectively.
- 13) The lowest and highest voltage gain values in CF converters are assigned to [213], [231], [234], [241] and [50], [65], [69], [110], [112], [132], respectively. The corresponding ratings are dedicated to [178], [215], [227], [230], [238] and [79], [84], [123] in VF topologies, respectively. It is clear that the CF converters provide higher voltage gain than the VF.
- 14) It is evident that the design and configuration of each NHSDC have pros and cons, where the initial aim in the design procedure is increasing output voltage gain while satisfying some other features. The superiority of these features depends on the application while keeping the other less-significant ones at a standard or acceptable level will be much better. As some examples, ICR and leakage current of FCs and PVs [10], [16], [19], [39], [42], [99], [162], [192], [231], [207], reliability of medical devices, thermoelectric generators and data centers power supplies [37], efficiency and reliability of aircrafts

and aerospace crafts [9], current stress of chargers [91], [138], [140], [161], OVR of electrical machinery and electroplating machines [68], [78], size of home appliances, power density of EVs [175], [209], extension capability of HVDC systems [18], [202], voltage ripple and power density of high dc voltage supply of inverters [2], control simplicity and cost of microgrids [14], [29], [34], [45], [47], [111], efficiency of AMOLED displays [9], sustainability of uninterruptable power supply (UPS) [25], [35], [61], [62], [87], [203], and voltage stress and ripple of X-ray, high-voltage vacuum tube drivers, plasma research, and pulsed laser devices [9] are the most demanding features along with the voltage gain. Note that the NHSDCs could be implemented as an independent stage or a preconditioning stage connected to other topologies.

- 15) The presented very high values of voltage gain in high D are only accessible in theoretical analytics. In practice, the voltage gain reaches zero at $D = 1$ and it is limited to low values at the duty cycles close to “1” due to high power loss [68].
- 16) It is noteworthy that the extendable [18], [19], [47], [63], [74], [75], [78], [88], [104], [114], [132], [134], [150], [151], [153], [154], [155], [158], [159], [160], [162], [164], [166], [167], [169], [170], [172], [173], [177], [195], [196], [183], [199], [202], [206] and impedance source [217], [218], [219], [220], [221], [222], [223], [224], [225], [226], [227], [228], [229], [230], [231], [232], [233], [234], [235], [236], [237], [238], [239], [240], [241] converters are excluded in Fig. 16, which will be investigated in a separate section.

2) *Voltage Stress*: Voltage stress along with the current stress of components plays the most crucial role in their design procedure, where the design of switches, diodes, capacitors, built-in transformers, protection systems, isolation materials, and the clearance between PCB traces are directly affected by their voltage stress tolerating across. In some previous literature works, the components voltage stresses of converters are compared through some criteria separate from other characteristics such as voltage gain [177], [235], [241], which seem to be unfair and incomplete assessments. In other words, higher voltage gain performance requires components with higher voltage ratings, especially in the output terminal, which should be considered in the evaluation of the figure of merit. In some other references, the components voltage stress is normalized with respect to the input voltage [116], [198], [224], [234], [236], [238], [240], which leads to a confusing evaluation metric. To clarify this, consider two topologies with the same output but different input voltage values. The one with lower input voltage has higher voltage gain (merit) and normalized voltage stress (demerit) since the input voltage is in the denominator of both metrics. This makes a contrast in the concept of normalization with respect to the input voltage. Therefore, one promising solution is to use the output voltage as the base value for normalization [11], [68], [77], [84], [121], [147], [148], [149], [179], [188], [231], in which higher output voltage increases the voltage gain (merit) and decreases the normalized voltage stress (merit).

Figs. 18–20 demonstrate the normalized accumulative voltage stresses of switch(es), diode(s), and capacitor(s), respectively. Moreover, the components voltage stresses of the interleaved converters with limited duty cycle range ($0.5 \leq D$) are depicted in Fig. 21. The following points summarize some results of these figures.

- 1) Despite the voltage gain results, the normalized accumulative switches voltage stress ($\hat{V}_S = \sum V_S/V_o$) has direct [40], [60], [106], [129], inverse [28], [103], [207], and no [90], [127], [204], [215] relation with D variation in different topologies (see Fig. 18). Moreover, the relation can either be linear [62], [140], [210], [216] or nonlinear [36], [126], [179], [187].
- 2) With respect to D variation, all converters have monotonic \hat{V}_S function except [68] and [147] with minimum \hat{V}_S in $D = 0.5$.
- 3) The suggested topologies in [62], [72], [129], [182], [204], [210], [211], [215] and in [52], [65], [66], [78], [87], [96], [109], [115], [134], [146], [148] have the highest and lowest \hat{V}_S during D variation, respectively. The corresponding ratings are assigned to [44], [50], [62], [110], [129], [133], [137] and [52], [63], [65], [66], [69], [78], [87], [109], [115], [126], [134], [146] according to N variation, respectively. It should be noted that [204], [215] and [62], [129], [133] suffer from undesired \hat{V}_S with a constant (or approximately constant) high value independent of D and N , respectively.
- 4) High \hat{V}_S is mainly caused by a high number of switches [204], [211], using switches close to the output high-voltage port [62], [129], [182], [210], [211], and low voltage gain [72], [133], [211], [215]. On the other hand, low \hat{V}_S is due to using less switches [52], [78], [87], [109], [115], [146], placing switches close to the input low-voltage port [52], [109], [115], [134], high voltage gain [65], [66], [69], [87], [109], [134], [148], and employing the passive VMC between the switch(es) and output port [78], [87], [109], [134], [146].
- 5) From the \hat{V}_S point of view, design of the topologies with low N values (especially close to $N = 1$) is not recommended in [12], [13], [27], [36], [57], [79], [101], which is dramatically improved with higher N .
- 6) Although the input CF or VF configuration seems not to have a logical correlation with \hat{V}_S , the studies of this article show that low \hat{V}_S is more likely in CF topologies.
- 7) Based on Fig. 19, the normalized accumulative diodes voltage stress ($\hat{V}_D = \sum V_D/V_o$) has higher varieties. From linear [86] to nonlinear [97], from constant [27] to highly sensitive [207], and from ascending [45] to descending [37] are all available in \hat{V}_D profiles. Note that most of the nonconstant profiles are nonlinear.
- 8) Considering \hat{V}_D , the converters have a monotonic function except [84], [123], [216], which reach the maximum \hat{V}_D in $D = 0.78$, 0.76 , and 0.78 , respectively.
- 9) According to D variation, the highest and lowest \hat{V}_D are assigned to [13], [25], [32], [46], [58], [112], [132] and [44], [51], [88], [89], [98], [101], respectively. Moreover, [25], [32], [46], [58], [68], [73], [124], [147] and [44],

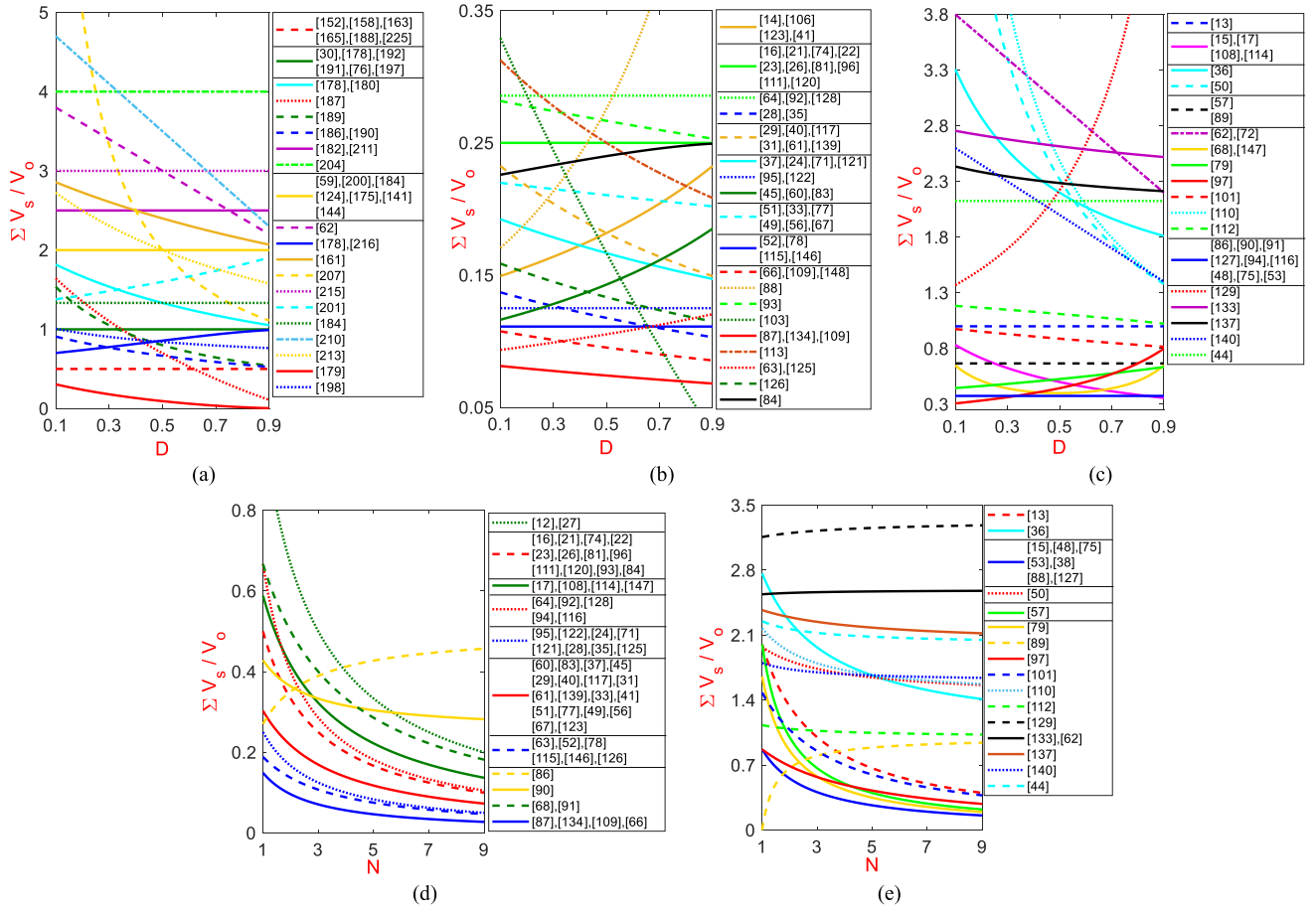


Fig. 18. Normalized accumulative switches voltage stress comparison of NHSDCs with regard to (a) duty cycle for the converters with only D -dependent voltage gain, (b), (c) duty cycle, and (d), (e) coupled magnetic components turns ratio.

[88], [98] have the highest and lowest \hat{V}_D with respect to N , respectively.

- 10) The suggested converters in [161], [204], and [211] have high \hat{V}_S and switches count simultaneously, which highlights the adverse effect on ISGC. It is noteworthy that these topologies lack coupled inductors. Moreover, high diodes count and \hat{V}_D appear in [25], [32], [46], [58], and [147].
- 11) Since the diodes count is usually more than the switches in a topology, and most of them are placed closer to the output port, it can be concluded with high probability that $\hat{V}_D \geq \hat{V}_S$. This outcome is verified by comparing Figs. 18 and 19, or the figures in Fig. 21. Nevertheless, the bidirectional configurations are exceptions.
- 12) It is worth mentioning that high \hat{V}_S in bidirectional topologies is basically caused by their requirement for more switches [44], [50], [62], [110], [129], [133], [137], [145], [204], [205], [210], [211], [213], [215]. Thus, their high \hat{V}_S should not be judged along with unidirectional topologies, since in bidirectional ones, usually $\hat{V}_D = 0$. Hence, in comparison of bidirectional and unidirectional structures, $\hat{V}_S + \hat{V}_D$ is a more reliable figure of merit. Among bidirectional converters, [142] has relatively low \hat{V}_S .

- 13) The normalized accumulative capacitors voltage stress ($\hat{V}_C = \sum V_C/V_o$) is the highest and lowest in [32], [59], [134], [159], [163], [188] and [12], [15], [30], [178], [180], [181], [182] with regard to D variation, and in [32], [54], [60], [66], [94], [98], [109], [118], [134] and [16], [17], [23], [44], [50], [68], [84], [107], [110], [120], [147], [164], [181] with regard to N variation, respectively.

- 14) It should be considered that the relation between components voltage stress and their cost is nonlinear with step changes.

3) *Current Stress*: The other figure of merit in a converter components design is their current stress, which has a decisive role in the design procedure of switches, diodes, magnetic components windings, cooling elements, protection systems, and PCB traces width. In this article, the normalized accumulative switches current stress ($\hat{I}_S = \sum I_S/I_i$) of the converters is evaluated, and the results for some selected topologies are depicted in Fig. 22. Dissimilar to the normalization of components voltage stress, input current is employed as the base value for \hat{I}_S . As shown in this figure, the relatively highest and lowest \hat{I}_S are devoted to the presented topologies in [13], [27], [42], [64], [73], [179] and [68], [118], [147], [207], respectively. Furthermore, [179] has the highest sensitivity with regard to D variation.

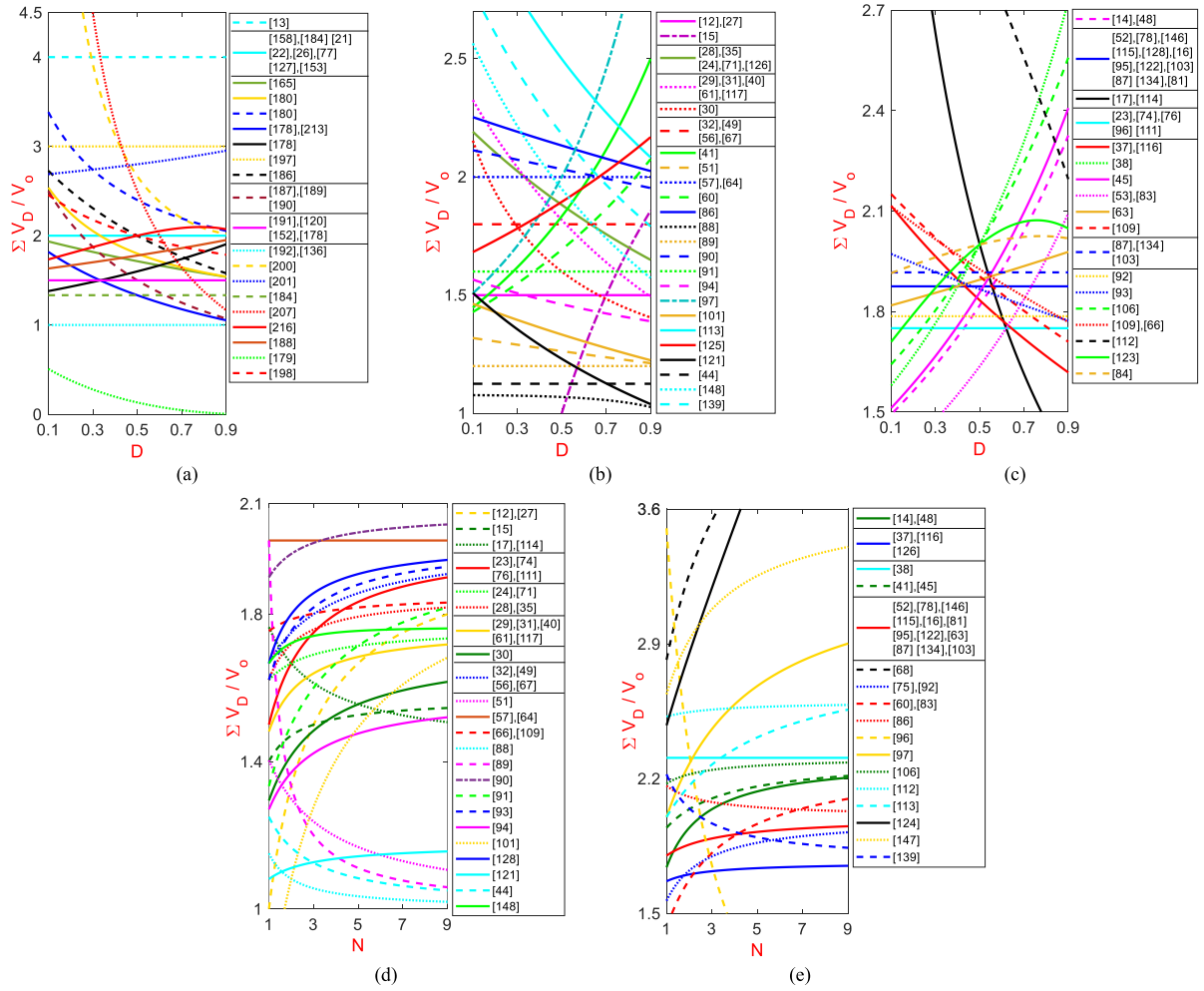


Fig. 19. Normalized accumulative diodes voltage stress comparison of NHSDCs with regard to (a) duty cycle for the converters with only D -dependent voltage gain, (b), (c) duty cycle, and (d), (e) coupled magnetic components turns ratio.

Using switches in an active voltage clamp circuit [13], [42], [64], [73], an integrated configuration [27], and an active SI in the converters input port [179] are the major reasons for high \hat{I}_S . Note that the calculated current stress in Fig. 22 represents only the continuous current (steady state) stress of switches where the pulsed current stresses, such as inrush and transient spikes, should also be considered in design and comparison studies meticulously. As some common examples, in the converters with diodes with uncompensated reverse recovery issues, high parasitic capacitance, fast switching of capacitive VMCs, high switching losses, and no leakage inductance energy absorption, the transient (usually high frequency) current spikes are much more dominant.

4) *Switch Utilization Factor (SUF)*: As a multiobjective metric evaluating both voltage and current stresses, SUF reflects the efficient employment of switches and is formulated as

$$\text{SUF} = \frac{P_o}{\sum_{j=1}^m V_{sj} I_{sj}} \quad (3)$$

where P_o , V_{sj} , I_{sj} , and m are output power, maximum steady-state switch voltage stress, switch current stress, and the number

of switches, respectively. The parameter I_{sj} can be replaced either with its maximum [243] or rms [244] value, where the first definition is assumed in this article. In a converter, higher SUF leads to higher efficiency, a smaller cooling system, and lower cost. Fig. 23(a) and (b) demonstrates the SUF diagrams for some of the converters with regard to D and N , respectively, which are less than “SUF = 1.” According to these figures, [68], [96], [118], [121], [134], [147], [191], [207] and [13], [42], [64], [73], [179], [182], [204], respectively, are the most and the least desired topologies with regard to SUF. Moreover, the most determinative factor for high SUF in [96], [134], [191] and [68], [118], [121], [147], [207], respectively, is their low \hat{V}_S and \hat{I}_S . On the other hand, high \hat{V}_S and \hat{I}_S lead to low SUF in [182], [204] and [13], [42], [64], [73], [179], respectively. According to the studies of this article, there is not any meaningful relation between stage type, using VMCs and improving SUF. It is worth noting that SUF can be similarly defined for diodes (DUF), and the summation of SUF and DUF is suggested in some literature [6]. In addition, it is a figure of merit to evaluate converters but not to design components.

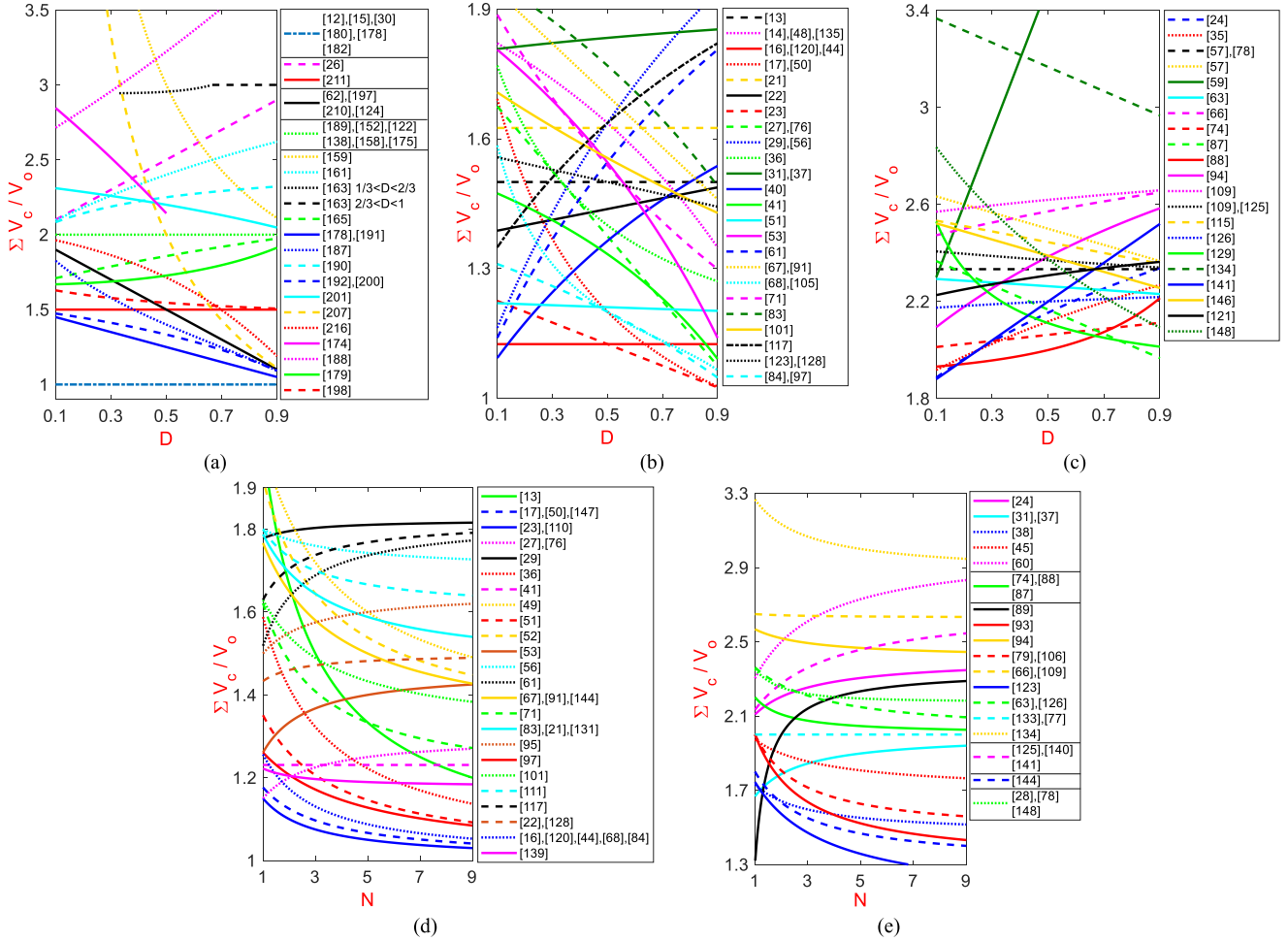


Fig. 20. Normalized accumulative capacitors voltage stress comparison of NHSDCs with regard to (a) duty cycle for the converters with only D -dependent voltage gain, (b), (c) duty cycle, and (d), (e) coupled magnetic components turns ratio.

5) *Input Current Ripple*: In Section III-A, the NHSDCs are classified into seven groups (A–G) according to their input port configuration. To evaluate more precisely with regard to the converters' operation point, one of these groups (the single-phase topologies with a single input inductor in group D) is selected and the normalized ICR ($\Delta i_L f_s L / V_o$) values are depicted in Fig. 24. It is noteworthy that Δi_L , f_s , L , and V_o are the ICR, switching frequency, input inductor, and average output voltage, respectively. According to Fig. 24(a) and (b), each normalized ICR diagram reaches a maximum point with respect to D variation, which is usually in $0.5 \geq D$. For instance, this maximum point occurs in $0.5 = D$ in [12], [23], [33], [49], [57], [89], [90], [91], [115], [134], [143], [144], [152], [175], [182], [203], and [209], which is the highest for this group of NHSDCs. Considering the preferred duty cycle range of $0.5 \leq D$ for NHSDCs, the operation point is often far from the maximum normalized ICR point. The results in Fig. 24 show that the presented topologies in [90], [112], [128], [139] and in [190], [204], [213] are the most and least preferred ones based on ICR, respectively. In addition, higher N usually leads to lower normalized ICR.

6) *Output Voltage Ripple*: In the applications sensitive to the OVR, this figure of merit can be considered as a reliable and

decisive evaluation metric to compare converters if it is normalized with respect to the output voltage value, and the effects of the duty cycle, switching frequency, output filter capacitor, and the number of output port levels are considered. For further clarification, the characteristics of the OVR in some NHSDCs are shown in Fig. 25. According to Fig. 25(a), an SS topology usually has a descending and an ascending output voltage waveform with the switching frequency of f_s when the main switch is ON and OFF, respectively [51], [152]. It is worth noting that this figure is drawn by ignoring the short demagnetization period of the coupled inductors or built-in transformers. However, if the same SS topology is extended to a two-phase interleaved configuration [13], [20], the OVR reduces and its frequency is $2f_s$ [see Fig. 25(b)]. In addition, in order to compare two possible conditions of multilevel structures, the output voltage waveforms of a two-level converter are shown in Fig. 25(c) and (d). Regarding these figures, the OVR of two output capacitors can either be additional [179] or subtractive [68] when they are charged and discharged simultaneously or separately in the corresponding time intervals, respectively. Similar to the normalized ICR, by using the duality concept in electrical circuitry, the normalized OVR can be defined as $\Delta v_o f_s C / I_i$, where, Δv_o , C , and I_i

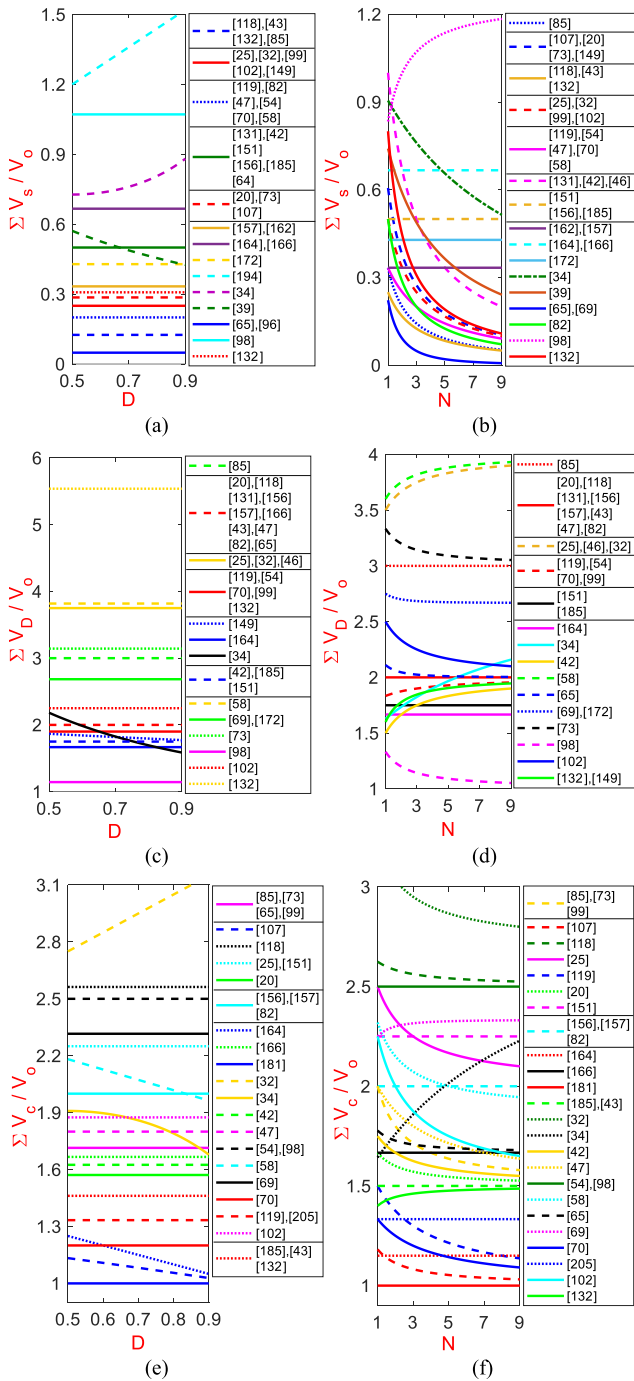


Fig. 21. Normalized accumulative voltage stress comparison of the interleaved NHSDCs with regard to D and N for (a), (b) switches, (c), (d) diodes, and (e), (f) capacitors.

are the OVR, output filter capacitor, and average input current, respectively.

7) *Efficiency*: One of the most practical goals in the NHSDCs design, operation, and implementation is achieving high efficiency in a wide range of light to full load, which determines the cooling system characteristics. In the literature, power loss (efficiency) calculation of presented topologies has been one of the most frequent sections. However, there are some necessary

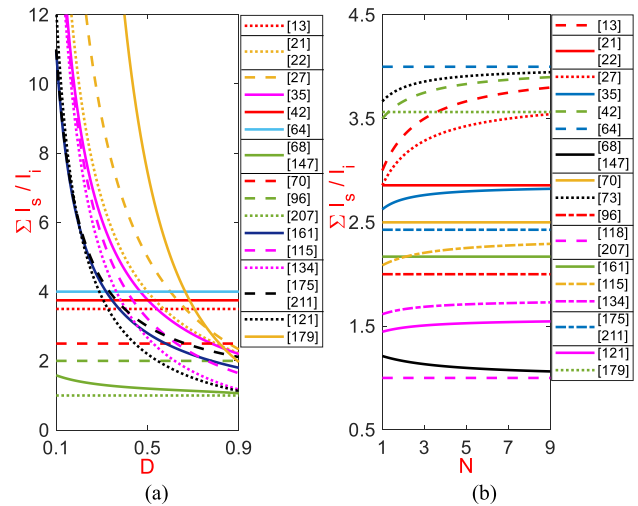


Fig. 22. Normalized accumulative switches current stress comparison of NHSDCs with regard to (a) D and (b) N .

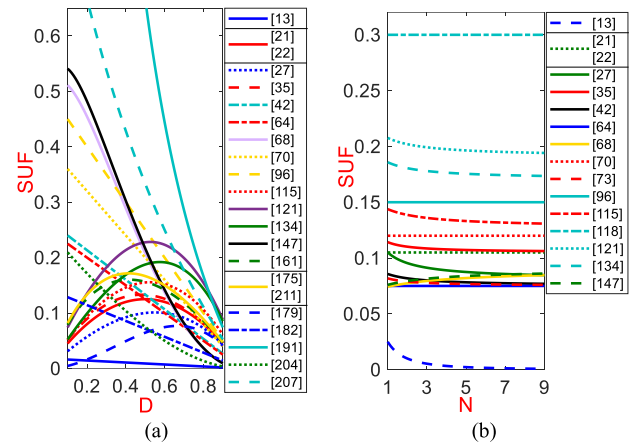


Fig. 23. SUF comparison of NHSDCs with regard to (a) D and (b) N .

and misunderstood points in the efficiency comparison of different converters.

- 1) The corresponding components should be considered with the same type, material, family, and characteristic for all topologies. It is clear that selecting expensive low-ON-resistance switches increases a converter's efficiency regardless of its operation principles.
- 2) The converters should be designed with the same nominal power, thermal considerations, switching frequency, components voltage and current safety margins, and ripples.
- 3) As mentioned earlier, in a single converter, there are different degrees of freedom, such as input voltage level, switching frequency, magnetic components turns ratio, duty cycle, phase shift angle, and load resistance, to variate output power that have different impacts on the converter efficiency [98], [116], [128], [184], [198], [199], [205], [209], [212], [213], [224], [231]. Therefore, the power axis in an efficiency diagram should be swept with the same approach for all converters.

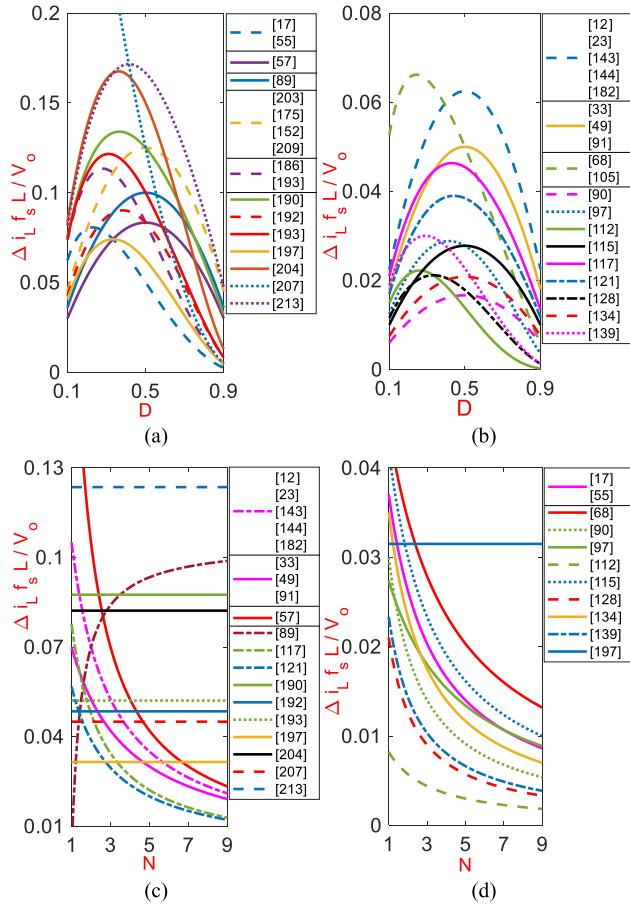


Fig. 24. Normalized ICR comparison of NHSDCs with regard to (a), (b) D and (c), (d) N .

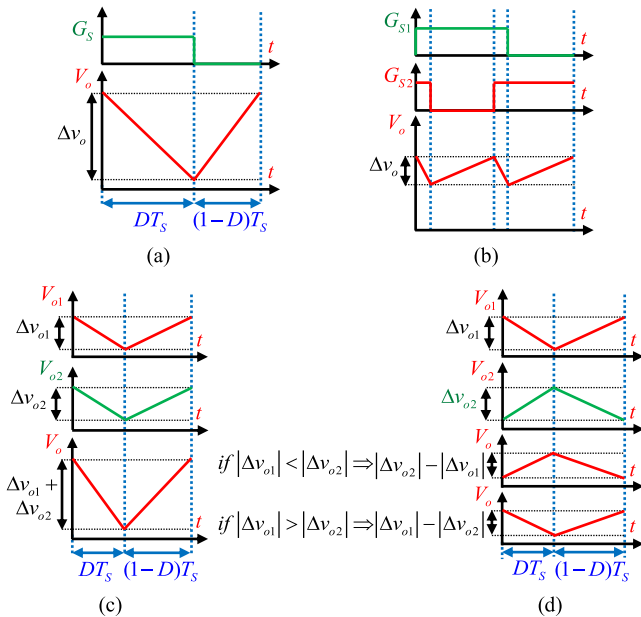


Fig. 25. OVR characterization. (a) SS converter. (b) Two-phase interleaved configuration. (c), (d) Two-level converter with an additional [179] or subtractive [68] style.

- 4) The effects of component's internal resistances, parasitic elements, magnetic components characteristics, free-wheeling currents, regenerative functionality, reverse recovery of diodes, switching transitions, leakage and magnetizing inductances energy, and auxiliary devices should be investigated more meticulously.

In addition, since the converters are usually designed for a specific operation region, their efficiency diagrams should be assessed in that same region based on the application. In some previously published literature works, efficiency is only evaluated in a single point [11], [88], [121], [201], [233], in a full load point [131], [149], [194], or in a maximum efficiency point [44], [76], [94], [98], [122], [126], [129], [163], [166], [170], [176], [179], [191], [224], [240] with different nominal power, output voltage, switching frequency, and duty cycle, which lead to some incomplete and unfair outcomes. Moreover, the efficiency is assessed in one reported point in [100] and [108]. According to the studies of this article among the references, the efficiency values of converters are usually compared where their corresponding components are of different characteristics, types, and families. This makes the comparison conclusions invalid (some examples are [76], [100], [108], [131], and [149]).

8) *Soft Switching*: Soft switching is a dominant approach to suppress switching loss, which is accomplished by resonant tanks [33], [183], [203], active resonant cells [46], [57], inductors in series with semiconductors [171], [235], clamp circuits [13], [16], [22], capacitors parallel with semiconductors [27], and leakage energy recycling [77], [119], [120], [132], [147]. However, it increases the conduction loss due to auxiliary components and intensifies the semiconductors voltage stress due to high-frequency ringing between the parasitic and resonance components, which highlights the significance of optimized operation and design region to reach low total power loss. Hence, the following points should be considered in the soft switching topologies comparison.

- 1) The width of acceptable soft switching range [27].
- 2) Interaction between the switching and conduction losses in the existence of soft switching components [18].
- 3) Switching frequency range [100], [181], [183].
- 4) Cost-effectiveness of auxiliary soft switching components.
- 5) Partial or full soft switching occurrence [11], [169].
- 6) Sensitivity of soft switching auxiliary components and the operation point to the environmental conditions (such as temperature) variation [148].

The zero voltage switching (ZVS) and ZCS of the NHSDCs are identified in Table VII. Regarding this table, satisfying ZVS and ZCS conditions in the switches and diodes, respectively, are the top trending issues in the literature.

9) *Reverse Recovery of Diodes*: Based on the power diodes physics, they do not turn OFF as soon as the anode–cathode current falls to zero due to the existence of charge carriers. Thus, a time period should be spent on removing the chargers, which is called reverse recovery. Although the period is short, its repetition in each turn–OFF transition generates remarkable power loss on a diode [84], [114], [188], [233]. Moreover, it

TABLE VII
NHSDCS ACCORDING TO THE SOFT SWITCHING CONDITION (ZCS: ZERO CURRENT SWITCHING; ZVS: ZERO VOLTAGE SWITCHING)

Ref	Switch		Diode		Ref	Switch		Diode	
	ZCS	ZVS	ZCS	ZVS		ZCS	ZVS	ZCS	ZVS
[11]	✓		✓		[107]		✓	✓	
[12]		✓			[108]	✓		✓	
[12]		✓			[111]	✓			
[13]		✓			[116]		✓	✓	
[18]		✓	✓		[117]	✓		✓	
[18]		✓	✓		[119]	✓		✓	
[20]	✓				[120]		✓	✓	
[21]		✓			[121]	✓		✓	✓
[22]		✓			[124]		✓	✓	
[23]		✓	✓		[127]		✓	✓	
[25]	✓				[128]		✓	✓	
[27]		✓			[130]		✓	✓	✓
[31]	✓	✓	✓		[131]		✓	✓	
[32]	✓				[132]	✓	✓	✓	
[33]	✓	✓			[132]	✓	✓	✓	
[42]		✓	✓		[133]	✓	✓	✓	
[44]		✓			[135]		✓	✓	
[45]			✓		[137]		✓	✓	
[46]	✓	✓			[138]		✓	✓	
[47]	✓				[140]		✓	✓	
[47]	✓				[141]		✓	✓	
[48]		✓			[142]	✓	✓	✓	
[49]	✓				[143]	✓	✓	✓	
[53]		✓	✓		[144]		✓	✓	
[54]	✓				[145]	✓	✓	✓	✓
[55]			✓		[148]		✓	✓	
[57]		✓			[149]			✓	
[57]		✓			[150]		✓	✓	
[57]		✓			[154]		✓	✓	
[58]	✓		✓		[161]		✓	✓	
[59]		✓			[162]	✓	✓	✓	✓
[64]		✓	✓		[168]		✓	✓	✓
[65]	✓		✓		[169]	✓	✓	✓	✓
[69]	✓		✓		[171]		✓	✓	
[70]	✓				[173]		✓	✓	
[73]		✓	✓		[175]		✓	✓	
[75]		✓			[181]		✓	✓	
[75]		✓			[182]		✓	✓	
[77]	✓		✓		[183]	✓	✓	✓	
[78]			✓		[184]		✓	✓	
[78]			✓		[184]		✓	✓	
[79]		✓	✓		[194]		✓	✓	
[81]	✓		✓		[195]	✓	✓	✓	
[82]	✓		✓		[201]	✓	✓	✓	
[85]		✓	✓		[202]	✓		✓	
[88]		✓			[203]		✓	✓	
[88]		✓			[204]	✓	✓	✓	
[89]		✓			[208]	✓	✓	✓	✓
[90]	✓	✓	✓		[209]	✓	✓	✓	
[91]		✓			[211]		✓	✓	
[92]		✓	✓		[213]	✓			
[93]	✓	✓			[214]		✓		
[94]		✓			[215]		✓	✓	
[98]		✓	✓		[218]	✓	✓	✓	✓
[99]		✓			[221]		✓	✓	✓
[100]	✓	✓	✓		[223]		✓	✓	
[101]		✓			[233]	✓	✓	✓	✓
[102]	✓								

leads to high di/dt , which may realize high voltage spikes with parasitic inductances [213]. The diode reverse recovery current passes through other components and increases their current stress. Hence, some approaches have been introduced in the literature to alleviate or eliminate the aforementioned obstacles, and coping with them can be considered as a valuable criterion that affects the converter power loss, components stresses,

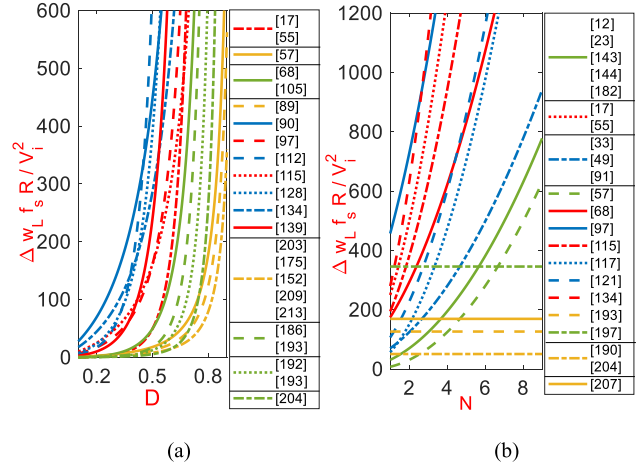


Fig. 26. Input inductor normalized transferred energy comparison of NHSDCs with regard to (a) D and (b) N .

cooling system size, and cost. Among these approaches, the following are the most applicable: ZCS in the turn-OFF transition [130], [133], [141], [142], [145], [148], [168], [208], [223], smooth turn-OFF due to inductive current [171], [235], placement of a coupled inductor leakage inductance in series with diodes [1], [77], [119], [120], [121], [122], [130], [131], [132], [147], [222], usage of resonant or quasi-resonant tanks [11], [117], [128], [201], control-base solutions such as operation in low duty cycles [44], [115], [134], employment of SiC diodes [212] (Note that SiC diodes have higher FW voltage drop.), and capability of using fast recovery diodes due to low voltage stress across diodes [118], [123], [137], [173].

10) *Energy*: In power electronic converters, the energy parameter is usually evaluated through the total energy volume of passive components [18], [64], which is defined as $\sum L\Delta I^2$ and $\sum C\Delta V^2$ for the inductors and capacitors, respectively. Since the volume of an inductor (capacitor) depends on its current and inductance (voltage and capacitance), energy reflects some data about the volume of passive components. However, voltage gain, active components, switching frequency, ripple values, and heatsink size are not considered in this criterion. Moreover, the transferred energy of different passive components may overlap. To overcome these deficiencies, normalized transferred energy is proposed. This metric can be calculated for converters' all passive components, but it is more practical in input and output filter components. In other words, since the whole converter energy passes through the input and output ports, their normalized transferred energy metric reflects useful data about energy, volume, power density, and voltage gain. In this article, the input inductor normalized transferred energy ($\Delta w_{L_s} f_s R / V_i^2$) is demonstrated in Fig. 26 for some converters of group D (the single-phase topologies with a single input inductor), where Δw_{L_s} , R , and V_i are the input inductor magnetic energy in one switching cycle, output load, and input voltage, respectively. Based on this figure, [112], [128], [139] and [152], [175], [190], [192], [193], [203], [204], [209], [213] owe the

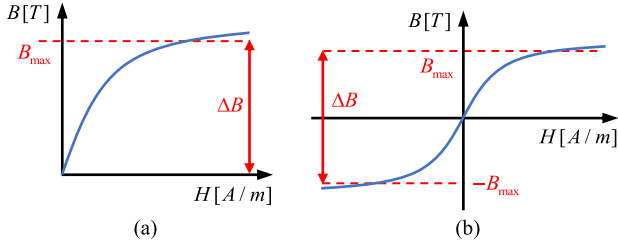


Fig. 27. Magnetic components B - H characteristic. (a) Single-quadrant operation. (b) Dual-quadrant operation.

highest and lowest normalized transferred energy on the input inductor among this group of NHSDCs, respectively.

11) *B-H Plane Characteristic*: Magnetic flux density (B) is a decisive parameter in the magnetic components design, which affects the core saturation, volume, and loss (hysteresis and eddy current). The B versus magnetic field strength (H) curve is the most essential characteristic of a core in datasheets. In single winding and most of the coupled inductors, this magnetic curve is in the first quadrant of the B - H plane, which is shown in Fig. 27(a). Operation in the first quadrant results in dc flux and limited ΔB as well as larger volume and lower efficiency. In order to cope with this obstacle, some interleaved coupled inductors [105] and built-in transformers [13], [25], [33], [58], [73], [85], [98], [144], [148], [149] are utilized in the NHSDCs with employing the first and third quadrants, which increase the applicable ΔB . In other words, for a certain ΔB , built-in transformers can be implemented with low $-B_{\max}$ cores [see Fig. 27(b)].

12) *Efficient Inductive Utilization*: With higher power density than the electric field, the magnetic field power is transferred through FL, FW, and (or) transformer-based mechanisms. FL and FW methodologies indicate the stored energy transfer of a coupled inductor or a built-in transformer when the main switch is OFF and ON, respectively. In addition, the transformer-based (TR) concept relates to the common power transfer through the induction between coupled windings. The more the aforementioned mechanisms are utilized in a converter, the more efficient inductive utilization. In other words, employing different inductive mechanisms leads to recycling the stored magnetizing and leakage energy, canceling the freewheeling currents, and then higher power density, voltage gain, and efficiency. In this article, different mechanisms of the inductive power transfer are checked in the NHSDCs and the results are tabulated in Table VIII.

13) *Output Voltage Sensitivity*: The sensitivity of a converter output voltage with respect to the control degree of freedom (such as D) plays a crucial role in extracting the control lookup table, designing the controller and output voltage regulation accuracy. Due to the nonlinear behavior of output voltage with regard to the control degree of freedom in most of the NHSDCs, the sensitivity is not constant in different operation points. Therefore, although higher sensitivity leads to higher voltage gain in ascending diagrams, it makes the output voltage regulation

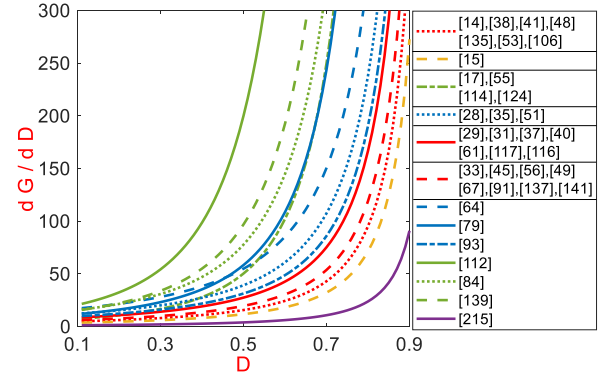


Fig. 28. Sensitivity comparison of voltage gain according to D variation.

harder and the corresponding control regions inaccessible. Note that these regions are also restricted due to higher power losses in experimental prototyping. In some literature works, the output voltage sensitivity is analyzed with its corresponding output power under the title of “output power regulation” [6]. Fig. 28 shows the sensitivity of voltage gain according to D variation (dG/dD) in some of the NHSDCs. The bidirectional topologies with high ISGC, ISGW, and ISGS in [50] and [110], the multistage topology with low ICR and high \hat{V}_D in [112], and most of the impedance source converters [217], [218], [219], [220], [221], [222], [223], [224], [225], [226], [227], [228], [229], [230], [231], [232], [233], [234], [235], [236], [237], [238], [239], [240], [241] have highly sensitive output voltage with respect to D .

The other concept in sensitivity analysis is the sensitivity of output voltage with respect to the passive components and parasitic elements values, which is highlighted in manufacturing tolerances, prototyping imprecision, and environmental changes. Regardless of ripples, switching frequency, and energy, the output voltage in the CCM operation of hard switching single-phase NHSDCs is the least sensitive to the passive components variation. Oppositely, the stresses, ripples, and voltage gain of the resonant [33], [183], [203], [208], [214], quasi-resonant [11], [23], [117], multiresonant [48], [74], [169], [194], switched-resonant [46], [57], [67], and interleaved [32], [39], [46], [82] structures are highly sensitive. The high sensitivity in the interleaved topologies can be partially or fully compensated by employing an appropriate current sharing control algorithm. In addition, the suitable operation of SC and SI cells is crucially sensitive to the similarity of the utilized capacitors and inductors values as well as their equivalent series resistance regardless of the converter type.

14) *Control Complexity*: Along with the improved configurative features of a converter, more straightforward control schemes facilitate higher flexibility, efficiency, and power density. However, control complexity is an intangible concept to be measured and compared. In other words, its evaluation with some qualitative criteria, such as “more” or “less” complex, seems to be vague. In this article, two figures of merit are introduced to ease the comparison process. The first metric is

TABLE VIII
MAGNETIC PERFORMANCE OF NHSDCS ACCORDING TO THE UTILIZED INDUCTIVE POWER TRANSFER MECHANISMS (FL: FLYBACK; FW: FORWARD; TR: TRANSFORMER-BASED; EIU: EFFICIENT INDUCTIVE UTILIZATION)

Ref	FL	FW	TR	EIU	Ref	FL	FW	TR	EIU	Ref	FL	FW	TR	EIU	Ref	FL	FW	TR	EIU
[11]	✓		✓	Yes	[50]			✓	No	[85]	✓	✓	✓	Yes	[123]	✓	✓	✓	Yes
[12]		✓	✓	No	[51]	✓		✓	Yes	[86]	✓		✓	Yes	[124]	✓			Yes
[12]	✓		✓	Yes	[52]	✓		✓	Yes	[87]	✓		✓	Yes	[125]	✓		✓	Yes
[13]			✓	No	[53]	✓	✓	✓	Yes	[88]	✓	✓	✓	Yes	[126]	✓		✓	Yes
[14]	✓		✓	Yes	[54]	✓	✓	✓	Yes	[88]	✓	✓	✓	Yes	[127]	✓		✓	Yes
[15]	✓			Yes	[55]	✓			Yes	[89]	✓	✓	✓	Yes	[128]	✓	✓	✓	Yes
[16]		✓	✓	Yes	[56]	✓	✓	✓	Yes	[90]	✓		✓	Yes	[129]	✓			No
[17]	✓	✓	✓	Yes	[57]	✓		✓	Yes	[91]	✓		✓	Yes	[130]	✓	✓		Yes
[18]			✓	No	[57]	✓		✓	Yes	[92]	✓	✓	✓	Yes	[131]	✓	✓	✓	Yes
[18]			✓	No	[57]	✓		✓	Yes	[93]			✓	No	[132]	✓	✓	✓	Yes
[19]			✓	No	[58]	✓		✓	No	[94]	✓		✓	Yes	[132]	✓	✓	✓	Yes
[20]	✓	✓	✓	Yes	[59]			✓	Yes	[95]	✓	✓	✓	Yes	[133]	✓		✓	Yes
[21]	✓		✓	Yes	[60]			✓	No	[96]	✓		✓	Yes	[134]		✓	✓	No
[22]	✓		✓	Yes	[61]	✓	✓	✓	Yes	[97]	✓	✓		Yes	[134]				No
[23]		✓	✓	No	[62]			✓	No	[98]			✓	No	[135]	✓		✓	Yes
[24]	✓		✓	Yes	[63]	✓		✓	Yes	[99]	✓		✓	Yes	[136]	✓		✓	Yes
[25]		✓	✓	No	[64]	✓	✓	✓	Yes	[100]	✓	✓	✓	Yes	[137]			✓	No
[26]	✓	✓	✓	Yes	[65]	✓	✓	✓	Yes	[101]	✓	✓	✓	Yes	[138]	✓	✓	✓	Yes
[27]	✓	✓	✓	Yes	[66]	✓		✓	Yes	[102]	✓	✓	✓	Yes	[139]	✓	✓	✓	Yes
[28]	✓	✓	✓	Yes	[67]	✓		✓	Yes	[103]			✓	No	[140]	✓		✓	Yes
[29]	✓	✓	✓	Yes	[68]	✓	✓	✓	Yes	[104]			✓	No	[141]	✓		✓	Yes
[30]	✓	✓		Yes	[69]	✓	✓	✓	Yes	[105]	✓	✓	✓	Yes	[142]	✓		✓	Yes
[31]	✓		✓	Yes	[70]	✓	✓	✓	Yes	[106]	✓		✓	Yes	[143]	✓		✓	Yes
[32]	✓	✓	✓	Yes	[71]	✓		✓	Yes	[107]			✓	No	[144]			✓	No
[33]		✓	✓	No	[72]	✓	✓	✓	Yes	[108]	✓		✓	No	[145]	✓	✓	✓	Yes
[34]		✓	✓	No	[73]	✓	✓	✓	Yes	[109]	✓		✓	Yes	[146]	✓		✓	Yes
[35]	✓		✓	Yes	[74]	✓	✓		Yes	[109]	✓		✓	Yes	[147]	✓	✓	✓	Yes
[36]	✓		✓	No	[74]	✓	✓		Yes	[110]	✓		✓	No	[148]	✓		✓	Yes
[37]	✓		✓	Yes	[74]	✓	✓		Yes	[111]	✓		✓	Yes	[149]			✓	No
[38]			✓	No	[75]	✓		✓	Yes	[112]			✓	No	[218]	✓		✓	Yes
[39]			✓	No	[75]	✓		✓	Yes	[113]	✓			Yes	[219]		✓	✓	No
[40]	✓	✓	✓	Yes	[76]	✓		✓	Yes	[114]	✓			Yes	[220]	✓	✓		Yes
[41]	✓	✓	✓	Yes	[77]	✓	✓	✓	Yes	[114]	✓			Yes	[221]	✓	✓	✓	Yes
[42]	✓	✓	✓	Yes	[78]	✓		✓	No	[115]	✓	✓		Yes	[222]	✓		✓	Yes
[43]	✓	✓	✓	Yes	[78]	✓		✓	No	[116]	✓		✓	Yes	[223]	✓		✓	Yes
[44]	✓	✓	✓	Yes	[79]			✓	No	[117]	✓	✓		Yes	[224]	✓	✓	✓	Yes
[45]	✓		✓	Yes	[80]			✓	No	[118]	✓		✓	Yes	[233]			✓	No
[46]	✓	✓	✓	Yes	[81]	✓	✓	✓	Yes	[119]	✓	✓	✓	Yes	[235]			✓	No
[47]	✓	✓	✓	Yes	[82]	✓		✓	Yes	[120]	✓	✓	✓	Yes	[236]			✓	No
[48]	✓		✓	Yes	[83]	✓		✓	Yes	[121]	✓		✓	Yes	[239]			✓	No
[49]	✓	✓	✓	Yes	[84]	✓	✓		Yes	[122]	✓		✓	Yes				✓	No

the number of operation modes (OMs) (time subintervals) of a converter, which contains some useful vision about accessible control region, acceptable operation width of the control degree of freedom, output voltage regulation range, required controller clock-pulse frequency, gate driver accuracy, and switching loss. In Table IX, the numbers of OMs are compared, where the very short time intervals of coupled inductors or built-in transformers demagnetization are ignored in some literature [51], [62], [68], [103]. According to this table, [13], [42], [46], [64], [73], [98], [181], and [208] have the most OMs. However, it should be considered that the high OM count and a more complex control scheme are sometimes the negative side effects of achieving other features. For instance, employment of active clamp circuits to meet soft switching in interleaved topologies [13], [64], [73], [98], an active clamp circuit and a leakage energy recycling mechanism to improve efficiency [42], two active resonant tanks and an SCI unit for soft switching and voltage boosting [46], a resonant cell to achieve ZVT [181], and a soft switching technique to alleviate the switching and reverse recovery losses of the main and auxiliary semiconductors [208] are the leading reasons for OM increment. On the other side, the converters with two OMs and no additional restriction on the

main switch duty cycle range (such as resonance or dead band) retain the drive and control characteristics of the conventional PWM boost converter (for example, [245], [246], [247], and [248]).

The next figure of merit is the number of series conducting semiconductors (SCS)s in the time subintervals, which affects the control complexity and power loss. The higher the SCS, the more the semiconductors conduction loss due to considering the impact of series and parallel connections of conducting semiconductors in the SCS metric. Furthermore, the SCS variation between consecutive subintervals includes some useful information about the number of total ON-OFF transitions, switching loss, control unit complexity, and required controller clock-pulse frequency. Note that this metric should be analyzed beside the semiconductors' voltage and current stresses. In Table IX, the maximum and minimum SCS values are listed for each converter. Based on this table, 1) minimum SCS of some subintervals is equal to zero in [37], [40], [53], [108], [113], and [143] in which the energy is transferred between the input source, semiconductors parallel capacitors, coupled inductors parasitic inductances, and the other passive components; 2) the presented control schemes in [15], [50], [60], [62], [67], [80],

TABLE IX
COMPARISON OF SCSs AND OMs COUNT

Ref	SCS		OM	Ref	SCS		OM	Ref	SCS		OM	Ref	SCS		OM
	min	max			min	max			min	max			min	max	
[11]	1	3	6	[65]	1	3	10	[120]	2	3	5	[185]	1	3	4
[12]	1	2	6	[66]	2	4	6	[121]	1	3	6	[186]	2	2	2
[13]	1	4	16	[67]	1	2	4	[122]	2	3	5	[187]	2	2	3
[14]	1	2	6	[68]	3	3	2	[123]	4	4	4	[188]	1	2	2
[15]	1	2	4	[69]	1	4	10	[124]	1	3	5	[189]	2	2	3
[16]	1	3	6	[70]	1	4	5	[125]	2	3	6	[190]	1	3	3
[17]	2	3	5	[71]	1	2	4	[126]	3	3	2	[191]	1	3	2
[18]	2	4	8	[72]	2	3	7	[127]	2	4	8	[192]	2	3	3
[20]	1	3	8	[73]	1	5	16	[128]	1	4	9	[193]	2	3	3
[21]	2	3	8	[74]	2	3	4	[129]	2	2	4	[194]	2	4	11
[22]	3	3	6	[75]	2	3	8	[130]	2	2	6	[197]	2	3	2
[23]	1	2	6	[76]	1	2	5	[131]	2	3	8	[198]	3	4	2
[24]	2	3	5	[77]	1	4	8	[132]	1	3	12	[200]	2	2	2
[25]	1	4	12	[78]	2	3	4	[133]	2	2	8	[201]	1	4	7
[26]	1	2	5	[79]	1	4	9	[134]	2	3	5	[203]	1	2	5
[27]	1	2	11	[80]	1	2	3	[135]	2	2	5	[204]	1	4	6
[28]	1	3	6	[81]	4	5	9	[136]	1	2	6	[205]	1	3	4
[29]	1	2	5	[82]	1	3	9	[137]	2	4	6	[207]	2	3	2
[30]	2	4	10	[83]	1	3	4	[138]	2	2	8	[208]	1	3	18
[31]	1	3	6	[84]	3	4	5	[139]	3	3	2	[209]	2	2	6
[32]	1	4	12	[85]	1	5	12	[140]	2	2	5	[210]	2	2	2
[33]	1	2	5	[86]	3	4	7	[141]	2	2	6	[211]	2	3	4
[34]	2	3	4	[87]	2	3	5	[142]	1	2	7	[212]	2	3	3
[35]	1	3	5	[88]	1	4	8	[143]	0	2	7	[213]	1	2	6
[36]	2	5	3	[89]	2	2	6	[144]	2	2	8	[214]			5
[37]	0	2	8	[90]	1	4	9	[145]	1	3	12	[215]	1	2	4
[38]	2	2	7	[91]	1	2	8	[146]	2	3	5	[216]	1	3	2
[39]	1	3	4	[92]	1	3	12	[147]	3	4	2	[217]	3	3	2
[40]	0	4	8	[93]	1	2	7	[148]	1	3	9	[219]	1	4	4
[41]	1	3	6	[94]	1	3	9	[149]	2	3	4	[220]	2	3	4
[42]	2	3	14	[95]	2	3	4	[150]	1	3	8	[221]	2	2	7
[43]	1	3	8	[96]	1	5	3	[151]	1	3	4	[222]	2	3	5
[44]	1	3	12	[97]	2	3	3	[152]	1	2	2	[223]	1	2	4
[45]	1	3	8	[98]	1	3	16	[156]	1	3	4	[224]	2	3	6
[46]	1	4	22	[99]	1	3	8	[157]	1	4	4	[225]	2	3	3
[47]	1	3	8	[100]	2	3	12	[158]	2	4	2	[226]	3	3	2
[48]	1	2	8	[101]	2	3	9	[161]	2	3	2	[227]	1	3	2
[49]	1	2	5	[102]	1	4	8	[163]	1	3	6	[228]	3	4	2
[50]	2	2	2	[103]	2	4	2	[164]	1	3	4	[229]	1	2	4
[51]			2	[105]	4	4	4	[165]	2	2	2	[230]	1	2	2
[52]	1	4	6	[106]	1	3	5	[168]	3	3	4	[231]	2	4	2
[53]	0	3	8	[107]	2	3	10	[171]	1	3	10	[232]	2	3	2
[54]	1	3	8	[108]	0	2	4	[174]	2	5	6	[233]	1	3	6
[55]	1	4	7	[109]	3	4	5	[175]	2	2	2	[234]	2	2	2
[56]	2	2	4	[109]	3	4	5	[176]	1	5	3	[235]	2	2	2
[57]	2	2	6	[110]	2	2	2	[178]	1	1	2	[236]	1	2	4
[57]	2	2	6	[111]	1	3	12	[178]	1	3	2	[237]	3	3	2
[57]	2	2	6	[112]	3	4	2	[178]	1	4	2	[238]	1	2	2
[58]	1	4	12	[113]	0	3	5	[179]	2	3	2	[238]	2	3	2
[59]	2	2	5	[114]	1	3	5	[180]	2	3	2	[238]	2	3	2
[60]	1	2	3	[115]	2	3	5	[180]	2	3	2	[239]	1	2	2
[61]	1	2	5	[116]	2	3	8	[181]	1	2	14	[240]	2	3	3
[62]	2	2	2	[117]	1	3	5	[182]	2	2	4	[240]	3	4	3
[63]	3	5	7	[118]	1	4	10	[184]	2	4	8	[241]	2	2	2
[64]	1	4	16	[119]	1	3	6	[184]	2	4	8				

[108], [110], [152], [165], [175], [178], [188], [210], [223], [230], [234], [235], [238], [239], and [241] lead to low OM and SCS values, which enable them to better control and efficiency metrics; and 3) high value for minimum or maximum SCS is not an appropriate case [36], [73], [85], [96], [176]; meanwhile, high values for both of them make the control and efficiency conditions much worse [63], [81], [105], [109], [112], [123],

[147], [158], [198], [228], [240]. In order to improve SCS effectiveness, its average form in the time subintervals is suggested as $SCS_1 D_1 + SCS_2 D_2 + \dots + SCS_{OM} D_{OM}$, where D_i and SCS_i are, respectively, the duty ratio and the number of SCSs in the subinterval "i." It is clear that $D_1 + D_2 + \dots + D_{OM} = 1$, and the improved SCS is equal to $SCS_1 \times D + SCS_2 \times (1 - D)$ for the converters with two time subintervals. Fig. 29

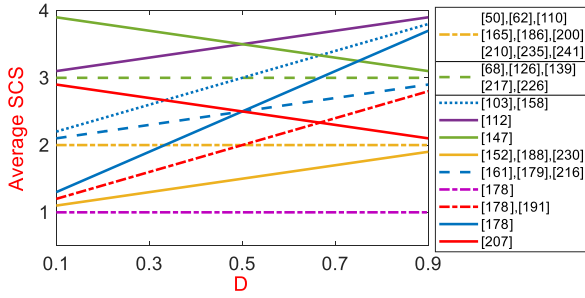


Fig. 29. Average SCSs comparison according to D variation.

demonstrates the average SCS with respect to D for some of the NHSDCs. According to this figure, SCS of “one” in OMs leads to less semiconductors power loss in [178].

One important subject that affects and is affected by the control scheme is the converter dynamics. In this two-way correlation, the converter dynamics play a significant role in the controller design and is resulted from the passive components configuration and semiconductors switching algorithm. These characteristics affect the converter transients, step-change response, output voltage regulation, and efficiency. It is worth to mention that the dynamic comparison of topologies should be done with the same condition of the passive components values’ and switching frequency. The higher the passive components values, the slower the dynamics and the lower ripples.

15) *Reliability*: Among the figures of merit, reliability analysis is the most emerging, which reflects some probabilistic data from the devices’ and converters’ mean time to failure, aging, degradation, maintenance, and repair cycles. In simple words, reliability estimates the lifetime of a converter and predicts its vulnerable components (or submodules) against faults according to the topology, control scheme, and experimental implementation. As some general rules, the series connection of components or submodules increases a converter’s total breakdown probability and decreases the reliability metric. Thus, cascading and using VMC worsen this figure of merit. On the other side, redundancy and parallel connection improve the reliability where interleaving and employment of multilevel structures are some examples (see Table IV). In [242], the reliability of an interleaved soft switching topology is modeled, analyzed, and compared with its SS configuration. Note that, as depicted in Fig. 30, reliability metrics in power electronics can be evaluated in the system, converter, and device levels, where the converter level is mainly concentrated in this article.

To be more detail, power loss distribution among components, components voltage and current safety margins, environmental conditions, devices materials’, PCB layout, failure modes, fault detection, fault tolerance, fault clearance, and derated power states are some of the considerable subjects in reliability analytics. From the analysis and comparison point of view, the same condition of efficiency calculation (discussed previously) should be considered in the reliability assessment. In [249], [250], [251], [252], [253], [254], and [255], some guidelines are given about the principles, modeling, analyses, and evaluation of

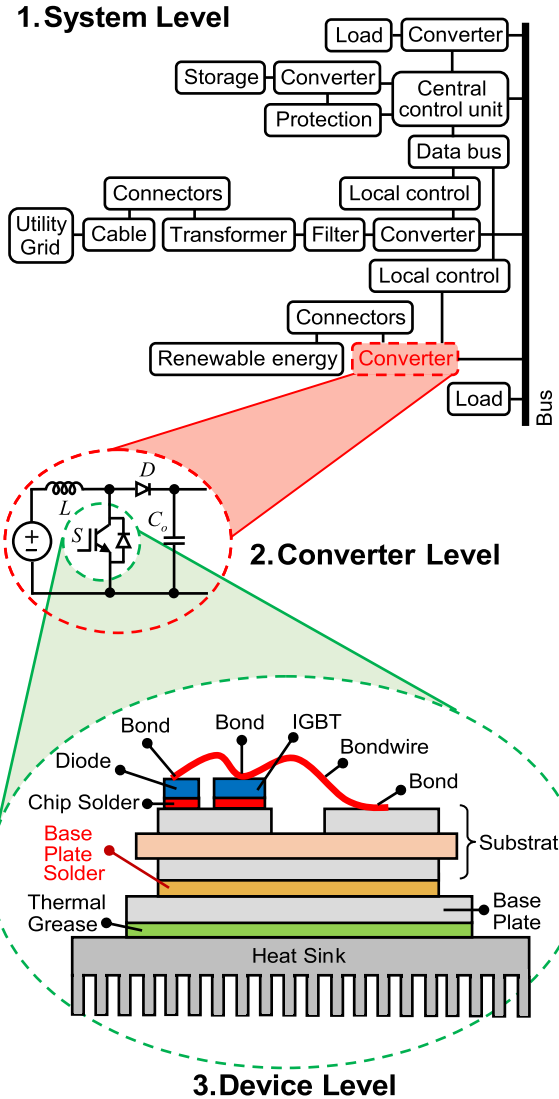


Fig. 30. Reliability evaluation levels in power electronics.

the reliability metric. Moreover, in [256] and [257], as two comprehensive review papers, some materials are provided about the lifetime and fault management techniques, respectively, to improve reliability in the power electronic converters. Some of the main topics in these literature works are failure mechanisms, failure modes, lifetime prediction, damage accumulation, parameter estimation, electrothermal modeling, fault compensation, redundancy methods, and unbalanced compensation. According to [249], [250], [251], [252], [253], [254], [255], [256], and [257], more reliable converters usually require higher cost; therefore, the reliability cost function is a determinative criterion in the optimized design of a converter. As a suggestion of this article, $\alpha_G \hat{G} - \alpha_C \hat{Cost} - \alpha_S \hat{Size} + \alpha_R \hat{Rel}$. is an applicable multiobjective figure of merit to assess converters if the same evaluation condition is considered for all of them. Note that, \hat{Rel} . is the normalized reliability, which is calculated as same as ISGC, ISGW, and ISGS. In addition, α_G , α_C , α_S , and α_R

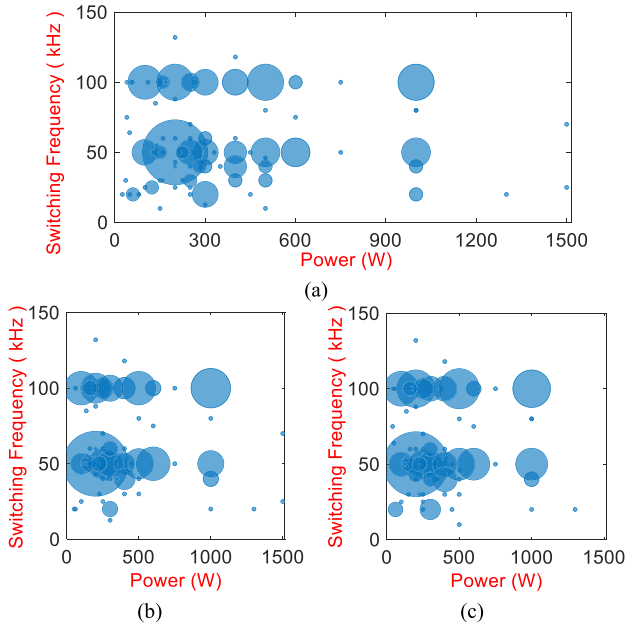


Fig. 31. Frequency versus power distribution. (a) All NHSDCs. (b) CI-based converters. (c) VMC-based converters.

coefficients are selected based on the application and design requirements.

16) *Power Versus Switching Frequency*: The P_o and f_s values are specified based on the converter application, components capability, and topological features. According to the components' operation limitations, these mutually incompatible design criteria usually cannot be selected in high values simultaneously. In other words, since the nominal current and voltage values and turn ON-OFF delays cannot be improved simultaneously in a semiconductor at least with nowadays technology, it is challenging to design a high-power converter with high f_s and vice versa. Moreover, large ΔV and ΔI and short switching transition periods lead to high voltage and current spikes, high parasitic components voltage drop, challenging protection considerations, and high power loss due to large dV/dt and dI/dt values, which restrict f_s increment in high power ranges. For example, the converters in [178] and [202] are designed for 40 W/100 kHz and 1 MW/4 kHz, respectively. Fig. 31 illustrates the f_s versus P_o bubble charts of the converters where Fig. 31(a)-(c) are dedicated to all NHSDCs, CI-based and VMC-based topologies. Although the design and implementation of the converters in literature are usually in the form of laboratory prototypes, the P_o versus f_s ratio gives some helpful design viewpoints. According to this figure, 200 W/50 kHz is mostly repeated in the NHSDCs. Furthermore, the similarity between Fig. 31(b) and (c) is caused by the simultaneous usage of CIs and VMCs in the converters.

IV. SPECIAL TYPES OF THE NHSDCS

According to the limited duty cycle range of impedance source converters (identified in Table I in the column named IS) and the variable configuration of extendable converters due to the

number of extended stages, these two groups are discussed in this separate section.

A. Impedance Source Converters

Since the first ZS network was presented in 2003 [258], many researchers have intended to improve its functionality by increasing boost factor (voltage gain), power range, and efficiency and decreasing components count, dead time, and stresses. These studies have resulted in some impedance source topologies, such as quasi-ZS, switched-ZS, embedded-ZS, semi-ZS, coupled inductor ZS, trans-ZS, Y-source, A-source, Γ -source, T-source, and Γ -ZS converters [259]. The improvement methodologies and techniques in the impedance source converters are as same as in the other NHSDCs. For instance, adding a passive clamp circuit to a ZS topology [217], an active soft switching tank and an SCI unit to a coupled inductor ZS topology [218], an SC or an SCI unit to a quasi-ZS topology [220], [224], [234], [237], a stacked configuration to a ZS or a quasi-ZS topology [221], [235], an SCI unit to a coupled inductor ZS topology [223], an SC or an SCI unit to a ZS topology [227], [232], the bidirectional operation feature to a ZS topology [229], [237], the CG operation feature to a ZS topology [230], an SC to a Sepic-based quasi-ZS topology [231], the resonance operation feature to a quasi-ZS topology [233], and a cascaded boost converter to a quasi-ZS topology [241] are some of these enhancement methodologies.

Dissimilar to the other types of VF(CF) converters, the ZS-based VF(CF) topologies cope with shoot-through(open circuit). The main features of these converters are listed as follows.

- 1) acceptable performance against EMI;
- 2) applicability as a voltage boosting interface of inverters in a cascaded structure;
- 3) current source behavior of the output port in the shoot-through modes;
- 4) modularity;
- 5) low- and medium-power applications.

Meanwhile, high current stress of impedance network components, high voltage stress of the main switch and output rectifier semiconductors, limited power range, high sensitivity of the output port voltage to the duty cycle in some control regions (hard output voltage regulation), limited duty cycle range, lack of CG in conventional structures, startup inrush current, and high ICR are the most considerable shortcomings or drawbacks [225]. The major applications of the impedance source topologies are low-power microgrids, adjustable speed drives, renewable energies, and UPS systems [259]. Note that the presented converters in [222] and [228] do not match the impedance source topologies' fundamental definition; however, their operation has some similarities to the impedance source. Thus, they are studied in this section.

In Fig. 32, operational features of the impedance source converters are compared in which voltage gain, \hat{V}_S , \hat{V}_D , \hat{V}_C , and the f_s versus P_o plots are expressed in Fig. 32(a)-(i), respectively. According to these figures, the following are concluded.

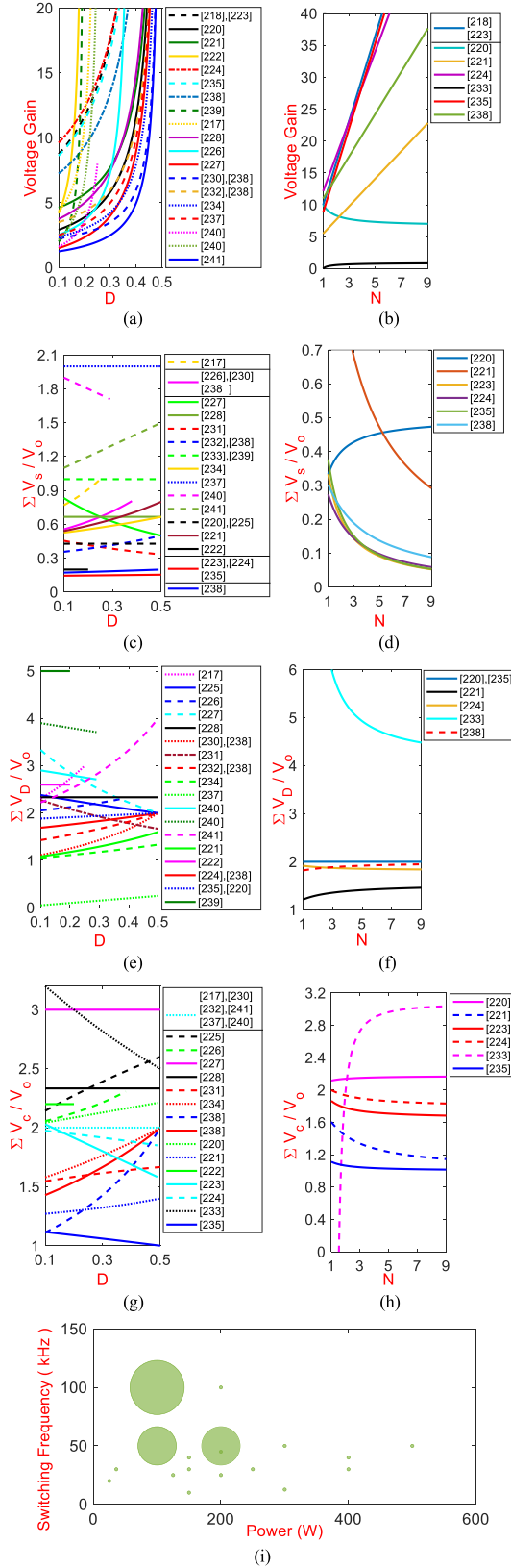


Fig. 32. Evaluation of impedance source NHSDCs with regard to D and N . (a), (b) Voltage gain. (c), (d) Normalized accumulative switches voltage stress. (e), (f) Normalized accumulative diodes voltage stress. (g), (h) Normalized accumulative capacitors voltage stress. (i) Frequency versus power.

- 1) The operation range of these converters is limited with respect to the D variation, which is the most in [217], [222], [239], and [240]. Although they provide high voltage gain, hard output voltage control restricts their industrial application.
- 2) The converters in [218], [223], [224], and [235] present the highest voltage gain with respect to N variation.
- 3) Unlike the voltage gain plots, \hat{V}_S , \hat{V}_D , and \hat{V}_C may have direct, inverse, or no relation with regards to D .
- 4) The \hat{V}_S is the lowest in [222], [223], [224], [235], and [238], which is mainly caused by the placement of passive VMCs close to the output high voltage port [222], [223], [224], utilizing multilevel structures [224], [235] and high output voltage as the base value for the normalization of \hat{V}_S [222].
- 5) The \hat{V}_S is the highest in [237], which is independent of D .
- 6) The \hat{V}_D is the highest and the lowest in [239], [240] and [234], [237], respectively.
- 7) In [237], high and low values of \hat{V}_S and \hat{V}_D , respectively, are resulted from the usage of six switches and one diode in a bidirectional topology. Meanwhile, $\hat{V}_S + \hat{V}_D$ is not high in [237].
- 8) Generally, from the voltage gain and voltage stress points of view, the work presented in [235] is the most desired candidate.
- 9) The design consideration of 100 W/100 kHz is the most trending in the impedance source converters.

B. Extendable Converters

The extension is a promising solution to accomplish high voltage and high power values, which is usually satisfied through interleaving [164], multistage structure [159], [160], multilevel connection [19], [150], [195], [202], VMC extension [47], [75], [78], [88], [151], [153], [154], [155], [158], [162], [164], [166], [167], or the combination of these approaches [18], [206]. Fig. 33(a)–(d) shows voltage gain, \hat{V}_S , \hat{V}_D , and \hat{V}_C of the extendable NHSDCs, respectively, in which the number of extended cells is assumed as $K = 3$. Based on these figures, the introduced topologies in [75], [63], [88], [199] and [153], [158] are the most desired with respect to the voltage gain, \hat{V}_S , \hat{V}_D , and \hat{V}_C , respectively.

V. DISCUSSION, OUTLOOK, AND CONCLUSION

This article aimed to review and evaluate the NHSDCs, as well as their associated voltage boosting and conditioning techniques, from various topological and operational points of view. It was tried to assess all the high-impact factor literature published after 2010. Unlike the other review papers, operation fundamentals discussion and classification of voltage boosting techniques were presented very concisely, and it was mainly focused on these techniques' merits and demerits. As one of the outstanding features of this article, the converters were redesigned under the same operation framework to counteract various design considerations and assumptions of each literature

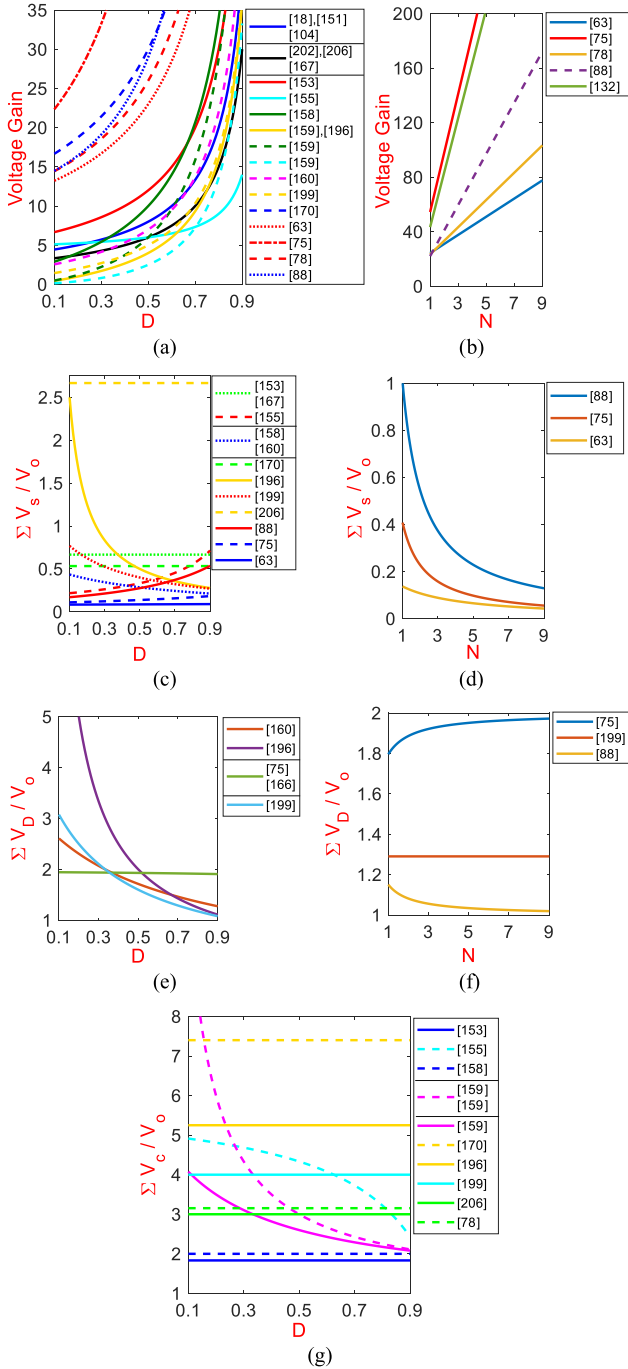


Fig. 33. Evaluation of extendable NHSDCs with regard to D and N . (a), (b) Voltage gain. (c), (d) Normalized accumulative switches voltage stress. (e), (f) Normalized accumulative diodes voltage stress. (g) Normalized accumulative capacitors voltage stress.

and to provide as real and fair comparison as possible. Each comparison section was followed with a comprehensive discussion to help readers deduce the pros and cons of the topologies more deeply. Moreover, the applications of each methodology were mentioned. Then, the article presented a holistic guideline for a fair comparison of not only the NHSDCs but also the whole power electronic converters. According to the industrial

applications and research literature, the NHSDCs have attracted one of the largest shares of investments and publications. New structures with various features have been continuously introduced, where most of them are the reconfiguration of previous methodologies. In this condition, evaluation of these methodologies is a bit confusing, challenging, and biased, which highlights the importance of effectiveness assessment of current figures of merit. After their extensive investigation, some improved metrics toward reliable comparison studies were proposed in this article.

Focusing on the NHSDCs and the employed techniques comparison study, some of the practical conclusions are as follows.

- 1) Using the minimum number of switches simplifies the control algorithm, decreases the OM count, and widens the duty cycle range, which is implementable in most NHSDCs. However, it imposes a high number of diodes usage that may magnify their reverse recovery effect and conduction loss. To accomplish high voltage gain with one switch, at least four diodes are required. The presented converters in [145] and [214] owe the most semiconductors, both of which are the interleaved topologies with soft switching mechanisms of passive clamp or resonant tanks.
- 2) Except for the synchronous PWM boost topology, which is not considered as a high step-up converter, at least three switches are needed for bidirectional NHSDCs.
- 3) Using one single-winding inductor is rarely preferred in the NHSDCs. In addition, coupled inductors are generally more proper choices than inductors where the best number of coupled windings is better to be selected based on the cooptimization of topological and operational criteria.
- 4) As the main reasons, interleaving and using separated clamp circuits and high-order SC units result in high capacitors count; meanwhile, interleaving, using resonant tanks and SI units, increases inductors count.
- 5) Simultaneous employment of at least two of the following techniques, units or circuits, is the main reason for the high components count in the NHSDCs: interleaving, VMCs, SC and SI units, integrated cells, stacked structures, soft switching tanks, voltage clamps, and snubber circuits. Moreover, from the configuration point of view, the components count will be high if multistage, interleaved, and (or) multilevel structures are coimplemented.
- 6) According to the reviewed literature, the converters with the highest voltage gain do not employ the highest number of components, which highlights the superiority of appropriate configuration style over the coimplementation of various voltage boosting techniques. In other words, high voltage gain with the desired operation characteristics is usually met by the wise coimplementation of capacitive and magnetic approaches, where coupled inductors and SCI are the most favorite candidates.

- 7) Extended interleaved CF topologies are the most desired converters with regard to ICR; however, their components count is high. On the other hand, VF topologies with discontinuous or partially negative input current are the worst cases. Although claimed in some literature works, they have limited applicability in the renewable energy systems. This is also valid for the FG configurations.
- 8) The maximum value of the normalized ICR usually occurs in $0.5 \geq D$, which is far from the preferred duty cycle range of the NHSDCs. Moreover, the higher the N , usually the lower the normalized ICR.
- 9) Using more than one SC, SI, and SCI technique improves the converter voltage gain; however, it does not guarantee high ISGC, ISGW, and ISGS values.
- 10) Voltage gain increases nonlinearly with the increment of D in the NHSDCs; however, \hat{V}_S , \hat{V}_D , and \hat{V}_C may have direct, inverse, or no relation with respect to D . The ramp of the voltage gain diagram is very high in some topologies, such as [50], [110], and [112], and most of the impedance source converters, which increases the voltage gain, restricts the applicable D range and hardens the control process.
- 11) According to N variation, most of the voltage gain profiles are linear with direct relation. However, \hat{V}_S decreases (nonlinearly) with the N increment except in some limited cases.
- 12) The main reasons for high \hat{V}_S are high switches count, using switches close to the output high-voltage port, and low voltage gain. Furthermore, low \hat{V}_S is more probable in the CF converters.
- 13) Achieving soft switching conditions by adding some auxiliary components does not guarantee lower total power loss in all operation regions due to the increment of conduction losses. Hence, an optimized operation region should be considered in the design procedure.
- 14) Employment of all FL, FW, and transformer-based mechanisms in a converter leads to higher efficiency, higher voltage gain, better magnetizing and leakage energy recycling, higher power density, and more efficient inductive utilization.
- 15) In the cascaded structures with independent control capability of stages, it is highly suggested to design the switching frequency of stages based on the cooptimized efficiency, reliability, stresses, size, weight, cost, and voltage gain results. This kind of cooptimization is helpful to determine the number of multilevel and interleaved stages, VMC order, number of extended cells, resonant tank characteristics, clamp and snubber circuits specifications, and components voltage and current safety margins.

Moreover, from the metrics applicability evaluation point of view, some of the main outcomes are summarized in the following.

- 1) The number of components count, of any kind, is not a respectable and reliable metric to assess converters;

the count of components from a single category, such as switches count, lacks the data of other components, and the total components count is a UCC without any real-world objectivity. These numbers should be transformed into some physical concepts, such as cost, size, and weight. In this article, some multiobjective figures of merit with different types of normalization forms were proposed and widely evaluated, some of which are ISGC, ISGW, and ISGS.

- 2) A high number of components and OMs, or high values of current and voltage stresses, should not be evaluated separately from the converters' other features. Sometimes, these demerits are the negative side effects of other operational and topological accomplishments.
- 3) According to some considerations, passive components and cooling systems are the most effective criteria on the converter's volume and weight, which can be used in the simplified comparison studies.
- 4) Similar to any engineering system, each converter has pros and cons, where their superiority is defined based on the application and design considerations. Therefore, the comparison study should be specified based on the applications.
- 5) As done in this article, redesign of the compared converters is required for a fair and proper evaluation. For most of the figures of merit, a fair and reliable comparison is satisfied in the same design specifications, such as nominal power, duty cycle, switching frequency, components characteristics', and thermal considerations. In other words, some of the comparison results in the previously published literature, which are provided under different operational and design conditions of converters, are incomplete or invalid.
- 6) The \hat{V}_S , \hat{I}_S , and SUF can reflect some useful data from the switch operation characteristics if \hat{V}_S and \hat{I}_S are normalized with respect to the output voltage and input current, respectively. The SUF metric is generalized by considering the summation of SUF and DUF for all semiconductors.
- 7) The input current and OVRs should be compared in their normalized form by considering the effects of switching frequency, duty cycle, input filter inductor, output filter capacitor, voltage gain, output power, and the number of output port levels and interleaved stages. The component's energy factor has the same comparison requirement.
- 8) Efficiency and reliability are two of the most challenging issues in the comparison studies that have been done inaccurately or improperly in some literature works. In other words, their evaluation is not as simple as done in some papers by comparing a single operation point, maximum values, or full load point under different operational and topological characteristics. To provide a valid comparison, the effects of nominal power, output voltage, duty cycle range, switching frequency, ripples, thermal considerations, and components voltage and current safety margins should be taken into account.

Moreover, the components should be selected with the same material, family, and characteristics for all compared topologies. Note that different combinations of design and control degrees of freedom lead to a certain output power range with different efficiency and reliability behavior. This makes the assessment more confusing; therefore, the degree of freedom should be the same to sweep the power values in all compared converters.

- 9) Operation in one or two quadrants of the B - H plane, utilization of FL, FW, and transformer-based mechanisms, and the normalized energy are the most applicable criteria to investigate the magnetic components operation. These simple metrics provide some information about power density, parasitic inductances' energy harvest, efficiency, and size.
- 10) Using the statement of “more” or “less” control complexity is not an appropriate approach for evaluation. Instead, OM, SCS, and average SCS were proposed in this article to evaluate control complexity and efficiency.
- 11) An example of relatively simple and comprehensive figure of merit, $\alpha_C \hat{G} - \alpha_C \hat{Cost} - \alpha_S \hat{Size} + \alpha_R \hat{Rel}$. was proposed. Weight and efficiency are excluded in this function since they are not completely independent of size and reliability, respectively.
- 12) The P_o versus f_s diagram helps to select the best ratio in the design procedure.
- 13) Multiobjective figures of merit are generally more reliable than single-objective ones. However, some of the single-objective metrics may include helpful information if they are provided within a fair evaluation condition.

As comprehensively studied in this article and according to the most recent publications in 2022 and 2023 [260], [261], [262], [263], [264], [265], [266], [267], [268], [269], [270], [271], [272], [273], [274], [275], [276], [277], most of these NHSDCs are the permutation or recombination of the current–voltage boosting techniques, which reveal itself in the frequent comment of the reviewers about the lack of novelty in the peer-review process. In addition, the current topologies have acceptably high voltage gain, and increasing the voltage gain to much higher values is not practical in most of the cases. Therefore, the helpful and probable prospects of these converters are toward finding new applications, matching the converter's features with their application requirements, developing bidirectional operation capabilities, enhancing the converter's dynamics and control features, decreasing the converter operation sensitivity to the components' precise values, widening the operation range, facilitating modularity and multiport operation with appropriate and independent power flow control of ports, improving reliability (fault tolerance) and power density, increasing the nominal power by suppressing the drawbacks such as high spikes and stresses, investigating the behavior of the converters with high switching frequencies in the presence of new magnetic materials, planar transformers and widebandgap semiconductors, analyzing and optimizing the effects of parasitic components in different switching frequency ranges, and easing the implementation process with low cost.

APPENDIX

A. Citing of Converters for the References With More Than One Topology

In some papers, more than one topology have been presented, which are listed as follows.

Ref. [R]	Converter cite in this paper	Converter figure in Ref. [R]	Ref. [R]	Converter cite in this paper	Converter figure in Ref. [R]
[12]	[12]	Fig. 3(b)	[134]	[134]	Fig. 1
	[12]	Fig. 3(c)		[134]	Fig. 14
[18]	[18]	Fig. 6	[150]	[150]	Fig. 5
	[18]	Fig. 2		[150]	Fig. 1
[47]	[47]	Fig. 2	[151]	[151]	Fig. 4
	[47]	Fig. 1		[151]	Fig. 3(f)
[57]	[57]	Fig. 2(a)	[158]	[158]	Fig. 3
	[57]	Fig. 2(b)		[158]	Fig. 2
	[57]	Fig. 2(c)		[159]	Fig. 8
[63]	[63]	Fig. 4	[159]	[159]	Fig. 13(a)
	[63]	Fig. 2(b)		[159]	Fig. 14
[74]	[74]	Fig. 1(a)	[164]	[164]	Fig. 1
	[74]	Fig. 1(b)		[164]	Fig. 5
	[74]	Fig. 6		[164]	Fig. 6
[75]	[75]	Fig. 3	[178]	[178]	Fig. 2(a)
	[75]	Fig. 1		[178]	Fig. 2(b)
[78]	[78]	Fig. 4	[180]	[178]	Fig. 2(c)
	[78]	Fig. 1		[180]	Fig. 3(a)
[88]	[88]	Fig. 3	[184]	[180]	Fig. 3(b)
	[88]	Fig. 1		[184]	Fig. 1(b)
[109]	[109]	Fig. 1(a)	[184]	[184]	Fig. 1(c)
	[109]	Fig. 1(c)		[193]	Fig. 2
[114]	[114]	Fig. 2(a)	[193]	[193]	Fig. 3
	[114]	Fig. 2(b)		[238]	Fig. 2(b)
[132]	[132]	Fig. 1(c)	[238]	[238]	Fig. 3(b)
	[132]	Fig. 1(b)		[238]	Fig. 4(b)
			[240]	[240]	Fig. 2
			[240]	[240]	Fig. 5

B. Calculation Example

In order to clarify the calculations and redesign characteristics of the NHSDCs in Table I, the design metrics are presented for [76] as an example, where IRFP260N, TLP250, LM7815, BYV44-400, EE55, and 400 V–33 μ F capacitors are selected for the switch (S), gate driver (GD), fixed voltage regulator (FVR), diode (D), inductor (L), and capacitor (C). Note that the core, bobbin, and windings are considered for each inductor. Moreover, “HS” represents the heatsink. Based on these redesign characteristics, the calculations for the cost, weight, size, FGC, SGC, ISGC, ISGW, and ISGS are as follows:

$$\begin{aligned} \text{Cost} &= \sum \text{Cost} (S + \text{GD} + \text{FVR} + D + L + C + \text{HS}) \\ &= 2.95 + 1.73 + 0.55 + 3.6 + 15.26 + 2.3 + 7.4 = 33.79 \text{€} \end{aligned}$$

$$\begin{aligned} \text{Weight} &= \sum \text{Weight} (S + \text{GD} + \text{FVR} + D + L + C + \text{HS}) \\ &= 5.5 + 2 + 2 + 11 + 260.6 + 10 + 83.7 = 374.8 \text{g}. \end{aligned}$$

$$\begin{aligned} \text{Size} &= \sum \text{Size} (S + \text{GD} + \text{FVR} + D + L + C + \text{HS}) \\ &= 2120 + 320 + 900 + 1786 + 132182.4 + 2009.6 + 50625 \\ &= 189\,943 \text{mm}^3 \end{aligned}$$

$$FGC = 13.33/33.79 = 0.3944$$

$$SGC = (13.33/159.25) - (33.79/102.39) = -0.2436$$

$$ISGC = \frac{13.33 - 3.33}{159.25 - 3.33} - \frac{33.79 - 33.79}{102.39 - 33.79} = 0.0641$$

$$ISGW = \frac{13.33 - 3.33}{159.25 - 3.33} - \frac{374.8 - 374.8}{1207.3 - 374.8} = 0.0641$$

$$ISGS = \frac{13.33 - 3.33}{159.25 - 3.33} - \frac{189943 - 189943}{601980 - 189943} = 0.0641.$$

REFERENCES

- [1] W. Li and X. He, "Review of nonisolated high-step-up DC/DC converters in photovoltaic grid-connected applications," *IEEE Trans. Ind. Electron.*, vol. 58, no. 4, pp. 1239–1250, Apr. 2011.
- [2] F. L. Tofoli, D. de Castro Pereira, W. J. de Paula, and D. de Sousa Oliveira Júnior, "Survey on non-isolated high-voltage step-up DC–DC topologies based on the boost converter," *IET Power Electron.*, vol. 8, no. 10, pp. 2044–2057, 2015.
- [3] Y. Guan, C. Cecati, J. M. Alonso, and Z. Zhang, "Review of high-frequency high-voltage-conversion-ratio DC–DC converters," *IEEE J. Emerg. Sel. Topics Ind. Electron.*, vol. 2, no. 4, pp. 374–389, Oct. 2021.
- [4] H. Liu, H. Hu, H. Wu, Y. Xing, and I. Batarseh, "Overview of high-step-up coupled-inductor boost converters," *IEEE J. Emerg. Sel. Topics Power Electron.*, vol. 4, no. 2, pp. 689–704, Jun. 2016.
- [5] A. M. S. S. Andrade, E. Mattos, L. Schuch, H. L. Hey, and M. L. da Silva Martins, "Synthesis and comparative analysis of very high step-up DC–DC converters adopting coupled-inductor and voltage multiplier cells," *IEEE Trans. Power Electron.*, vol. 33, no. 7, pp. 5880–5897, Jul. 2018.
- [6] L. Schmitz, D. C. Martins, and R. F. Coelho, "Comprehensive conception of high step-up DC–DC converters with coupled inductor and voltage multipliers techniques," *IEEE Trans. Circuits Syst. I, Reg. Papers*, vol. 67, no. 6, pp. 2140–2151, Jun. 2020.
- [7] J. M. de Andrade, M. A. Salvador, R. F. Coelho, and T. B. Lazzarin, "General method for synthesizing high gain step-up DC–DC converters based on differential connections," *IEEE Trans. Power Electron.*, vol. 35, no. 12, pp. 13239–13254, Dec. 2020.
- [8] M. A. Salvador, J. M. de Andrade, T. B. Lazzarin, and R. F. Coelho, "Methodology for synthesis of high-gain step-up DC–DC converters based on differential connections," *Int. J. Circuit Theory Appl.*, vol. 49, no. 2, pp. 306–326, 2021.
- [9] M. Forouzesh, Y. P. Siwakoti, S. A. Gorji, F. Blaabjerg, and B. Lehman, "Step-up DC-DC converters: A comprehensive review of voltage-boosting techniques, topologies, and applications," *IEEE Trans. Power Electron.*, vol. 32, no. 12, pp. 9143–9178, Dec. 2017.
- [10] M. S. Bhaskar et al., "Survey of DC-DC non-isolated topologies for unidirectional power flow in fuel cell vehicles," *IEEE Access*, vol. 8, pp. 178130–178166, 2020.
- [11] S. Hasanpour, M. Forouzesh, Y. P. Siwakoti, and F. Blaabjerg, "A novel full soft-switching high-gain DC/DC converter based on three-winding coupled-inductor," *IEEE Trans. Power Electron.*, vol. 36, no. 11, pp. 12656–12669, Nov. 2021.
- [12] K.-B. Park, G.-W. Moon, and M.-J. Youn, "Nonisolated high step-up stacked converter based on boost-integrated isolated converter," *IEEE Trans. Power Electron.*, vol. 26, no. 2, pp. 577–587, Feb. 2011.
- [13] W. Li, W. Li, X. He, D. Xu, and B. Wu, "General derivation law of nonisolated high-step-up interleaved converters with built-in transformer," *IEEE Trans. Ind. Electron.*, vol. 59, no. 3, pp. 1650–1661, Mar. 2012.
- [14] Y.-P. Hsieh, J.-F. Chen, T.-J. Liang, and L.-S. Yang, "A Novel high step-up DC–DC converter for a microgrid system," *IEEE Trans. Power Electron.*, vol. 26, no. 4, pp. 1127–1136, Apr. 2011.
- [15] G. M. L. Chu, D. D. C. Lu, and V. G. Agelidis, "Flyback-based high step-up converter with reduced power processing stages," *IET Power Electron.*, vol. 5, no. 3, pp. 349–357, Mar. 2012.
- [16] K.-C. Tseng, C.-C. Huang, and W.-Y. Shih, "A high step-up converter with a voltage multiplier module for a photovoltaic system," *IEEE Trans. Power Electron.*, vol. 28, no. 6, pp. 3047–3057, Jun. 2013.
- [17] S.-M. Chen, T.-J. Liang, L.-S. Yang, and J.-F. Chen, "A Cascaded high step-up DC–DC converter with single switch for microsource applications," *IEEE Trans. Power Electron.*, vol. 26, no. 4, pp. 1146–1153, Apr. 2011.
- [18] S. Park, Y. Park, S. Choi, W. Choi, and K.-B. Lee, "Soft-switched interleaved boost converters for high step-up and high-power applications," *IEEE Trans. Power Electron.*, vol. 26, no. 10, pp. 2906–2914, Oct. 2011.
- [19] S. V. Araujo, R. P. Torrico-Bascope, and G. V. Torrico-Bascope, "Highly efficient high step-up converter for fuel-cell power processing based on three-state commutation cell," *IEEE Trans. Ind. Electron.*, vol. 57, no. 6, pp. 1987–1997, Jun. 2010.
- [20] W. Li, Y. Zhao, Y. Deng, and X. He, "Interleaved converter with voltage multiplier cell for high step-up and high-efficiency conversion," *IEEE Trans. Power Electron.*, vol. 25, no. 9, pp. 2397–2408, Sep. 2010.
- [21] Y. Zhao, X. Xiang, C. Li, Y. Gu, W. Li, and X. He, "Single-phase high step-up converter with improved multiplier cell suitable for half-bridge-based PV inverter system," *IEEE Trans. Power Electron.*, vol. 29, no. 6, pp. 2807–2816, Jun. 2014.
- [22] N. Molavi, E. Adib, and H. Farzanehfar, "Soft-switched non-isolated high step-up DC-DC converter with reduced voltage stress," *IET Power Electron.*, vol. 9, no. 8, pp. 1711–1718, 2016.
- [23] K.-B. Park, G.-W. Moon, and M.-J. Youn, "High step-up boost converter integrated with a transformer-assisted auxiliary circuit employing quasi-resonant operation," *IEEE Trans. Power Electron.*, vol. 27, no. 4, pp. 1974–1984, Apr. 2012.
- [24] A. Ajami, H. Ardi, and A. Farakhor, "A novel high step-up DC/DC converter based on integrating coupled inductor and switched-capacitor techniques for renewable energy applications," *IEEE Trans. Power Electron.*, vol. 30, no. 8, pp. 4255–4263, Aug. 2015.
- [25] W. Li, W. Li, X. Xiang, Y. Hu, and X. He, "High step-up interleaved converter with built-in transformer voltage multiplier cells for sustainable energy applications," *IEEE Trans. Power Electron.*, vol. 29, no. 6, pp. 2829–2836, Jun. 2014.
- [26] S.-M. Chen, T.-J. Liang, L.-S. Yang, and J.-F. Chen, "A safety enhanced, high step-up DC–DC converter for AC photovoltaic module application," *IEEE Trans. Power Electron.*, vol. 27, no. 4, pp. 1809–1817, Apr. 2012.
- [27] H.-W. Seong, H.-S. Kim, K.-B. Park, G.-W. Moon, and M.-J. Youn, "High step-up DC-DC converters using zero-voltage switching boost integration technique and light-load frequency modulation control," *IEEE Trans. Power Electron.*, vol. 27, no. 3, pp. 1383–1400, Mar. 2012.
- [28] Y.-P. Hsieh, J.-F. Chen, T.-J. Liang, and L.-S. Yang, "Novel high step-up DC–DC converter with coupled-inductor and switched-capacitor techniques," *IEEE Trans. Ind. Electron.*, vol. 59, no. 2, pp. 998–1007, Feb. 2012.
- [29] Y.-P. Hsieh, J.-F. Chen, T.-J. Liang, and L.-S. Yang, "Novel high step-up DC–DC converter for distributed generation system," *IEEE Trans. Ind. Electron.*, vol. 60, no. 4, pp. 1473–1482, Apr. 2013.
- [30] L.-S. Yang, T.-J. Liang, H.-C. Lee, and J.-F. Chen, "Novel high step-up DC–DC converter with coupled-inductor and voltage-doubler circuits," *IEEE Trans. Ind. Electron.*, vol. 58, no. 9, pp. 4196–4206, Sep. 2011.
- [31] B. Axelrod, Y. Beck, and Y. Berkovich, "High step-up DC–DC converter based on the switched-coupled-inductor boost converter and diode-capacitor multiplier: Steady state and dynamics," *IET Power Electron.*, vol. 8, no. 8, pp. 1420–1428, Feb. 2015.
- [32] W. Li, Y. Zhao, J. Wu, and X. He, "Interleaved high step-up converter with winding-cross-coupled inductors and voltage multiplier cells," *IEEE Trans. Power Electron.*, vol. 27, no. 1, pp. 133–143, Jan. 2012.
- [33] Y. Deng, Q. Rong, W. Li, Y. Zhao, J. Shi, and X. He, "Single-switch high step-up converters with built-in transformer voltage multiplier cell," *IEEE Trans. Power Electron.*, vol. 27, no. 8, pp. 3557–3567, Aug. 2012.
- [34] C.-M. Lai, C.-T. Pan, and M.-C. Cheng, "High-efficiency modular high step-up interleaved boost converter for DC-microgrid applications," *IEEE Trans. Ind. Appl.*, vol. 48, no. 1, pp. 161–171, Jan./Feb. 2012.
- [35] Y.-P. Hsieh, J.-F. Chen, T.-J. P. Liang, and L.-S. Yang, "Novel high step-up DC–DC converter with coupled-inductor and switched-capacitor techniques for a sustainable energy system," *IEEE Trans. Power Electron.*, vol. 26, no. 12, pp. 3481–3490, Dec. 2011.
- [36] S. Dwari and L. Parsa, "An efficient high-step-up interleaved DC–DC converter with a common active clamp," *IEEE Trans. Power Electron.*, vol. 26, no. 1, pp. 66–78, Jan. 2011.
- [37] I. Laird and D. D.-C. Lu, "High step-up DC/DC Topology and MPPT algorithm for use with a thermoelectric generator," *IEEE Trans. Power Electron.*, vol. 28, no. 7, pp. 3147–3157, Jul. 2013.
- [38] K. I. Hwu and Y. T. Yau, "High step-up converter based on coupling inductor and bootstrap capacitors with active clamping," *IEEE Trans. Power Electron.*, vol. 29, no. 6, pp. 2655–2660, Jun. 2014.

- [39] C.-T. Pan and C.-M. Lai, "A high-efficiency high step-up converter with low switch voltage stress for fuel-cell system applications," *IEEE Trans. Ind. Electron.*, vol. 57, no. 6, pp. 1998–2006, Jun. 2010.
- [40] S.-K. Changchien, T.-J. Liang, J.-F. Chen, and L.-S. Yang, "Novel high step-up DC–DC converter for fuel cell energy conversion system," *IEEE Trans. Ind. Electron.*, vol. 57, no. 6, pp. 2007–2017, Jun. 2010.
- [41] K.-C. Tseng, J.-T. Lin, and C.-C. Huang, "High step-up converter with three-winding coupled inductor for fuel cell energy source applications," *IEEE Trans. Power Electron.*, vol. 30, no. 2, pp. 574–581, Feb. 2015.
- [42] M. Forouzes, Y. Shen, K. Yari, Y. P. Siwakoti, and F. Blaabjerg, "High-efficiency high step-up DC–DC converter with dual coupled inductors for grid-connected photovoltaic systems," *IEEE Trans. Power Electron.*, vol. 33, no. 7, pp. 5967–5982, Jul. 2018.
- [43] Y.-T. Chen, Z.-X. Lu, and R.-H. Liang, "Analysis and Design of a novel high-step-up DC/DC converter with coupled inductors," *IEEE Trans. Power Electron.*, vol. 33, no. 1, pp. 425–436, Jan. 2018.
- [44] M. R. Mohammadi, A. Amoozezaei, S. A. Khajehoddin, and K. Moez, "A high step-up/step-down LVS-parallel HVS-series ZVS bidirectional converter with coupled inductors," *IEEE Trans. Power Electron.*, vol. 37, no. 2, pp. 1945–1961, Feb. 2022.
- [45] J. Ai and M. Lin, "High step-up DC–DC converter with low power device voltage stress for a distributed generation system," *IET Power Electron.*, vol. 11, no. 12, pp. 1955–1963, Oct. 2018.
- [46] L. He, X. Xu, J. Chen, J. Sun, D. Guo, and T. Zeng, "A plug-play active resonant soft switching for current-auto-balance interleaved high step-up DC/DC converter," *IEEE Trans. Power Electron.*, vol. 34, no. 8, pp. 7603–7616, Aug. 2019.
- [47] Y. Zheng and K. M. Smedley, "Interleaved high step-up converter integrating coupled inductor and switched capacitor for distributed generation systems," *IEEE Trans. Power Electron.*, vol. 34, no. 8, pp. 7617–7628, Aug. 2019.
- [48] S. Sathyan, H. M. Suryawanshi, M. S. Ballal, and A. B. Shitole, "Soft-switching DC–DC converter for distributed energy sources with high step-up voltage capability," *IEEE Trans. Ind. Electron.*, vol. 62, no. 11, pp. 7039–7050, Nov. 2015.
- [49] H. Ardi, A. Ajami, and M. Sabahi, "A novel high step-up DC–DC converter with continuous input current integrating coupled inductor for renewable energy applications," *IEEE Trans. Ind. Electron.*, vol. 65, no. 2, pp. 1306–1315, Feb. 2018.
- [50] E. Babaei and Z. Saadatizadeh, "High voltage gain DC–DC converters based on coupled inductors," *IET Power Electron.*, vol. 11, no. 3, pp. 434–452, Mar. 2018.
- [51] Y. Cao, V. Samavatian, K. Kaskani, and H. Eshraghi, "A novel nonisolated ultra-high-voltage-gain DC–DC converter with low voltage stress," *IEEE Trans. Ind. Electron.*, vol. 64, no. 4, pp. 2809–2819, Apr. 2017.
- [52] X. Hu, J. Wang, L. Li, and Y. Li, "A three-winding coupled-inductor DC–DC converter topology with high voltage gain and reduced switch stress," *IEEE Trans. Power Electron.*, vol. 33, no. 2, pp. 1453–1462, Feb. 2018.
- [53] A. B. Shitole, S. Sathyan, H. M. Suryawanshi, G. G. Talapur, and P. Chaturvedi, "Soft-switched high voltage gain boost-integrated flyback converter interfaced single-phase grid-tied inverter for SPV integration," *IEEE Trans. Ind. Appl.*, vol. 54, no. 1, pp. 482–493, Jan./Feb. 2018.
- [54] Y. Zheng, W. Xie, and K. M. Smedley, "Interleaved high step-up converter with coupled inductors," *IEEE Trans. Power Electron.*, vol. 34, no. 7, pp. 6478–6488, Jul. 2019.
- [55] S.-W. Lee and H.-L. Do, "High step-up coupled-inductor cascade boost DC–DC converter with lossless passive snubber," *IEEE Trans. Ind. Electron.*, vol. 65, no. 10, pp. 7753–7761, Oct. 2018.
- [56] G. Wu, X. Ruan, and Z. Ye, "High step-up DC–DC converter based on switched capacitor and coupled inductor," *IEEE Trans. Ind. Electron.*, vol. 65, no. 7, pp. 5572–5579, Jul. 2018.
- [57] A. Kumar and P. Sensarma, "Ripple-free input current high voltage gain DC–DC converters with coupled inductors," *IEEE Trans. Power Electron.*, vol. 34, no. 4, pp. 3418–3428, Apr. 2019.
- [58] T. Nouri, N. Vosoughi, S. H. Hosseini, E. Babaei, and M. Sabahi, "An interleaved high step-up converter with coupled inductor and built-in transformer voltage multiplier cell techniques," *IEEE Trans. Ind. Electron.*, vol. 66, no. 3, pp. 1894–1905, Mar. 2019.
- [59] H. Liu, L. Wang, Y. Ji, and F. Li, "A novel reversal coupled inductor high-conversion-ratio bidirectional DC–DC converter," *IEEE Trans. Power Electron.*, vol. 33, no. 6, pp. 4968–4979, Jun. 2018.
- [60] Y. P. Siwakoti and F. Blaabjerg, "Single switch nonisolated ultra-step-up DC–DC converter with an integrated coupled inductor for high boost applications," *IEEE Trans. Power Electron.*, vol. 32, no. 11, pp. 8544–8558, Nov. 2017.
- [61] T.-J. Liang, S.-M. Chen, L.-S. Yang, J.-F. Chen, and A. Ioinovici, "Ultra-large gain step-up switched-capacitor DC–DC converter with coupled inductor for alternative sources of energy," *IEEE Trans. Circuits Syst. I, Reg. Papers*, vol. 59, no. 4, pp. 864–874, Apr. 2012.
- [62] A. R. N. Akhormeh, K. Abbaszadeh, M. Moradzadeh, and A. Shahirinia, "High-gain bidirectional quadratic DC–DC converter based on coupled inductor with current ripple reduction capability," *IEEE Trans. Ind. Electron.*, vol. 68, no. 9, pp. 7826–7837, Sep. 2021.
- [63] J. Ding, S. W. Zhao, H. J. Yin, P. Qin, and G. B. Zeng, "High step-up DC/DC converters based on coupled inductor and switched capacitors," *IET Power Electron.*, vol. 13, no. 14, pp. 3099–3109, Nov. 2020.
- [64] H. Moradisizkoochi, N. Elsayed, and O. A. Mohammed, "An integrated interleaved ultrahigh step-up DC–DC converter using dual cross-coupled inductors with built-in input current balancing for electric vehicles," *IEEE J. Emerg. Sel. Topics Power Electron.*, vol. 8, no. 1, pp. 644–657, Mar. 2020.
- [65] M. Shaneh, E. Adib, and M. Niroomand, "An ultrahigh step-up nonisolated interleaved converter with low input current ripple," *IEEE J. Emerg. Sel. Topics Power Electron.*, vol. 8, no. 2, pp. 1584–1592, Jun. 2020.
- [66] K.-C. Tseng, C.-C. Huang, and C.-A. Cheng, "A Single-switch converter with high step-up gain and low diode voltage stress suitable for green power-source conversion," *IEEE J. Emerg. Sel. Topics Power Electron.*, vol. 4, no. 2, pp. 363–372, Jun. 2016.
- [67] S. B. Santra, D. Chatterjee, Y. P. Siwakoti, and F. Blaabjerg, "Generalized switch current stress reduction technique for coupled-inductor-based single-switch high step-up boost converter," *IEEE J. Emerg. Sel. Topics Power Electron.*, vol. 9, no. 2, pp. 1863–1875, Apr. 2021.
- [68] H. Tarzarni, P. Kolahian, and M. Sabahi, "High step-up DC–DC converter with efficient inductive utilization," *IEEE Trans. Ind. Electron.*, vol. 68, no. 5, pp. 3831–3839, May 2021.
- [69] M. Shaneh, M. Niroomand, and E. Adib, "Ultrahigh-step-up nonisolated interleaved boost converter," *IEEE J. Emerg. Sel. Topics Power Electron.*, vol. 8, no. 3, pp. 2747–2758, Sep. 2020.
- [70] S.-W. Seo, J.-H. Ryu, Y. Kim, and J.-B. Lee, "Ultra-high step-up interleaved converter with low voltage stress," *IEEE Access*, vol. 9, pp. 37167–37178, 2021.
- [71] M. Mahmoudi, A. Ajami, and E. Babaei, "A non-isolated high step-up DC–DC converter with integrated 3 winding coupled inductor and reduced switch voltage stress," *Int. J. Circuit Theory Appl.*, vol. 46, no. 10, pp. 1879–1898, May 2018.
- [72] A. R. Majarshin and E. Babaei, "High step-up DC–DC converter with reduced voltage and current stress of elements," *IET Power Electron.*, vol. 12, no. 11, pp. 2884–2894, Sep. 2019.
- [73] T. Nouri, M. Shaneh, and A. Ghorbani, "Interleaved high step-up ZVS DC–DC converter with coupled inductor and built-in transformer for renewable energy systems applications," *IET Power Electron.*, vol. 13, no. 16, pp. 3537–3548, 2020.
- [74] Y. Ye, W. Peng, and B. Jiang, "High step-up DC–DC converter with multi-winding CL and switched capacitor," *IET Power Electron.*, vol. 11, no. 14, pp. 2232–2240, Nov. 2018.
- [75] P. Mohseni, S. Mohammadsalehian, M. R. Islam, K. M. Muttaqi, D. Sutanto, and P. Alavi, "Ultrahigh voltage gain DC–DC boost converter with ZVS switching realization and coupled inductor extendable voltage multiplier cell techniques," *IEEE Trans. Ind. Electron.*, vol. 69, no. 1, pp. 323–335, Jan. 2022.
- [76] R. Afzal, Y. Tang, H. Tong, and Y. Guo, "A high step-up integrated coupled inductor-capacitor DC–DC converter," *IEEE Access*, vol. 9, pp. 11080–11090, 2021.
- [77] X. Hu, X. Liu, Y. Zhang, Z. Yu, and S. Jiang, "A hybrid cascaded high step-up DC–DC converter with ultralow voltage stress," *IEEE J. Emerg. Sel. Topics Power Electron.*, vol. 9, no. 2, pp. 1824–1836, Apr. 2021.
- [78] W. Hassan, D. D.-C. Lu, and W. Xiao, "Single-switch high step-up DC–DC converter with low and steady switch voltage stress," *IEEE Trans. Ind. Electron.*, vol. 66, no. 12, pp. 9326–9338, Dec. 2019.
- [79] P. Mohseni, S. H. Hosseini, and M. Maalandish, "A new soft switching DC–DC converter with high voltage gain capability," *IEEE Trans. Ind. Electron.*, vol. 67, no. 9, pp. 7386–7398, Sep. 2020.
- [80] V. Marzang, S. M. Hashemzadeh, P. Alavi, A. Khoshkbar-Sadigh, S. H. Hosseini, and M. Z. Malik, "A modified triple-switch triple-mode high step-up DC–DC converter," *IEEE Trans. Ind. Electron.*, vol. 69, no. 8, pp. 8015–8027, Aug. 2022.
- [81] X. Hu, W. Liang, X. Liu, and Z. Yu, "A hybrid interleaved DC–DC converter with a wide step-up regulation range and ultralow voltage stress," *IEEE Trans. Ind. Electron.*, vol. 67, no. 7, pp. 5479–5489, Jul. 2020.

- [82] T. Liu, M. Lin, and J. Ai, "High step-up interleaved DC-DC converter with asymmetric voltage multiplier cell and coupled inductor," *IEEE J. Emerg. Sel. Topics Power Electron.*, vol. 8, no. 4, pp. 4209–4222, Dec. 2020.
- [83] M. Das, M. Pal, and V. Agarwal, "Novel high gain, high efficiency DC-DC converter suitable for solar PV module integration with three-phase grid tied inverters," *IEEE J. Photovolt.*, vol. 9, no. 2, pp. 528–537, Mar. 2019.
- [84] M. Rezaie and V. Abbasi, "Ultrahigh step-up DC-DC converter composed of two stages boost converter, coupled inductor, and multiplier cell," *IEEE Trans. Ind. Electron.*, vol. 69, no. 6, pp. 5867–5878, Jun. 2022.
- [85] T. Nouri, N. Nouri, and N. Vosoughi, "A novel high step-up high efficiency interleaved DC-DC converter with coupled inductor and built-in transformer for renewable energy systems," *IEEE Trans. Ind. Electron.*, vol. 67, no. 8, pp. 6505–6516, Aug. 2020.
- [86] J. Ai, M. Lin, and M. Yin, "A family of high step-up cascade DC-DC converters with clamped circuits," *IEEE Trans. Power Electron.*, vol. 35, no. 5, pp. 4819–4834, May 2020.
- [87] M. E. Azizkandi, F. Sedaghati, H. Shayeghi, and F. Blaabjerg, "A high voltage gain DC-DC converter based on three winding coupled inductor and voltage multiplier cell," *IEEE Trans. Power Electron.*, vol. 35, no. 5, pp. 4558–4567, May 2020.
- [88] P. Alavi, P. Mohseni, E. Babaei, and V. Marzang, "An ultra-high step-up DC-DC converter with extendable voltage gain and soft-switching capability," *IEEE Trans. Ind. Electron.*, vol. 67, no. 11, pp. 9238–9250, Nov. 2020.
- [89] A. Mirzaee and J. S. Moghani, "Coupled inductor-based high voltage gain DC-DC converter for renewable energy applications," *IEEE Trans. Power Electron.*, vol. 35, no. 7, pp. 7045–7057, Jul. 2020.
- [90] R. Fani, E. Farshidi, E. Adib, and A. Kosarian, "Analysis, design, and implementation of a ZVT high step-up DC-DC converter with continuous input current," *IEEE Trans. Ind. Electron.*, vol. 67, no. 12, pp. 10455–10463, Dec. 2020.
- [91] Y. Zheng, B. Brown, W. Xie, S. Li, and K. Smedley, "High step-up DC-DC converter with zero voltage switching and low input current ripple," *IEEE Trans. Power Electron.*, vol. 35, no. 9, pp. 9416–9429, Sep. 2020.
- [92] K. R. Kothapalli, M. R. Ramteke, H. M. Suryawanshi, N. K. Reddi, and R. B. Kalahasthi, "A coupled inductor based high step-up converter for DC microgrid applications," *IEEE Trans. Ind. Electron.*, vol. 68, no. 6, pp. 4927–4940, Jun. 2021.
- [93] S. Gao, Y. Wang, Y. Liu, Y. Guan, and D. Xu, "A novel DCM soft-switched SEPIC-based high-frequency converter with high step-up capacity," *IEEE Trans. Power Electron.*, vol. 35, no. 10, pp. 10444–10454, Oct. 2020.
- [94] X. Zhang et al., "Novel high step-up soft-switching DC-DC converter based on switched capacitor and coupled inductor," *IEEE Trans. Power Electron.*, vol. 35, no. 9, pp. 9471–9481, Sep. 2020.
- [95] Y. Ye, S. Chen, and Y. Yi, "Switched-capacitor and coupled-inductor-based high step-up converter with improved voltage gain," *IEEE J. Emerg. Sel. Topics Power Electron.*, vol. 9, no. 1, pp. 754–764, Feb. 2021.
- [96] M. L. Alghaythi, R. M. O'Connell, N. E. Islam, M. M. S. Khan, and J. M. Guerrero, "A high step-up interleaved DC-DC converter with voltage multiplier and coupled inductors for renewable energy systems," *IEEE Access*, vol. 8, pp. 123165–123174, 2020.
- [97] S. Hasanpour, Y. P. Siwakoti, A. Mostaan, and F. Blaabjerg, "New semiquadratic high step-up DC/DC converter for renewable energy applications," *IEEE Trans. Power Electron.*, vol. 36, no. 1, pp. 433–446, Jan. 2021.
- [98] T. Nouri, N. Vosoughi Kurdkandi, and M. Shaneh, "A novel ZVS high-step-up converter with built-in transformer voltage multiplier cell," *IEEE Trans. Power Electron.*, vol. 35, no. 12, pp. 12871–12886, Dec. 2020.
- [99] S.-W. Seo, D.-K. Lim, and H. H. Choi, "High step-up interleaved converter mixed with magnetic coupling and voltage lift," *IEEE Access*, vol. 8, pp. 72768–72780, 2020.
- [100] B. Akhlaghi and H. Farzanehfard, "Soft switching interleaved high step-up converter with multifunction coupled inductors," *IEEE J. Emerg. Sel. Topics Ind. Electron.*, vol. 2, no. 1, pp. 13–20, Jan. 2021.
- [101] Y. Tang, H. Tong, R. Afzal, and Y. Guo, "High step-up ZVT converter based on active switched coupled inductors," *IEEE Access*, to be published, doi: [10.1109/ACCESS.2020.3041004](https://doi.org/10.1109/ACCESS.2020.3041004).
- [102] S.-W. Seo, J.-H. Ryu, Y. Kim, and H. H. Choi, "Non-isolated high step-up DC/DC converter with coupled inductor and switched capacitor," *IEEE Access*, vol. 8, pp. 217108–217122, 2020.
- [103] R. Ebrahimi, H. Madadi Kojabadi, L. Chang, and F. Blaabjerg, "Coupled-inductor-based high step-up DC-DC converter," *IET Power Electron.*, vol. 12, no. 12, pp. 3093–3104, 2019.
- [104] F. L. Tofoli, D. de Souza Oliveira, R. P. Torrico-Bascopé, and Y. J. A. Alcazar, "Novel nonisolated high-voltage gain DC-DC converters based on 3SSC and VMC," *IEEE Trans. Power Electron.*, vol. 27, no. 9, pp. 3897–3907, Sep. 2012.
- [105] M. Sabahi, H. Tarzamni, and P. Kolahian, "Operation and design analysis of an interleaved high step-up DC-DC converter with improved harnessing of magnetic energy," *Int. J. Circuit Theory Appl.*, vol. 49, no. 2, pp. 221–243, 2021.
- [106] H. Chen, X. Hu, Y. Huang, M. Zhang, and B. Gao, "Improved DC-DC converter topology for high step-up applications," *IET Circuits, Devices Syst.*, vol. 13, no. 1, pp. 51–60, Jan. 2019.
- [107] Y. Hu, Y. Deng, J. Long, and X. Lu, "High step-up passive absorption circuit used in non-isolated high step-up converter," *IET Power Electron.*, vol. 7, pp. 1945–1953, 2014.
- [108] W. Hassan, D. D.-C. Lu, and W. Xiao, "Analysis and experimental verification of a single-switch high-voltage gain ZCS DC-DC converter," *IET Power Electron.*, vol. 12, no. 8, pp. 2146–2153, Jul. 2019.
- [109] M. E. Azizkandi, F. Sedaghati, H. Shayeghi, and F. Blaabjerg, "Two-and three-winding coupled-inductor-based high step-up DC-DC converters for sustainable energy applications," *IET Power Electron.*, vol. 13, no. 1, pp. 144–156, 2019.
- [110] E. Babaei, Z. Saadatizadeh, and C. Cecati, "High step-up high step-down bidirectional DC/DC converter," *IET Power Electron.*, vol. 10, no. 12, pp. 1556–1571, Oct. 2017.
- [111] F. Li, H. Liu, C. Zhang, and P. Wheeler, "Novel high step-up dual switches converter with reduced power device voltage stress for distributed generation system," *IET Power Electron.*, vol. 10, no. 14, pp. 1–10, Aug. 2017.
- [112] A. Lahooti Eshkevari, A. Mosallanejad, and M. S. Sepasian, "Design analysis and implementation of a new high-gain p-type step-up DC/DC converter with continuous input current and common ground," *IET Power Electron.*, vol. 14, no. 1, pp. 225–238, 2021.
- [113] H. Bahrami, H. Iman-Eini, B. Kazemi, and A. Taheri, "Modified step-up boost converter with coupled-inductor and super-lift techniques," *IET Power Electron.*, vol. 8, no. 6, pp. 898–905, Jun. 2015.
- [114] C.-L. Shen and P.-C. Chiu, "Buck-boost-flyback integrated converter with single switch to achieve high voltage gain for PV or fuel-cell applications," *IET Power Electron.*, vol. 9, no. 6, pp. 1228–1237, 2016.
- [115] N. H. Jabarullah, E. Geetha, M. Arun, and V. Vakhnina, "Design, analysis, and implementation of a new high step-up DC-DC converter with low input current ripple and ultra-high-voltage conversion ratio," *IET Power Electron.*, vol. 13, no. 15, pp. 3243–3253, Sep. 2020.
- [116] K. Zaoskoufis and E. C. Tatakis, "An Improved Boost-based DC/DC converter with high-voltage step-up ratio for DC microgrids," *IEEE J. Emerg. Sel. Topics Power Electron.*, vol. 9, no. 2, pp. 1837–1853, Apr. 2021.
- [117] M. Forouzesh, K. Yari, A. Baghrarian, and S. Hasanpour, "Single-switch high step-up converter based on coupled inductor and switched capacitor techniques with quasi-resonant operation," *IET Power Electron.*, vol. 10, no. 2, pp. 240–250, 2017.
- [118] R. Fani, E. Farshidi, E. Adib, and A. Kosarian, "Interleaved non-isolated DC-DC converter for ultra-high step-up applications," *IET Power Electron.*, vol. 13, no. 18, pp. 4261–4269, Nov. 2020.
- [119] M. Fekri, N. Molavi, E. Adib, and H. Farzanehfard, "High voltage gain interleaved DC-DC converter with minimum current ripple," *IET Power Electron.*, vol. 10, no. 14, pp. 1924–1931, 2017.
- [120] S. Heidari Beni, S. M. M. Mirtalaei, A. Kianpour, and S. Aghababaei Beni, "Design and improvement of a soft switching high step-up boost converter with voltage multiplier," *IET Power Electron.*, vol. 10, no. 15, pp. 2163–2169, Dec. 2017.
- [121] S. Hasanpour, M. Forouzesh, Y. P. Siwakoti, and F. Blaabjerg, "A new high-gain, high-efficiency SEPIC-based DC-DC converter for renewable energy applications," *IEEE J. Emerg. Sel. Topics Ind. Electron.*, vol. 2, no. 4, pp. 567–578, Oct. 2021.
- [122] W. Hassan, Y. Lu, M. Farhangi, D. D. Lu, and W. Xiao, "Design analysis and experimental verification of a high voltage gain and high-efficiency DC-DC converter for photovoltaic applications," *IET Renew. Power Gener.*, vol. 14, no. 10, pp. 1699–1709, Jul. 2020.
- [123] Y.-T. Chen, M.-H. Tsai, and R.-H. Liang, "DC-DC converter with high voltage gain and reduced switch stress," *IET Power Electron.*, vol. 7, no. 10, pp. 2564–2571, Oct. 2014.

- [124] S. W. Lee and H. L. Do, "High step-up cascade synchronous boost converter with zero voltage switching," *IET Power Electron.*, vol. 11, no. 31, pp. 618–625, Mar. 2018.
- [125] Y.-T. Chen, Z.-X. Lu, R.-H. Liang, and C.-W. Hung, "Analysis and implementation of a novel high step-up DC–DC converter with low switch voltage stress and reduced diode voltage stress," *IET Power Electron.*, vol. 9, no. 9, pp. 2003–2012, Jul. 2016.
- [126] M. Hoseinzadeh Lish, R. Ebrahimi, H. Madadi Kojabadi, J. M. Guerrero, N. Nourani Esfetanaj, and L. Chang, "Novel high gain DC–DC converter based on coupled inductor and diode capacitor techniques with leakage inductance effects," *IET Power Electron.*, vol. 13, no. 11, pp. 2380–2389, 2020.
- [127] B. Poorali, H. M. Jazi, and E. Adib, "Single-core soft-switching high step-up three-level boost converter with active clamp," *IET Power Electron.*, vol. 9, no. 14, pp. 2692–2699, Mar. 2016.
- [128] P. Upadhyay, R. Kumar, and S. Sathyan, "Coupled-inductor-based high-gain converter utilising magnetising inductance to achieve soft-switching with low voltage stress on devices," *IET Power Electron.*, vol. 13, no. 3, pp. 576–591, Feb. 2020.
- [129] S. M. Fardahar and M. Sabahi, "High step-down/high step-up interleaved bidirectional DC–DC converter with low voltage stress on switches," *IET Power Electron.*, vol. 13, no. 1, pp. 104–115, Jan. 2020.
- [130] N. Molavi, E. Adib, and H. Farzanehfard, "Soft-switching bidirectional DC–DC converter with high voltage conversion ratio," *IET Power Electron.*, vol. 11, no. 1, pp. 33–42, Feb. 2018.
- [131] H. G. Sadighi, S. E. Afjei, and A. Salemmia, "High step-up DC–DC converter based on coupled-inductor for renewable energy systems," *IET Power Electron.*, vol. 13, no. 18, pp. 4315–4324, 2020.
- [132] H. Moradi Sizkoohi, J. Milimonfared, M. Taheri, and S. Salehi, "High step-up soft-switched dual-boost coupled-inductor-based converter integrating multipurpose coupled inductors with capacitor-diode stages," *IET Power Electron.*, vol. 8, no. 9, pp. 1786–1797, Sep. 2015.
- [133] M. Vesali, M. Delshad, E. Adib, and M. R. Amini, "A new nonisolated soft switched DC–DC bidirectional converter with high conversion ratio and low voltage stress on the switches," *Int. Trans. Elect. Energy Syst.*, vol. 31, no. 1, Jan. 2021, Art. no. e12666.
- [134] H. Radmanesh, M. R. Soltanpour, and M. E. Azizkandi, "Design and implementation of an ultra-high voltage DC-DC converter based on coupled inductor with continuous input current for clean energy applications," *Int. J. Circuit Theory Appl.*, vol. 49, pp. 348–379, 2020.
- [135] Y.-P. Hsieh, J.-F. Chen, L.-S. Yang, C.-Y. Wu, and W.-S. Liu, "High-conversion-ratio bidirectional DC–DC converter with coupled inductor," *IEEE Trans. Ind. Electron.*, vol. 61, no. 1, pp. 210–222, Jan. 2014.
- [136] T.-J. Liang, H.-H. Liang, S.-M. Chen, J.-F. Chen, and L.-S. Yang, "Analysis, design, and implementation of a bidirectional double-boost DC–DC converter," *IEEE Trans. Ind. Appl.*, vol. 50, no. 6, pp. 3955–3962, Nov./Dec. 2014.
- [137] M. Aamir, S. Mekhilef, and H.-J. Kim, "High-gain zero-voltage switching bidirectional converter with a reduced number of switches," *IEEE Trans. Circuits Syst. II, Exp. Briefs*, vol. 62, no. 8, pp. 816–820, Aug. 2015.
- [138] H. Wu, K. Sun, L. Chen, L. Zhu, and Y. Xing, "High step-up/step-down soft-switching bidirectional DC–DC converter with coupled-inductor and voltage matching control for energy storage systems," *IEEE Trans. Ind. Electron.*, vol. 63, no. 5, pp. 2892–2903, May 2016.
- [139] H. Tarzamni, N. V. Kurdkandi, H. S. Gohari, M. Lehtonen, O. Husev, and F. Blaabjerg, "Ultra-high step-up DC-DC converters based on center-tapped inductors," *IEEE Access*, vol. 9, pp. 136373–136383, 2021.
- [140] M. P. S., M. Das, and V. Agarwal, "Design and development of a novel high voltage gain, high-efficiency bidirectional DC–DC converter for storage interface," *IEEE Trans. Ind. Electron.*, vol. 66, no. 6, pp. 4490–4501, Jun. 2019.
- [141] Z. Hosseinzadeh, N. Molavi, and H. Farzanehfard, "Soft-switching high step-up/down bidirectional DC–DC converter," *IEEE Trans. Ind. Electron.*, vol. 66, no. 6, pp. 4379–4386, Jun. 2019.
- [142] M. Packnezhad and H. Farzanehfard, "Soft-switching high step-up/down converter using coupled inductors with minimum number of components," *IEEE Trans. Ind. Electron.*, vol. 68, no. 9, pp. 7938–7945, Sep. 2021.
- [143] J. Yao, A. Abramovitz, and K. M. Smedley, "Analysis and design of charge pump-assisted high step-up tapped inductor SEPIC converter with an 'inductorless' regenerative snubber," *IEEE Trans. Power Electron.*, vol. 30, no. 10, pp. 5565–5580, Oct. 2015.
- [144] H. Wu, Y. Lu, L. Chen, P. Xu, and Y. Xing, "High step-up/step-down non-isolated BDC with built-in DC-transformer for energy storage systems," *IET Power Electron.*, vol. 9, no. 13, pp. 2571–2579, Oct. 2016.
- [145] M. Shaneh, M. Niroomand, and E. Adib, "Non-isolated interleaved bidirectional DC–DC converter with high step voltage ratio and minimum number of switches," *IET Power Electron.*, vol. 12, no. 6, pp. 1510–1520, 2019.
- [146] M. E. Azizkandi, F. Sedaghati, and E. Babaei, "A topology of coupled inductor DC–DC converter with large conversion ratio and reduced voltage stress on semiconductors," *IET Power Electron.*, vol. 13, no. 15, pp. 3339–3350, 2020.
- [147] H. Tarzamni, M. Sabahi, S. Rahimpour, M. Lehtonen, and P. Dehghanian, "Operation and design consideration of an ultrahigh step-up DC-DC converter featuring high power density," *IEEE J. Emerg. Sel. Topics Power Electron.*, vol. 9, no. 5, pp. 6113–6123, Oct. 2021.
- [148] T. Nouri, N. V. Kurdkandi, and O. Husev, "An improved ZVS high step-up converter based on coupled inductor and built-in transformer," *IEEE Trans. Power Electron.*, vol. 36, no. 12, pp. 13802–13816, Dec. 2021.
- [149] M. F. Guepfrih, G. Waltrich, and T. B. Lazzarin, "High step-up DC-DC converter using built-in transformer voltage multiplier cell and dual boost concepts," *IEEE J. Emerg. Sel. Topics Power Electron.*, vol. 9, no. 6, pp. 6700–6712, Dec. 2021.
- [150] S. Lee, P. Kim, and S. Choi, "High step-up soft-switched converters using voltage multiplier cells," *IEEE Trans. Power Electron.*, vol. 28, no. 7, pp. 3379–3387, Jul. 2013.
- [151] L. W. Zhou, B. X. Zhu, Q. M. Luo, and S. Chen, "Interleaved non-isolated high step-up DC/DC converter based on the diode–capacitor multiplier," *IET Power Electron.*, vol. 7, no. 2, pp. 390–397, Feb. 2014.
- [152] G. Wu, X. Ruan, and Z. Ye, "Nonisolated high step-up DC–DC converters adopting switched-capacitor cell," *IEEE Trans. Ind. Electron.*, vol. 62, no. 1, pp. 383–393, Jan. 2015.
- [153] C.-M. Young, M.-H. Chen, T.-A. Chang, C.-C. Ko, and K.-K. Jen, "Cascade Cockcroft–Walton voltage multiplier applied to transformerless high step-up DC–DC Converter," *IEEE Trans. Ind. Electron.*, vol. 60, no. 2, pp. 523–537, Feb. 2013.
- [154] Y. Huang, Y. Mei, S. Xiong, S.-C. Tan, C. Y. Tang, and S. Y. Hui, "Reverse electro dialysis energy harvesting system using high-gain step-up DC/DC converter," *IEEE Trans. Sustain. Energy*, vol. 9, no. 4, pp. 1578–1587, Oct. 2018.
- [155] M. Maalandish, S. H. Hosseini, T. Jalilzadeh, and N. Vosoughi, "High step-up DC-DC converter using one switch and lower losses for photovoltaic applications," *IET Power Electron.*, vol. 11, no. 13, pp. 2081–2092, Nov. 2018.
- [156] B. P. Baddipadiga and M. Ferdowsi, "A high-voltage-gain DC-DC converter based on modified dickson charge pump voltage multiplier," *IEEE Trans. Power Electron.*, vol. 32, no. 10, pp. 7707–7715, Oct. 2017.
- [157] A. Alzahrani, M. Ferdowsi, and P. Shamsi, "High-voltage-gain DC–DC step-up converter with bifold dickson voltage multiplier cells," *IEEE Trans. Power Electron.*, vol. 34, no. 10, pp. 9732–9742, Oct. 2019.
- [158] T. Shanthi, S. U. Prabha, and K. Sundaramoorthy, "Non-isolated n-stage high step-up DC-DC converter for low voltage DC source integration," *IEEE Trans. Energy Convers.*, vol. 36, no. 3, pp. 1625–1634, Sep. 2021.
- [159] M. Abbasi, E. Babaei, and B. Tousei, "New family of non-isolated step-up/down and step-up switched-capacitor-based DC-DC converters," *IET Power Electron.*, vol. 12, no. 7, pp. 1706–1720, 2019.
- [160] E. Babaei, T. Jalilzadeh, M. Sabahi, M. Maalandish, and R. S. Alishah, "High step-up DC–DC converter with reduced voltage stress on devices," *Int. Trans. Elect. Energy Syst.*, vol. 29, no. 4, 2019, Art. no. e2789.
- [161] Z. Wang, P. Wang, B. Li, X. Ma, and P. Wang, "A bidirectional DC–DC converter with high voltage conversion ratio and zero ripple current for battery energy storage system," *IEEE Trans. Power Electron.*, vol. 36, no. 7, pp. 8012–8027, Jul. 2021.
- [162] B. Zhu, S. Chen, Y. Zhang, and Y. Huang, "An interleaved zero-voltage zero-current switching high step-up DC-DC converter," *IEEE Access*, vol. 9, pp. 5563–5572, 2021.
- [163] Y. Zheng, W. Xie, and K. M. Smedley, "A family of interleaved high step-up converters with diode–capacitor technique," *IEEE J. Emerg. Sel. Topics Power Electron.*, vol. 8, no. 2, pp. 1560–1570, Jun. 2020.
- [164] G. Lin and Z. Zhang, "Low input ripple high step-up extendable hybrid DC-DC converter," *IEEE Access*, vol. 7, pp. 158744–158752, 2019.
- [165] M. A. Salvador, J. M. de Andrade, T. B. Lazzarin, and R. F. Coelho, "Non-isolated high-step-up DC-DC converter derived from switched-inductors and switched-capacitors," *IEEE Trans. Ind. Electron.*, vol. 67, no. 10, pp. 8506–8516, Oct. 2020.
- [166] M. Meraj, M. S. Bhaskar, A. Iqbal, N. Al-Emadi, and S. Rahman, "Interleaved multilevel boost converter with minimal voltage multiplier components for high-voltage step-up applications," *IEEE Trans. Power Electron.*, vol. 35, no. 12, pp. 12816–12833, Dec. 2020.

- [167] M. S. Bhaskar, D. J. Almkhles, S. Padmanaban, F. Blaabjerg, U. Subramaniam, and D. M. Ionel, "Analysis and investigation of hybrid DC-DC non-isolated and non-inverting Nx interleaved multilevel boost converter (Nx-IMBC) for high voltage step-up applications: Hardware implementation," *IEEE Access*, vol. 8, pp. 87309–87328, 2020.
- [168] W. Xie and K. M. Smedley, "Seven switching techniques for the ladder resonant switched-capacitor converters with full-range voltage regulation," *IEEE Trans. Ind. Electron.*, vol. 69, no. 8, pp. 7897–7908, Aug. 2022.
- [169] H. Trazamni, E. Babaei, and M. Sabahi, "Full soft-switching high step-up DC-DC converter based on active resonant cell," *IET Power Electron.*, vol. 10, no. 13, pp. 1729–1739, 2017.
- [170] M. Maalandish, S. H. Hosseini, and T. Jalilzadeh, "High step-up DC/DC converter using switch-capacitor techniques and lower losses for renewable energy applications," *IET Power Electron.*, vol. 11, no. 10, pp. 1718–1729, Aug. 2018.
- [171] Q. m. Luo, H. Yan, S. Chen, and L. W. Zhou, "Interleaved high step-up zero-voltage-switching boost converter with variable inductor control," *IET Power Electron.*, vol. 7, no. 12, pp. 3083–3089, 2014.
- [172] B. Zhu, S. Liu, Y. Huang, and C. Tan, "Non-isolated high step-up DC/DC converter based on a high degrees of freedom voltage gain cell," *IET Power Electron.*, vol. 10, no. 15, pp. 2023–2033, Dec. 2017.
- [173] B. Zhu, L. Ren, X. Wu, and K. Song, "ZVT high step-up DC/DC converter with a novel passive snubber cell," *IET Power Electron.*, vol. 10, no. 5, pp. 599–605, 2017.
- [174] Z. Saadatizadeh, P. C. Heris, E. Babaei, and F. Sadikoglu, "Expandable interleaved high voltage gain boost DC-DC converter with low switching stress," *Int. J. Circuit Theory Appl.*, vol. 47, pp. 782–804, 2019.
- [175] Y. Zhang, Y. Gao, L. Zhou, and M. Sumner, "A switched-capacitor bidirectional DC-DC converter with wide voltage gain range for electric vehicles with hybrid energy sources," *IEEE Trans. Power Electron.*, vol. 33, no. 11, pp. 9459–9469, Nov. 2018.
- [176] V. Marzang, S. H. Hosseini, N. Rostami, P. Alavi, P. Mohseni, and S. M. Hashemzadeh, "A high step-up nonisolated DC-DC converter with flexible voltage gain," *IEEE Trans. Power Electron.*, vol. 35, no. 10, pp. 10489–10500, Oct. 2020.
- [177] N. Vosoughi, M. Abbasi, E. Abbasi, and M. Sabahi, "A Zeta-based switched-capacitor DC-DC converter topology," *Int. J. Circuit Theory Appl.*, vol. 47, no. 8, pp. 1302–1322, 2019.
- [178] L.-S. Yang, T.-J. Liang, and J.-F. Chen, "Transformerless DC-DC converters with high step-up voltage gain," *IEEE Trans. Ind. Electron.*, vol. 56, no. 8, pp. 3144–3152, Aug. 2009.
- [179] B. Krishna and V. Karthikeyan, "Active Switched-inductor network step-up DC-DC converter with wide range of voltage-gain at the lower range of duty cycles," *IEEE J. Emerg. Sel. Topics Ind. Electron.*, vol. 2, no. 4, pp. 431–441, Oct. 2021.
- [180] Y. Tang, D. Fu, T. Wang, and Z. Xu, "Hybrid switched-inductor converters for high step-up conversion," *IEEE Trans. Ind. Electron.*, vol. 62, no. 3, pp. 1480–1490, Mar. 2015.
- [181] K.-J. Lee, B.-G. Park, R.-Y. Kim, and D.-S. Hyun, "Nonisolated ZVT two-inductor boost converter with a single resonant inductor for high step-up applications," *IEEE Trans. Power Electron.*, vol. 27, no. 4, pp. 1966–1973, Apr. 2012.
- [182] H. Kang and H. Cha, "A new nonisolated high-voltage-gain boost converter with inherent output voltage balancing," *IEEE Trans. Ind. Electron.*, vol. 65, no. 3, pp. 2189–2198, Mar. 2018.
- [183] M. Mousavi, Y. Sangsefidi, and A. Mehrizi-Sani, "A Multistage resonant DC-DC converter for step-up applications," *IEEE Trans. Power Electron.*, vol. 36, no. 8, pp. 9251–9262, Aug. 2021.
- [184] H. Choi, M. Jang, M. Ciobotaru, and V. G. Agelidis, "Performance evaluation of interleaved high-gain converter configurations," *IET Power Electron.*, vol. 9, no. 9, pp. 1852–1861, 2016.
- [185] C.-T. Pan, C.-F. Chuang, and C.-C. Chu, "A novel transformer-less adaptable voltage quadrupler DC converter with low switch voltage stress," *IEEE Trans. Power Electron.*, vol. 29, no. 9, pp. 4787–4796, Sep. 2014.
- [186] J. Leyva-Ramos, R. Mota-Varona, M. G. Ortiz-Lopez, L. H. Diaz-Saldierna, and D. Langarica-Cordoba, "Control strategy of a quadratic boost converter with voltage multiplier cell for high-voltage gain," *IEEE J. Emerg. Sel. Topics Power Electron.*, vol. 5, no. 4, pp. 1761–1770, Dec. 2017.
- [187] Y. Gu, Y. Chen, B. Zhang, D. Qiu, and F. Xie, "High step-up DC-DC converter with active switched LC-network for photovoltaic systems," *IEEE Trans. Energy Convers.*, vol. 34, no. 1, pp. 321–329, Mar. 2019.
- [188] A. M. S. S. Andrade, T. M. K. Faistel, A. Toebe, and R. A. Guisso, "Family of transformerless active switched inductor and switched capacitor Ćuk DC-DC converter for high voltage gain applications," *IEEE J. Emerg. Sel. Topics Ind. Electron.*, vol. 2, no. 4, pp. 390–398, Oct. 2021.
- [189] S. A. Ansari and J. S. Moghani, "A novel high voltage gain noncoupled inductor SEPIC converter," *IEEE Trans. Ind. Electron.*, vol. 66, no. 9, pp. 7099–7108, Sep. 2019.
- [190] C. H. Basha and C. Rani, "Design and analysis of transformerless, high step-up, boost DC-DC converter with an improved VSS-RBFA based MPPT controller," *Int. Trans. Elect. Energy Syst.*, vol. 30, no. 12, 2020, Art. no. e12633.
- [191] S. Sadaf, M. S. Bhaskar, M. Meraj, A. Iqbal, and N. Al-Emadi, "Transformer-less boost converter with reduced voltage stress for high voltage step-up applications," *IEEE Trans. Ind. Electron.*, vol. 69, no. 2, pp. 1498–1508, Feb. 2022.
- [192] V. Karthikeyan, S. Kumaravel, and G. Gurukumar, "High step-up gain DC-DC converter with switched capacitor and regenerative boost configuration for solar PV applications," *IEEE Trans. Circuits Syst. II, Exp. Briefs*, vol. 66, no. 12, pp. 2022–2026, Dec. 2019.
- [193] V. F. Pires, A. Cordeiro, D. Foito, and J. F. Silva, "High step-up DC-DC converter for fuel cell vehicles based on merged quadratic Boost-Ćuk," *IEEE Trans. Veh. Technol.*, vol. 68, no. 8, pp. 7521–7530, Aug. 2019.
- [194] H. Lei, R. Hao, X. You, and F. Li, "Nonisolated high step-up soft-switching DC-DC converter with interleaving and dickson switched-capacitor techniques," *IEEE J. Emerg. Sel. Topics Power Electron.*, vol. 8, no. 3, pp. 2007–2021, Sep. 2020.
- [195] C. Sun, X. Zhang, and X. Cai, "A step-up nonisolated modular multilevel DC-DC converter with self-voltage balancing and soft switching," *IEEE Trans. Power Electron.*, vol. 35, no. 12, pp. 13017–13030, Dec. 2020.
- [196] B. Zhu, G. Liu, Y. Zhang, Y. Huang, and S. Hu, "Single-switch high step-up zeta converter based on coat circuit," *IEEE Access*, vol. 9, pp. 5166–5176, 2021.
- [197] M. Rezaie and V. Abbasi, "Effective combination of quadratic boost converter with voltage multiplier cell to increase voltage gain," *IET Power Electron.*, vol. 13, no. 11, pp. 2322–2333, Aug. 2020.
- [198] J. Melo de Andrade, R. F. Coelho, and T. B. Lazzarin, "High step-up DC-DC converter based on modified active switched-inductor and switched-capacitor cells," *IET Power Electron.*, vol. 13, no. 14, pp. 3127–3137, 2020.
- [199] B. Zhu, H. Wang, and D. M. Vilathgamuwa, "Single-switch high step-up boost converter based on a novel voltage multiplier," *IET Power Electron.*, vol. 12, no. 14, pp. 3732–3738, Nov. 2019.
- [200] S. A. Gorji, A. Mostaan, H. T. My, and M. Ektesabi, "Non-isolated buck-boost DC-DC converter with quadratic voltage gain ratio," *IET Power Electron.*, vol. 12, no. 6, pp. 1425–1433, 2019.
- [201] L. He and Z. Zheng, "High step-up DC-DC converter with switched-capacitor and its zero-voltage switching realisation," *IET Power Electron.*, vol. 10, no. 6, pp. 630–636, Dec. 2016.
- [202] X. Zhang and T. C. Green, "The modular multilevel converter for high step-up ratio DC-DC conversion," *IEEE Trans. Ind. Electron.*, vol. 62, no. 8, pp. 4925–4936, Aug. 2015.
- [203] Y. Park, B. Jung, and S. Choi, "Nonisolated ZVZCS resonant PWM DC-DC converter for high step-up and high-power applications," *IEEE Trans. Power Electron.*, vol. 27, no. 8, pp. 3568–3575, Aug. 2012.
- [204] R. H. Ashique and Z. Salam, "A high-gain, high-efficiency nonisolated bidirectional DC-DC converter with sustained ZVS operation," *IEEE Trans. Ind. Electron.*, vol. 65, no. 10, pp. 7829–7840, Oct. 2018.
- [205] F. Wang, Y. Wang, B. Su, and C. Teng, "Three-phase interleaved high step-up bidirectional DC-DC converter," *IET Power Electron.*, vol. 13, no. 12, pp. 2469–2480, Sep. 2020.
- [206] Y. Qin, Y. Yang, S. Li, Y. Huang, S.-C. Tan, and S. Y. Hui, "A high-efficiency DC/DC converter for high-voltage-gain, high-current applications," *IEEE J. Emerg. Sel. Topics Power Electron.*, vol. 8, no. 3, pp. 2812–2823, Sep. 2020.
- [207] A. Sarikhani, B. Allahverdienejad, and M. Hamzeh, "A nonisolated Buck-Boost DC-DC converter with continuous input current for photovoltaic applications," *IEEE J. Emerg. Sel. Topics Power Electron.*, vol. 9, no. 1, pp. 804–811, Feb. 2021.
- [208] R. Eskandari, E. Babaei, M. Sabahi, and S. R. Ojaghkandi, "Interleaved high step-up zero-voltage zero-current switching boost DC-DC converter," *IET Power Electron.*, vol. 13, no. 1, pp. 96–103, Jan. 2020.
- [209] M. Kwon, S. Oh, and S. Choi, "High gain soft-switching bidirectional DC-DC converter for eco-friendly vehicles," *IEEE Trans. Power Electron.*, vol. 29, no. 4, pp. 1659–1666, Apr. 2014.

- [210] H. Ardi, A. Ajami, F. Kardan, and S. N. Avilagh, "Analysis and implementation of a nonisolated bidirectional DC-DC converter with high voltage gain," *IEEE Trans. Ind. Electron.*, vol. 63, no. 8, pp. 4878-4888, Aug. 2016.
- [211] Y. Zhang, Y. Gao, J. Li, and M. Sumner, "Interleaved switched-capacitor bidirectional DC-DC converter with wide voltage-gain range for energy storage systems," *IEEE Trans. Power Electron.*, vol. 33, no. 5, pp. 3852-3869, May 2018.
- [212] J. Bauman and M. Kazerani, "A novel capacitor-switched regenerative snubber for DC/DC boost converters," *IEEE Trans. Ind. Electron.*, vol. 58, no. 2, pp. 514-523, Feb. 2011.
- [213] M. P. Hirth, R. Gules, and C. H. Illa Font, "A wide conversion ratio bidirectional modified SEPIC converter with nondissipative current snubber," *IEEE J. Emerg. Sel. Topics Power Electron.*, vol. 9, no. 2, pp. 1350-1360, Apr. 2021.
- [214] Y. Huang, S.-C. Tan, and S. Y. Hui, "Multiphase-interleaved high step-up DC/DC resonant converter for wide load range," *IEEE Trans. Power Electron.*, vol. 34, no. 8, pp. 7703-7718, Aug. 2019.
- [215] C. Chen, J. Liu, and H. Lee, "A 2-MHz 9-45-V input high-efficiency three-switch ZVS step-up/down hybrid converter," *IEEE J. Solid-State Circuits*, vol. 56, no. 3, pp. 855-865, Mar. 2021.
- [216] K. Varesi, N. Hassanpour, and S. Saeidabadi, "Novel high step-up DC-DC converter with increased voltage gain per devices and continuous input current suitable for DC microgrid applications," *Int. J. Circuit Theory Appl.*, vol. 48, no. 10, pp. 1820-1837, Oct. 2020.
- [217] J. Zhao and D. Chen, "Switched-capacitor high voltage gain Z-source converter with common ground and reduced passive component," *IEEE Access*, vol. 9, pp. 21395-21407, 2021.
- [218] B. Poorali, H. M. Jazi, and E. Adib, "Improved high step-up Z-source DC-DC converter with single core and ZVT operation," *IEEE Trans. Power Electron.*, vol. 33, no. 11, pp. 9647-9655, Nov. 2018.
- [219] Y. Ji, H. Liu, Y. Feng, F. Wu, and P. Wheeler, "High step-up y-source coupled-inductor impedance network boost DC-DC converters with common ground and continuous input current," *IEEE J. Emerg. Sel. Topics Power Electron.*, vol. 8, no. 3, pp. 3174-3183, Sep. 2020.
- [220] A. Samadian, S. H. Hosseini, M. Sabahi, and M. Maalandish, "A new coupled inductor nonisolated high step-up quasi Z-source DC-DC converter," *IEEE Trans. Ind. Electron.*, vol. 67, no. 7, pp. 5389-5397, Jul. 2020.
- [221] B. Poorali and E. Adib, "Soft-switched high step-up quasi-z-source DC-DC converter," *IEEE Trans. Ind. Electron.*, vol. 67, no. 6, pp. 4547-4555, Jun. 2020.
- [222] Q. Pan, H. Liu, P. Wheeler, and F. Wu, "High step-up cascaded DC-DC converter integrating coupled inductor and passive snubber," *IET Power Electron.*, vol. 12, no. 9, pp. 2414-2423, Aug. 2019.
- [223] B. Poorali, A. Torkan, and E. Adib, "High step-up Z-source DC-DC converter with coupled inductors and switched capacitor cell," *IET Power Electron.*, vol. 8, pp. 1394-1402, 2015.
- [224] A. Samadian, S. H. Hosseini, and M. Sabahi, "A new three-winding coupled inductor nonisolated quasi-Z-source high step-up DC-DC converter," *IEEE Trans. Power Electron.*, vol. 36, no. 10, pp. 11523-11531, Oct. 2021.
- [225] M. M. Haji-Esmaili, E. Babaei, and M. Sabahi, "High step-up quasi-Z source DC-DC converter," *IEEE Trans. Power Electron.*, vol. 33, no. 12, pp. 10563-10571, Dec. 2018.
- [226] X. Zhu, B. Zhang, and K. Jin, "Hybrid nonisolated active quasi-switched DC-DC converter for high step-up voltage conversion applications," *IEEE Access*, vol. 8, pp. 222584-222598, 2020.
- [227] J. Zhao, D. Chen, and J. Jiang, "Transformerless high step-up DC-DC converter with low voltage stress for fuel cells," *IEEE Access*, vol. 9, pp. 10228-10238, 2021.
- [228] S. Miao, W. Liu, and J. Gao, "Single-inductor boost converter with ultrahigh step-up gain, lower switches voltage stress, continuous input current, and common grounded structure," *IEEE Trans. Power Electron.*, vol. 36, no. 7, pp. 7841-7852, Jul. 2021.
- [229] M. Ortega, M. V. Ortega, F. Jurado, J. Carpio, and D. Vera, "Bidirectional DC-DC converter with high gain based on impedance source," *IET Power Electron.*, vol. 12, no. 8, pp. 2069-2078, Jun. 2019.
- [230] H. Shen, B. Zhang, D. Qiu, and L. Zhou, "A common grounded Z-source DC-DC converter with high voltage gain," *IEEE Trans. Ind. Electron.*, vol. 63, no. 5, pp. 2925-2935, May 2016.
- [231] N. Elsayad, H. Moradisizkoobi, and O. Mohammed, "A new SEPIC-based step-up DC-DC converter with wide conversion ratio for fuel cell vehicles: Analysis and design," *IEEE Trans. Ind. Electron.*, vol. 68, no. 8, pp. 6390-6400, Aug. 2021.
- [232] S. Rostami, V. Abbasi, and T. Kerekes, "Switched capacitor based Z-source DC-DC converter," *IET Power Electron.*, vol. 12, no. 13, pp. 3582-3589, Sep. 2019.
- [233] M. Rezvanyardom, A. Mirzaei, and S. Heydari, "Fully soft-switching nonisolated quasi-ZS-source DC-DC converter with high-voltage gain," *IEEE J. Emerg. Sel. Topics Power Electron.*, vol. 9, no. 2, pp. 1854-1862, Apr. 2021.
- [234] M. Veerachary and P. Kumar, "Analysis and design of quasi-Z-source equivalent DC-DC boost converters," *IEEE Trans. Ind. Appl.*, vol. 56, no. 6, pp. 6642-6656, Nov./Dec. 2020.
- [235] A. Torkan and M. Ehsani, "A novel nonisolated Z-source DC-DC converter for photovoltaic applications," *IEEE Trans. Ind. Appl.*, vol. 54, no. 5, pp. 4574-4583, Sep./Oct. 2018.
- [236] Y. P. Siwakoti, P. C. Loh, F. Blaabjerg, S. J. Andreasen, and G. E. Town, "Y-source boost DC/DC converter for distributed generation," *IEEE Trans. Ind. Electron.*, vol. 62, no. 2, pp. 1059-1069, Feb. 2015.
- [237] A. Kumar, X. Xiong, X. Pan, M. Reza, A. R. Beig, and K. A. Jaafari, "A wide voltage gain bidirectional DC-DC converter based on quasi Z-source and switched capacitor network," *IEEE Trans. Circuits Syst. II, Exp. Briefs*, vol. 68, no. 4, pp. 1353-1357, Apr. 2021.
- [238] Y. Chen, B. Zhang, F. Xie, W. Xiao, D. Qiu, and Y. Chen, "Common ground quasi-Z-source series DC-DC converters utilizing negative output characteristics," *IEEE J. Emerg. Sel. Topics Power Electron.*, vol. 10, no. 4, pp. 3861-3872, Aug. 2022.
- [239] Y. P. Siwakoti, F. Blaabjerg, V. P. Galigekere, A. Ayachit, and M. K. Kazimierczuk, "A-source impedance network," *IEEE Trans. Power Electron.*, vol. 31, no. 12, pp. 8081-8087, Dec. 2016.
- [240] M. R. A. Pahlavani and M. H. B. Nozadian, "High step-up active Z-source DC/DC converters; analyses and control method," *IET Power Electron.*, vol. 12, no. 4, pp. 790-800, Apr. 2019.
- [241] K. Patidar and A. C. Umarikar, "High step-up pulse-width modulation DC-DC converter based on quasi-Z-source topology," *IET Power Electron.*, vol. 8, no. 4, pp. 477-488, 2015.
- [242] H. Tarzamni, E. Babaei, A. Zarrin Gharehkhoushan, and M. Sabahi, "Interleaved full ZVZCS DC-DC boost converter: Analysis, design, reliability evaluations and experimental results," *IET Power Electron.*, vol. 10, no. 7, pp. 835-845, Jun. 2017.
- [243] M. K. Kazimierczuk, *Pulse-Width Modulated DC-DC Power Converters*. Hoboken, NJ, USA: Wiley, 2008.
- [244] R. W. Erickson and D. Maksimovic, *Fundamentals of Power Electronics*. Berlin, Germany: Springer, 2020.
- [245] B. Zhu, F. Ding, and D. M. Vilathgamuwa, "Coat circuits for DC-DC converters to improve voltage conversion ratio," *IEEE Trans. Power Electron.*, vol. 35, no. 4, pp. 3679-3687, Apr. 2020.
- [246] M. R. Banaei and S. G. Sani, "Analysis and implementation of a new SEPIC-based single-switch buck-boost DC-DC converter with continuous input current," *IEEE Trans. Power Electron.*, vol. 33, no. 12, pp. 10317-10325, Dec. 2018.
- [247] B. Zhu, Y. Liu, S. Zhi, K. Wang, and J. Liu, "A family of bipolar high step-up zeta-buck-boost converter based on 'coat circuit'," *IEEE Trans. Power Electron.*, vol. 38, no. 3, pp. 3328-3339, Mar. 2023.
- [248] M. R. Banaei and H. A. F. Bonab, "A novel structure for single-switch nonisolated transformerless buck-boost DC-DC converter," *IEEE Trans. Ind. Electron.*, vol. 64, no. 1, pp. 198-205, Jan. 2017.
- [249] H. Tarzamni et al., "Thermal analysis of non-isolated conventional PWM-based DC-DC converters with reliability consideration," *IET Power Electron.*, vol. 14, no. 2, pp. 337-351, Feb. 2021.
- [250] H. Tarzamni et al., "Reliability assessment of conventional isolated PWM DC-DC converters," *IEEE Access*, vol. 9, pp. 46191-46200, 2021.
- [251] H. Tarzamni, F. Tahami, M. Fotuhi-Firuzabad, and F. Blaabjerg, "Improved Markov model for reliability assessment of isolated multiple-switch PWM DC-DC converters," *IEEE Access*, vol. 9, pp. 33666-33674, 2021.
- [252] H. Tarzamni, F. Tahami, M. Fotuhi-Firuzabad, and F. P. Esmaelnia, "Reliability analysis of buck-boost converter considering the effects of operational factors," in *Proc. 10th Int. Power Electron., Drive Syst. Technol. Conf.*, 2019, pp. 647-652.
- [253] H. Tarzamni, F. P. Esmaelnia, M. Fotuhi-Firuzabad, F. Tahami, S. Tohid, and P. Dehghanian, "Comprehensive analytics for reliability evaluation of conventional isolated multiswitch PWM DC-DC converters," *IEEE Trans. Power Electron.*, vol. 35, no. 5, pp. 5254-5266, May 2020.
- [254] M. Hasanisadi, H. Tarzamni, and F. Tahami, "Comprehensive reliability assessment of buck quasi-resonant converter," in *Proc. IEEE 20th Int. Power Electron. Motion Control Conf.*, 2022, pp. 614-620.

- [255] H. Tarzamni, E. Babaei, F. P. Esmaelnia, P. Dehghanian, S. Tohidi, and M. B. B. Sharifian, "Analysis and reliability evaluation of a high step-up soft switching push-pull DC-DC converter," *IEEE Trans. Rel.*, vol. 69, no. 4, pp. 1376–1386, Dec. 2020.
- [256] S. Rahimpour, H. Tarzamni, N. V. Kurdkandi, O. Husev, D. Vinnikov, and F. Tahami, "An overview of lifetime management of power electronic converters," *IEEE Access*, vol. 10, pp. 109688–109711, 2022, doi: [10.1109/ACCESS.2022.3214320](https://doi.org/10.1109/ACCESS.2022.3214320).
- [257] S. Rahimpour, O. Husev, D. Vinnikov, N. V. Kurdkandi, and H. Tarzamni, "Fault management techniques to enhance the reliability of power electronic converters: An overview," *IEEE Access*, vol. 11, pp. 13432–13446, 2023, doi: [10.1109/ACCESS.2023.3242918](https://doi.org/10.1109/ACCESS.2023.3242918).
- [258] F. Z. Peng, "Z-source inverter," *IEEE Trans. Ind. Appl.*, vol. 39, no. 2, pp. 504–510, Mar./Apr. 2003.
- [259] M. Hasan Babayi, E. Babaei, S. H. Hosseini, and E. Shokati Asl, "Switched Z-source networks: A review," *IET Power Electron.*, vol. 12, no. 7, pp. 1616–1633, Jun. 2019.
- [260] S. Hasanpour, Y. P. Siwakoti, and F. Blaabjerg, "A new high efficiency high step-up DC/DC converter for renewable energy applications," *IEEE Trans. Ind. Electron.*, vol. 70, no. 2, pp. 1489–1500, Feb. 2023.
- [261] S. Abbasian, H. S. Gohari, M. Farsijani, K. Abbaszadeh, H. Hafezi, and S. Filizadeh, "Single-switch resonant soft-switching ultra-high gain DC-DC converter with continuous input current," *IEEE Access*, vol. 10, pp. 33482–33491, 2022.
- [262] S. Shabani, M. Delshad, R. Sadeghi, and H. H. Alhelou, "A high step-up PWM non-isolated DC-DC converter with soft switching operation," *IEEE Access*, vol. 10, pp. 37761–37773, 2022.
- [263] M. Zhang, Z. Wei, M. Zhou, F. Wang, Y. Cao, and L. Quan, "A high step-up DC-DC converter with switched-capacitor and coupled-inductor techniques," *IEEE J. Emerg. Sel. Topics Ind. Electron.*, vol. 3, no. 4, pp. 1067–1076, Oct. 2022.
- [264] S. Hasanpour, "New structure of single-switch ultra-high-gain DC/DC converter for renewable energy applications," *IEEE Trans. Power Electron.*, vol. 37, no. 10, pp. 12715–12728, Oct. 2022.
- [265] X. Ding, M. Zhou, Y. Cao, B. Li, Y. Sun, and X. Hu, "A high step-up coupled-inductor-integrated DC-DC multilevel boost converter with continuous input current," *IEEE J. Emerg. Sel. Topics Power Electron.*, vol. 10, no. 6, pp. 7346–7360, Dec. 2022.
- [266] S. R. V and K. S., "Ultra-voltage gain bidirectional DC-DC converter with reduced switch voltage stress and improved efficiency," *IEEE Trans. Circuits Syst. II, Exp. Briefs*, vol. 69, no. 11, pp. 4468–4472, Nov. 2022.
- [267] V. Abbasi, S. Rostami, S. Hemmati, and S. Ahmadian, "Ultrahigh step-up quadratic boost converter using coupled inductors with low voltage stress on the switches," *IEEE J. Emerg. Sel. Topics Power Electron.*, vol. 10, no. 6, pp. 7733–7743, Dec. 2022.
- [268] I. P. Rosas, E. Agostini, and C. B. Nascimento, "Single-switch high-step-up DC-DC converter employing coupled inductor and voltage multiplier cell," *IEEE Access*, vol. 10, pp. 82626–82635, 2022.
- [269] S. Abbasian, M. Farsijani, M. Tavakoli bina, and A. Shahirinia, "A non-isolated common-ground high step-up soft switching DC-DC converter with single active switch," *IEEE Trans. Ind. Electron.*, vol. 7, no. 6, pp. 5728–5738, Jun. 2023.
- [270] J. Wang, X. Wu, Z. Liu, X. Cui, and Z. Song, "Modified SEPIC DC-DC converter with wide step-up/step-down range for fuel cell vehicles," *IEEE Trans. Power Electron.*, to be published, doi: [10.1109/TPEL.2022.3203151](https://doi.org/10.1109/TPEL.2022.3203151).
- [271] H. S. Gohari, S. Abbasian, N. A. Mardakheh, K. Abbaszadeh, and F. Blaabjerg, "Coupled inductor-based current-fed ultra-high step-up DC-DC converter featuring low input current ripple," *IEEE Trans. Circuits Syst. II, Exp. Briefs*, to be published, doi: [10.1109/TCSII.2022.3206231](https://doi.org/10.1109/TCSII.2022.3206231).
- [272] S. Habibi, R. Rahimi, M. Ferdowsi, and P. Shamsi, "Coupled inductor based single-switch quadratic high step-up DC-DC converters with reduced voltage stress on switch," *IEEE J. Emerg. Sel. Topics Ind. Electron.*, vol. 4, no. 2, pp. 434–446, Apr. 2023.
- [273] S. Hasanpour, T. Nouri, F. Blaabjerg, and Y. P. Siwakoti, "High step-up SEPIC-based trans-inverse DC-DC converter with quasi-resonance operation for renewable energy applications," *IEEE Trans. Ind. Electron.*, vol. 70, no. 1, pp. 485–497, Jan. 2023.
- [274] A. Gupta, N. Korada, and R. Ayyanar, "Quadratic-extended-duty-ratio boost converters for ultra high gain application with low input current ripple and low device stress," *IEEE Trans. Ind. Appl.*, vol. 59, no. 1, pp. 938–948, Jan./Feb. 2022.
- [275] H. Li, C. Li, X. Sun, L. Cheng, and W. Li, "An interleaved high step-up DC/DC converter-based three-winding coupled inductors with symmetrical structure," *IEEE Trans. Power Electron.*, vol. 38, no. 5, pp. 6642–6652, May 2023, doi: [10.1109/TPEL.2023.3244809](https://doi.org/10.1109/TPEL.2023.3244809).
- [276] P. Luo, T.-J. Liang, K.-H. Chen, and S.-M. Chen, "Design and Implementation of a high step-up DC-DC converter with active switched inductor and coupled inductor," *IEEE Trans. Ind. Appl.*, vol. 59, no. 3, pp. 3470–3480, May/Jun. 2023, doi: [10.1109/TIA.2023.3238701](https://doi.org/10.1109/TIA.2023.3238701).
- [277] V. Abbasi, N. Talebi, M. Rezaie, A. Arzani, and F. Y. Moghadam, "Ultrahigh step-up DC-DC converter based on two boosting stages with low voltage stress on its switches," *IEEE Trans. Ind. Electron.*, vol. 70, no. 12, pp. 12387–12398, Dec. 2023, doi: [10.1109/TIE.2023.3236064](https://doi.org/10.1109/TIE.2023.3236064).



Hadi Tarzamni (Student Member, IEEE) was born in Tabriz, Iran, in 1992. He received the B.Sc. and M.Sc. degrees (Hons.) in power electrical engineering from the Faculty of Electrical and Computer Engineering, University of Tabriz, Tabriz, Iran, in 2014 and 2016, respectively. He is currently working toward the dual Ph.D. degree in power electronics engineering with the School of Electrical Engineering, Sharif University of Technology, Tehran, Iran, and the Department of Electrical Engineering and Automation, Aalto University, Espoo, Finland.

He has authored and coauthored more than 35 journal and conference papers. He also holds six patents in the area of power electronics. Since January 2021, he has been a Researcher with the Department of Electrical Engineering and Automation and the Department of Electronics and Nanoengineering, Aalto University, Espoo. His research interests include power electronic converters analysis and design, dc-dc and dc-ac converters, high step-up power conversion, soft-switching and resonant converters, and reliability analysis.

Mr. Tarzamni was the recipient of the Best Paper Award at the 10th International Power Electronics, Drive Systems and Technologies Conference in 2019. He has been awarded a three-year Aalto ELEC Doctoral School Grant, a Jenny and Antti Wihuri Foundation Grant, and a Walter Ahlström Foundation Grant in 2021, 2022, and 2023, respectively.



Homayon Soltani Gohari was born in Kerman, Iran, in December 1994. He received the M.Sc. degree in power electrical engineering and power electronics from the Faculty of Electrical Engineering, K. N. Toosi University of Technology, Tehran, Iran, in 2020.

His research interests include design, analysis, and control of power electronic converters, particularly EV chargers, grid-connected PV inverters, high step-up/down converters, and single/three-phase rectifiers with PFC.



Mehran Sabahi was born in Tabriz, Iran, in 1968. He received the B.S. degree in electronic engineering from the University of Tabriz, Tabriz, in 1991, the M.S. degree in electrical engineering from Tehran University, Tehran, Iran, in 1994, and the Ph.D. degree in electrical engineering from the University of Tabriz, Tabriz, in 2009.

In 2009, he joined the Faculty of Electrical and Computer Engineering, University of Tabriz, where he has been a Professor since 2019. His current research interests include power electronic converters

and renewable energy systems.



Jorma Kyrrä (Member, IEEE) received the M.Sc., Lic.Sc., and D.Sc. degrees in electrical engineering from the Helsinki University of Technology (TKK), which is now Aalto University, Helsinki, Finland, in 1987, 1991, and 1995, respectively.

Since 1985, he has been with the university in various positions. Since 1996, he has been an Associate Professor of power electronics, and since 1998, a Professor of power electronics. From 2008 to 2009, he was the Dean with the Faculty of Electronics, Communications and Automation, TKK, and from

2009 to 2011, the Vice President of Aalto University, Espoo, Finland. He is currently the Head of the Department of Electrical Engineering and Automation with Aalto University. His research interest is power electronics at large. The Power Electronics Group at Aalto University has expertise, e.g., in power electronics for ac drives, dc-dc converters, modeling of converters, filtering of EMI, power factor correction, and distributed power systems.